BIOMIMETIC SYNTHESIS OF HYBRID MATERIALS FOR POTENTIAL APPLICATIONS

RAMAKRISHNA MALLAMPATI

(M.Sc. University of Pune, India)

A THESIS SUBMITTED

FOR THE DEGREE OF DOCTOR OF PHILOSOPHY

DEPARTMENT OF CHEMISTRY

NATIONAL UNIVERSITY OF SINGAPORE

2013

DECLARATION

I hereby declare that this thesis is my original work and it has been written by me in its entirety, under the supervision of Assoc. Prof. Suresh Valiyaveettil, (in the "Materials Research Laboratory," S5-01-01) Department Of Chemistry, National University of Singapore, between 03rd August, 2009 and 02nd August, 2013.

I have duly acknowledged all the sources of information which have been used in the thesis.

This thesis has also not been submitted for any degree in any university previously.

The content of the thesis has been partly published in:

1. R. Mallampati and S. Valiyaveettil, Simple and efficient biomimetic synthesis of Mn_3O_4 hierarchical structures and their application in water treatment, **Journal of Nanoscience and Nanotechnology**, 2011, 11, 1–5.

2. R. Mallampati and S. Valiyaveettil, Application of Tomato peel as an efficient adsorbent for water purification – Alternative Biotechnology? **RSC Advances**, 2012, 2, 9914–9920.

3. R. Mallampati and S. Valiyaveettil, Biomimetic synthesis of metal oxides for the extraction of nanoparticles from water, **Nanoscale**, 2013, 5, 3395-3399.

4. R. Mallampati and S. Valiyaveettil, Apple peels – a versatile biomass for water purification?, **ACS applied materials & Interfaces**, 2013, 5, 4443−4449.

Name	Signature	Date

ACKNOWLEDGEMENTS

First and foremost, my sincere gratitude goes to my supervisor Assoc. Prof. Suresh Valiyaveettil for his guidance, support and encouragement during the course of this work. He gave me a lot of opportunities to try and learn new things and many helpful suggestions when things just would not seem to work right. I must be very thankful to him for his patience and helping me in my toughest time during research with moral support.

Many people have contributed their time and effort in helping me to accomplish this research. I sincerely thank all the current and former members of the group for their cordiality and friendship. Special thanks to Dr. Narahari, Dr. Pradipta, Dr. Sajini, Dr. Jhinuk, Dr. Vinod, Dr. Bala, Dr. Jitendra, Dr. Brahathees, Dr. Kaali, Dr. Qureshi, Dr. Mithun, Dr. Lekha, Evelyn, Kiruba, Deepa, Roshan, Daisy, Ping sen for all the good times in the lab and helping exchange knowledge and skills. Special thanks to Ashok and Chunyan for travelling all along four years with me and making this journey memorable.

Technical assistance provided by the staffs of CMMAC, Lab-suppies and Chemistry admistrative office and the Faculty of Science is gratefully acknowledged.

I am indebted forever to my friends Janardhan, Raghavendra and many others for their true love and affection and never left me feel alone in this journey.

I whole heartedly thank my parents, brother and sister-in-law for their support and encouragement.

Graduate Scholarship and financial help from the National University of Singapore is gratefully acknowledged.

TABLE OF CONTENTS

Title page

Declaration i

Acknowledgements ii

Table of Contents iii

Summary vii

List of Tables ix

List of Figures xi

List of Illustrations xvi

List of publications and presentations xviii

Chapter 1: Introduction

1.1. Biowaste - origin 2

1.2. Use of biowaste 2

1.3. water pollution: Different treatment methods 3

1.4. Adsorption: biowaste as novel adsorbent 8

1.5. Biopeels as efficient adsorbents 10

1.6. Factors effecting biosorption 12

1.7. Mechanism of biosorption 12

1.8. Isotherms 14

1.9. Kinetics 16

1.10. Modification of biopeels 17

1.11. Challenges 20

1.12. Scope and outline of the thesis 21

1.13. References 22

Chapter 2: Materials and methods

2.1. Commercially purchased chemicals 37

2.2. Synthesis of materials

2.2.1. Preparation of apple and tomato peels as adsorbents 37

2.2.2. Immobilization of Apple peel 38

2.2.3. Synthesis of Au and Ag nanoparticles 38

2.2.4. Synthesis of ESM + NP composites 38

2.2.5. Synthesis of metal oxides from ESM 39
2.3. Characterisation and analysis techniques 39
2.4. Batch adsorption studies
2.4.1. Effect of initial adsorbate concentration and time 40
2.4.2. Kinetic and isotherm studies 41
2.4.3. Effect of solution pH 41
2.4.4. Desorption studies 42
Chapter 3: Evaluation of biopeels for the extraction of different pollutants from water
3.1. Introduction 44
3.2. Results and discussion
3.2.1. Characterization of adsorbents 47
3.2.2. Effects of initial pollutant concentration and contact time 50
3.2.3. Effect of pH on the adsorption of different pollutants 53
3.3. Conclusion 55
3.4. References 57
Chapter 4: Application of tomato and apple peels as efficient adsorbents for water purification
4.1. Introduction 61
4.2. Characterisation of tomato and apple peel 63
4.3. Batch adsorption experiments
4.3.1. Effect of pH 64
4.3.2. Effect of initial pollutant concentration and contact time 66
4.3.3. Isotherm studies 68
4.3.4. Adsorption kinetics 72
4.3.5. Effect of temperature on adsorption 76
4.3.6. Diffusion rate constant study 77
4.3.7. Regeneration of adsorbent 80
4.4. Conclusions 80
4.5. References 82
Chapter 5 : Removal of anions and nanoparticles by using immobilized apple peel
5.1. Introduction 86

5.2. Characterisation of adsorbent 88

5.3.Characterisation of nanoparticles 92

5.4. Batch adsorption experiments

5.4.1. Effect of initial adsorbate concentration and time 93

5.4.2. Effect of solution pH 95

5.4.3. Isotherm studies 96

5.4.4. Adsorption kinetics 100

5.5. Analysis of adsorbent after adsorption 104

5.6. Desorption studies 107

5.7. Conclusions 108

5.8. References 109

Chapter 6: Biomimetic metal oxides for the extraction of nanoparticles from water

6.1. Introduction 113

6.2. Characterization 114

6.3. Adsorption of nanoparticles 120

6.4. Plausible mechanism 124

6.5. Conclusions 125

6.6. References 127

Chapter 7: Biomimetic synthesis of Mn_3O_4 hierarchical structures and their application in water treatment

7.1 Introduction 130

7.2 Characterization 132

7.3 Adsorption experiments 137

7.4 Conclusions 140

7.5 References 141

Chapter 8: Eggshell membrane supported recyclable noble metal catalysts for organic reactions

8.1 Introduction 145

8.2 Characterization 146

8.3 Reduction of *p*-nitrophenol 148

8.4 Synthesis of propargylamine 152

8.5 Conclusions 155
8.6 References 156

Chapter 9: Conclusions and future studies

9.1. Conclusions 161
9.2. Future studies 163

SUMMARY

One of the common problems throughout the world that needs to be addressed immediately is the availability of quality drinking water. Water is being contaminated by different pollutants like pesticides, heavy metal ions and dyes which create health problems in living organisms. Different water treatment techniques have been developed but none of them can extract all pollutants due to diversity in the chemical and physical properties of the pollutants. In this work, adsorbents were prepared from readily available biomass for water treatment. Biowaste materials are used directly as adsorbents and as templates to prepare other hybrid materials. These adsorbents were characterized using different analytical methods such as scanning electron microscopy (SEM), thermo gravimetric analysis (TGA), transmission electron microscopy (TEM) and X-ray diffraction analysis (powder XRD). The adsorption efficiency of each material was evaluated using batch adsorption studies. Langmuir and Freundlich isotherm models were used to validate the adsorption process. Kinetic studies were done to further understand the adsorption process.

In chapter one, a brief review of literature related to the usage of biopeels for water treatment is given. Advantages and challenges of different existing treatment methods were discussed. Chapter two includes different chemicals, analytical techniques and methods used in the research process. In chapter three, many viable biomembranes were screened against different pollutants and a few were selected for further adsorption experiments. The adsorption capacities of different biopeels towards different pollutants were investigated and identified that these peels can adsorb cationic pollutants more efficiently than anionic pollutants. Tomato and apple peels were tested as efficient adsorbents among all biomembranes screened due to their easy availability and high efficiency. Both peels were tested to extract different contaminants including dyes, pesticides, and heavy metal ions shown in chapter four. Results indicated that these biomembranes were more efficient in removing most of the pollutants. Apple peel was treated with zirconium ions to make it suitable adsorbent for anions. We

evaluated the performance of chemically treated apple peel against different anions and nanoparticles in chapter five. Results indicated that zirconium treated apple peels can extract chromate, arsenate and nanoparticles efficiently. Chaper six includes the bioinspired synthesis of metal oxides to remove nanocontaminants from water. Eggshell membrane was used as template to get porous metal oxide structures. These metal oxides including ZnO, NiO, CuO, CeO_2 and Co_3O_4 were characterized and employed in extraction of engineered gold and silver nanoparticles. Some of the metal oxides (NiO) showed efficient adsorption of NPs. Similar synthetic procedure is used to get Mn_3O_4. Chapter seven discusses the removal of different dyes, Phosphate and pesticides by Mn_3O_4. It is concluded from this chapter that Mn_3O_4 can be employed as efficient adsorbent for different pollutants. In chapter eight, various functional groups on eggshell membrane were exploited to synthesize stable gold and silver nanoparticles on its surface in chapter eight. These nanoparticles were tested for their catalytic activity in different organic reactions. Reduction of nitrophenol and synthesis of propargylamine were selected as model reactions to evaluate the catalytic activity of synthesized nanoparticles. It is proved that these biotemplated nanoparticles work as economic and efficient catalysts for various reactions.

Chapter nine summarizes the conclusions and future studies that can be carried out using our functional biowaste materials.

LIST OF TABLES

Table. No.	Title of the Table	Page No.
	Chapter 1	
Table 1.1.	Comparison of Different water treatment techniques.	7
Table 1.2.	List of biopeels (Fruit & vegetable) used for adsorption of different pollutants.	10
Table 1.3.	Different approaches to modify of biopeels for applications in water treatment.	19
	Chapter 3	
Table 3.1.	CHNS analysis data of different biosorbents.	50
Table 3.2.	Maximum experimental adsorption capacities of different pollutants using biopeels.	56
	Chapter 4	
Table 4.1.	Langumir and Freundlich isotherm model constants and correlation coefficients for adsorption of different pollutants on tomato peel.	69
Table 4.2.	Langumir and Freundlich isotherm model constants and correlation coefficients for adsorption of different pollutants on apple peel.	70
Table 4.3.	Pseudo first order and pseudo second order constants and correlation coefficients for adsorption of different pollutants on tomato peel.	75
Table 4.4.	Pseudo first order and pseudo second order constants and correlation coefficients for adsorption of different pollutants on apple peel.	76
Table 4.5.	Adsorption capacities tomato peels towards different pollutants at different temperatures.	77
Table 4.6.	Intraparticle diffusion model constants and correlation coefficients for adsorption of different pollutants on tomato peel.	79

Table 4.7. Intraparticle diffusion model constants and correlation coefficients for adsorption of different pollutants on apple peel. 79

Chapter 5

Table 5.1. Dynamic light scattering analysis of NPs. 93

Table 5.2. Langmuir and Freundlich isotherm model constants and correlation coefficients for adsorption of different anions on Zr immobilized apple peel surface. 100

Table 5.3. Pseudo first order and pseudo second order constants and correlation coefficients for adsorption of different anionic contaminants on treated apple peel. 104

Chapter 6

Table 6.1. Summary of the BET surface area (m^2/g) and IEPS values for the metal oxides. 120

Chapter 8

Table 8.1. K_{app} of different borohydide reduction reactions in presence of Au + ESM and Ag + ESM. 151

Table 8.2. Table showing reaction time of five consecutive reactions using NP-ESM catalysts. 152

Table 8.3. Percentage yields of propargylamine reaction with different reactants. 153

Table 8.4. Percentage yields of propargylamine reactions for five consecutive runs. 154

LIST OF FIGURES

Figure. No.	Title of the Figure	Page No.
	Chapter 3	
Figure 3.1.	Structure of epicatechin.	46
Figure 3.2.	FT-IR spectra of avocado, hami melon, dragon fruit, longan and kiwi peels.	47
Figure 3.3.	FT-IR spectra of avocado peel and hami melon peel before and after adsorption of pollutants.	48
Figure 3.4.	FESEM images of the surface of treated avocado (a), hami melon (b), dragon fruit (c), longan (d) and kiwi (e) peels.	49
Figure 3.5.	Variation of adsorption capacity of dyes (a, b, c, d and e) and heavy metal ions (i, ii, iii, iv and v) for avocado (a, i), hami melon (b, ii), dragon fruit (c, iii), longan (d, iv) and kiwi (e, v) peels.	53
Figure 3.6.	Effect of pH on adsorption capacity of dyes (a, b, c, d and e) and heavy metal ions (i, ii, iii, iv and v) for avocado (a, i), hami melon (b, ii), dragon fruit (c, iii), longan (d, iv) and kiwi (e, v) peels.	55
	Chapter 4	
Figure 4.1.	Schematic representation of the pollutant extraction by Tomato peel. Different dots indicate different classes of pollutants in water	62
Figure 4.2.	FT-IR spectrum of tomato peel before and after adsorption of pollutants (a) and apple peel (b).	63
Figure 4.3.	FESEM (a, b) and EDS (c, d) of tomato peel (a, c) and apple peel (b, d) surface.	64
Figure 4.4.	Effect of pH on the adsorption of dyes (a, d), metal ions (b, e) and pesticides (c, f).	65
Figure 4.5.	The variation of adsorption capacity of dyes (a, d), heavy metal ions (b, e) and pesticides (c, f) with time.	67

Figure 4.6. Langumir isotherms for dyes (a, c) and metal ions (b, d). 69

Figure 4.7. Freundlich isotherms for the adsorption of dyes (a, c) and metal ions (b, d) on tomato (a, b) and apple (c, d) peel. 72

Figure 4.8. Pseudo first order kinetics for adsorption dyes (a, c) and heavy metal ions (b, d) on to tomato (a, b) and apple (c, d) peel. 73

Figure 4.9. Pseudo second order kinetics for adsorption dyes (a, c) and heavy metal ions (b, d) on to tomato (a, b) and apple (c, d) peel 74

Figure 4.10. Weber and Morris intraparticle diffusion plots for removal of dyes (a, c) and heavy metal ions (b, d) by tomato (a, b) and apple (c, d) peel. 78

Chapter 5

Figure 5.1. FT-IR spectrum of raw apple peel and Zr treated apple peel. 89

Figure 5.2. FESEM micrographs (a, b) and EDS (i, ii) analysis of apple peel surface before (a, i) and after (b, ii) Zr treatment. Inset in (a) and (b) shows the magnified surface image . 90

Figure 5.3. XPS profile (a) and expanded region for Zr peaks (b) of treated apple peel surface. 91

Figure 5.4. TEM images of Ag and Au NPs with different capping agents. 92

Figure 5.5. UV-Vis spectra of different NPs. 92

Figure 5.6. The variation of adsorption capacity of Zr treated apple peel towards different anions (a) and nanoparticles (b) with change in time. 94

Figure 5.7. The variation of % removal of Zr treated apple peel towards different anions with change in pH. 95

Figure 5.8. Langmuir isotherms for anions (a) and NPs (b) adsorption. 97

Figure 5.9. Freundlich isotherms for anions (a) and NPs (b) adsorption. 99

Figure 5.10. Pseudo-first order (a, b) and pseudo-second order (c, d) kinetics for the adsorption of anions (a, c) and NPs (b, d) on to the Zr treated apple peel. 103

Figure 5.11. SEM (a, b) and EDS (i, ii) analysis of Zr treated apple peel with Ag (a, i) and Au (b, ii) adsorbed on the surface. 105

Figure 5.12. EDS analysis of Zr treated apple peel surface after adsorption of chromate (a) and arsenate (b) anions. 106

Figure 5.13. Desorption of anions from the Zr immobilized apple peel surface at various pH under ambient conditions. 107

Chapter 6

Figure 6.1. TGA curves of natural ESM and copper nitrate adsorbed on ESM 115

Figure 6.2. X-ray diffraction pattern of a) natural ESM, b) CeO_2, c) Co_3O_4, d) CuO, e) NiO and f) ZnO 116

Figure 6.3. EDX analysis of ESM copper composite a) before calcination and b) after calcination 117

Figure 6.4. SEM images of (a) natural ESM and oxides (b) CeO_2, (c) Co_3O_4, (d) CuO, (e) NiO and (f) ZnO synthesized on ESM template. 118

Figure 6.5. Magnified SEM images of (a) NiO, (b) CeO_2, (c) opened cavity of a CeO_2 tubes and (d) TEM of CeO_2 nanoparticles 119

Figure 6.6. TEM images of (a) Ag-PVP, (b) Au-PVP nanoparticles and the corresponding (c) UV-VIS spectra 121

Figure 6.7. UV-VIS spectra (a) Ag-PVP and (b) Au-PVP and corresponding optical images of (c) Ag-PVP and (d) Au-PVP nanoparticle solutions at different time intervals. Nickel oxide (20 mg of metal oxides to 10 mL of 2.5×10^{-4} M) were added into the vials 122

containing nanoparticle solutions and stirred for a duration mentioned above and filtered.

Figure 6.8. Adsorption capacities of different metal oxides towards (a) Ag-PVP and (b) Au-PVP nanoparticles. C_0 is the initial concentration of the nanoparticle solution and C is the remaining concentration at different time intervals during the extraction. 122

Figure 6.9. TEM images of (a) Au and (b) Ag nanoparticles on NiO particles after extraction. Inset shows the magnified images of metal oxide surface showing the presence of nanoparticles. 123

Figure 6.10. EDX analysis of a) Au NPs on NiO surface and b) Ag NPs on NiO surface 123

Chapter 7

Figure 7.1. X-ray diffraction pattern of the Mn_3O_4 sample. 132

Figure 7.2. EDX spectra of Mn_3O_4, showing peaks corresponding to Manganese and Oxygen. 133

Figure 7.3. TGA curves of natural ESM and manganese nitrate impregnated egg membrane (ESM+ $Mn(NO_3)_2.4H_2O$) 133

Figure 7.4. SEM image of a) natural ESM b) $Mn(NO_3)_2.4H_2O$ infiltred ESM composite calcinated at 700^oC and c) magnified image of b. 134

Figure 7.5. TEM image of Mn_3O_4 crystals dispersed in ethanol. 135

Figure 7.6. Nitrogen adsorption–desorption isotherms plot (a) and corresponding pore-size distribution plot (b) of Mn_3O_4. 136

Figure 7.7. UV spectra of a solution of Victoria blue (100 mg L^{-1}, 50 mL) in the presence of Mn_3O_4 hollow microfibers (0.01 g) at different time intervals of 0, 2, 4, 6 and 8 min, respectively. 137

Figure 7.8. Adsorption rate of the Victoria Blue on a) as prepared Mn_3O_4; b) secondary; c) third; d) fourth regenerated particles, respectively. C_0 (mg L^{-1}) is the 137

initial concentration of the Victoria Blue solution and C (mg L^{-1}) is the remaining concentration at different time intervals during the extraction.

Figure 7.9. Adsorption capacities of dyes (a) and pesticides (b) using Mn_3O_4 as adsorbent. 139

Chapter 8

Figure 8.1. SEM images of natural ESM (a), Au NPs (b) and Ag NPs (c) on ESM fibers. 146

Figure 8.2. SEM - EDS spot analysis of Ag NP (a) and Au NP (b) on ESM 147

Figure 8.3. XPs spectra of Au NP (a) and Ag NP (b) on ESM. Spectra were recorded using ESM-NPs. 147

Figure 8.4. UV-Vis spectra (a) and XRD pattern (b) of Au-ESM and Ag-ESM at ambient conditions. 148

Figure 8.5. Time dependant UV- Vis spectra of the reduction of *p*-nitrophenol by Au-ESM with time. 149

Figure 8.6. UV- Vis spectra of time dependant reduction of *ortho*-(a) and *meta* – nitrophenol (b) by Au-ESM. 150

Figure 8.7. Graph of ln A versus Time (sec) where A is absorbance. 150

Figure 8.8. Nanoparticles catalysed coupling reactions to form propargylamine derivatives. 152

Figure 8.9. FESEM images of Au-ESM (a) and Ag-ESM (b) after five consecutive reactions. 155

ABBREVIATIONS AND SYMBOLS

λ	Wavelength
%	Percentage
nm	Nanometer(s)
μm	Micrometer(s)
θ	Diffraction angle
NP	Nanoparticle
conc.	Concentration
cm	Centimeter
et. al	In Latin - et alii (and others)
g	Gram(s)
min	Minutes
h	Hour(s)
i.e.	That is (Latin id est)
kV	Kilovolts
keV	Kilo electron volts
mg	Milligram(s)
ml	Milliliter(s)
mmol	Milli molar
nm	nanometer
RT	Room temperature
rpm	Revolutions per minute
ESM	Eggshell Membrane
SEM	Scanning electron microscope
DSC	Differential scanning calorimetry
TGA	Thermo gravimetric analysis
EDX	Energy dispersive X-ray analysis
FT-IR	Fourier transform infrared spectroscopy
NMR	Nuclear magnetic resonance
FESEM	Field emission scanning electron microscope

ICP-OES	Inductive coupled plasma Optical Emission spectroscopy
UV-Vis	Ultra-Violet visible spectroscopy
XRD	X-ray diffraction
XPS	X-ray photoelectron spectroscopy

LIST OF PUBLICATIONS

1. R. Mallampati and S. Valiyaveettil, Simple and efficient biomimetic synthesis of Mn3O4 hierarchical structures and their application in water treatment, Journal of Nanoscience and Nanotechnology, 2011, 11, 1–5.

2. R. Mallampati and S. Valiyaveettil, Application of Tomato peel as an efficient adsorbent for water purification – Alternative Biotechnology? RSC Advances, 2012, 2, 9914–9920.

3. R. Mallampati and S. Valiyaveettil, Biomimetic synthesis of metal oxides for the extraction of nanoparticles from water, Nanoscale, 2013, 5, 3395-3399.

4. R. Mallampati and S. Valiyaveettil, Apple peels – a versatile biomass for water purification?, ACS applied materials & Interfaces, 2013, 5, 4443−4449.

5. R. Mallampati and S. Valiyaveettil, Efficient and recyclable noble metal catalysts for different organic reactions, ChemCatChem, 2013, (In press)

Invited Conferences and Presentations

1. **R. Mallampati** and S. Valiyaveettil, Bioinspired synthesis of metal oxide structures for Water Treatment, **IWA-WCE 2012, Ireland.**

2. **R. Mallampati** and S. Valiyaveettil, Biomimetic synthesis of Mn_3O_4 hierarchical network like structures and their application in water treatment, **ASIANANO 2011, Japan.**

3. **R. Mallampati** and S. Valiyaveettil, Efficient noble metal catalysts for different organic reactions. **MRS 2011, Boston, USA.**

4. **R. Mallampati** and S. Valiyaveettil, Utilization of tomato peel as a potential adsorbent for various pollutants in water, **5th MRS-S-2012, Singapore.**

5. **R. Mallampati** and S. Valiyaveettil, Bioinspired Synthesis of Hierarchical Metal Oxide Structures for Water Treatment, **SIWW 2012, Singapore.**

6. **R. Mallampati** and S. Valiyaveettil, Utilization of Bio Waste as a Potential Adsorbent for Various Pollutants in Water, **ICYRAM 2012, Singapore.**

7. R. Mallampati and S. Valiyaveettil, **Simple and Efficient Bio Mimetic Synthesis Mn_3O_4 Hierarchical Network Like Structures and Their Application in Water Treatment, ICMAT 2011, Singapore.**

8. R. Mallampati and S. Valiyaveettil, **Utilization of biowaste as a potential adsorbent for various pollutants in water, 244th ACS National Meeting 2012, Philadelphia USA.**

9. R. Mallampati and S. Valiyaveettil, Extraction of nanoparticles by Zr(IV) Loaded Biomembrane, **MRS 2013, USA.**

10. R. Mallampati and S. Valiyaveettil, Efficient Removal of nanoparticles by chemically modified Biomembrane, **SICC-7, 2012, Singapore.**

11. R. Mallampati and S. Valiyaveettil, Removal of Au and Ag NPs by Zr(IV) Loaded Biomembrane, **ICMAT 2013, Singapore.**

CHAPTER 1

INTRODUCTION

1.1. Biowaste – origin

Biowaste is defined as biodegradable waste materials generated from various sources. Nature contains abundant amount of biological matter which eventually converts into biowaste. Daily human activities also produce large quantities of biowaste, which include biowaste from, (1) industries; (2) domestic sources and (3) agricultural lands. Firstly, the food processing industries produce different biowastes such as nuts, outer peels of vegetables and fruits. Secondly, remains of the crops after harvesting are being disposed in different forms. The third category is domestic sources which includes food and kitchen waste from households, caterers and retail premises. Currently most of the biowaste is disposed by burning or dumping them in landfills. The landfilling of biodegradable waste is known to contribute to environmental pollution, mainly through the production of toxic leachate and methane gas.

1.2. Use of biowaste

The biological treatment of waste includes composting and anaerobic digestion. Composting is biological decomposition in aerobic and thermophilic conditions. The recycling of compost is considered as an efficient way of maintaining or restoring the quality of soils due to fertilisation and improving properties of organic matter present in them. It also contributes to the carbon sequestration and possibly replaces peat and fertilizers. However, the application of compost to soil could raise environmental problems related to the introduction of heavy metals, excessive or unbalanced supply of nutrients, organic pollutants and the spreading of pathogens. Furthermore, the application of biowaste and vegetable waste compost in agriculture has shown a low nitrogen fertilizer value of composts. Anaerobic digestion is similar to composting but it takes place in the absence of oxygen. This process turns most of the carbon dioxide emissions into methane and which then burns to generate energy by producing a soil conditioner. Biomass can be burnt directly to supply heat energy or to generate steam in order to produce electricity. Pyrolysis and gasification are thermal technologies like incineration which breaks down carbon-based wastes by using high temperatures. The pyrolysis process degrades waste to produce oil, char (or ash) and synthetic gas (syngas).

However, many proposals are emerging that aim to treat mixed household waste, such disposal of biowaste is an expensive and less efficient process. In addition, biowaste disposal involves many environmental concerns. Biomass burning produces lot of toxic gases like NO_2, SO_2 and CO_2. Developing a route to use biowaste for water treatment solves the problem of waste disposal and serves as an alternative biotechnology. Biomass contains mostly cellulose and hemicellulose carbohydrate polymers with different functional groups such as -NH_2, -OH and –COOH and these act as potential sites for binding metals, ions and molecules. This binding ability of biowaste can be employed to use them as adsorbents in water treatment and templates to prepare efficient catalysts.

1.3. Water pollution: different treatment methods

Water is vital to almost all life forms in existence and it is believed that, even, the first life started in water. Although more than 70% of earth surface is covered with water, majority of it is not suitable to sustain human life and only limited potable water resources are available. The inquisitive nature of human mind resulted in many rewarding innovations which eventually led to the age of industrialization of the world. The extensive use of chemicals for various purposes in day-to-day life and the growing industrialization led to unwanted contamination of our existing natural resources by the release of diverse organic and inorganic pollutants into water system.[1-3] Among various pollutants, heavy metal ions and dissolved organics (pesticides and dyes) are most dangerous to human health.[4] Since, it is impossible to completely prevent the drainage of hazardous chemicals into drinking water resources, the best way is to develop efficient water purifying technologies to provide clean water to the living communities. Consequently, many novel water purification techniques have been developed which include chemical precipitation, chemical oxidation and reduction, electrochemical treatment, ion exchange, membrane processes, coagulation, adsorption, dialysis, foam-flotation, osmosis, photo catalytic degradation and biological methods.[5] Continuous research is going on to develop an efficient method to remove most of these pollutants effectively and simultaneously.

Water treatment methods

Chemical precipitation is generally employed for heavy metal removal from inorganic effluent.[6] The pH is adjusted to the basic conditions (pH 11), metal ions are transformed to the insoluble solid through a chemical reaction with a precipitating agent such as lime. Generally, the metal precipitated from the solution is in the form of hydroxide.[7] Lime or calcium hydroxide is the most commonly used precipitating agent due to its low cost and high availability. This can be employed to treat inorganic pollutants with a metal concentration of higher than 1000 mg/L. Simplicity of the process, requirement of inexpensive equipment, convenient and safe operations are other advantages. Chemical precipitation needs large amount of chemicals to remove metals. Another limitation is the excessive production of sludge that requires further treatment. Moreover, increasing cost of sludge disposal, poor settling, aggregation of metal precipitates and slow metal precipitation needs to be answered.

Coagulation–flocculation: This method can be employed to treat wastewater containing heavy metals and organics. The coagulant destabilizes colloidal particles and results in sedimentation.[8] Particle size is increased by coagulation of the unstable particles into bigger floccules. This technique involves pH adjustment and the addition of ferric/alum salts as the coagulant. pH ranging from 11.0 to 11.5 is generally found to be effective in the removal of heavy metals by the coagulation–flocculation process.[9-11] Efficient sludge settling is the major advantage of this technique. On the other hand, the toxic sludge must be transformed into a stabilized product to arrest leaking of heavy metals into the environment. It has limitations such as high operational cost due to chemical consumption.[12] Electro-coagulation also creates a floc of metallic hydroxides, which requires further purification.

Flotation: Flotation is utilised to separate solids from a liquid phase using bubble attachment. Among the various types of flotation, dispersed-air flotation is the most commonly used for the treatment of metal-contaminated wastewater.[13-15] Low cost materials such as zeolite and chabazite have been used as effective collectors with high removal efficiency. Heavy metal

removal by flotation has the potential for industrial application even though it is a physical separation process.[16-18] Flotation can be used to remove some of the dissolved metal ions and organics.

Membrane filtration: Membrane filtration process has been effectively applied in the removal of suspended solid, organic compounds and inorganic contaminants such as heavy metals. Various types of filtration such as ultrafiltration, nanofiltration and reverse osmosis are being employed depending on the size of the particle that can be retained.[19-22]

Ultrafiltration (UF): On the basis of the pore size (5 – 20 nm) and molecular weight of the pollutants (1000 – 100,000 Da), UF utilizes permeable membrane to separate macromolecules, heavy metals and suspended solids from inorganic solution.[23-25] UF can achieve more than 90% of removal efficiency depending on the membrane properties; with a metal concentration ranging from 20 to 100 mg/L. UF has some advantages including lower driving force and a smaller space requirement. However, membrane fouling decreases the UF performance hindering its application in wastewater treatment. Fouling has many adverse effects such as decrease in flux with time, and degradation of the membrane materials,[26] which then add high operational costs for the membrane system.

Nanofiltration (NF): The separation mechanism of NF involves electrical and steric effects. A potential is created between the ions in the effluent and the charged anions in the NF membrane to reject the latter. Generally, NF membrane can treat inorganic effluent with high metal concentration. Depending on the membrane characteristics, NF can effectively remove pollutants at a wide pH range of 3 – 8.[27-29] However, NF efficiency is still under investigation for the removal of different pollutants.

Reverse osmosis (RO): This is a pressure driven membrane process where water can pass through the membrane, while the heavy metal is retained. Cationic compounds can be separated from water by applying a greater hydro-static pressure. RO is more effective for heavy metal removal from inorganic solution than UF and NF. RO works effectively at a wide pH range of 3–11 depending on the characteristics of the membrane such as the material,

porosity, thickness, hydrophilicity, roughness and charge of the membrane. High water flux rate, high salt rejection, resistance to biological attack, mechanical strength, chemical stability and the ability to withstand high temperatures are various advantages of using RO technique.[30] However, suspended solids such as chlorine oxides block the small pores of the membrane leading to fouling. This warrants the replacement of the membrane resulting to high operational costs.[31-33] Other drawbacks are the high energy consumption and the need for experienced work force to run the process.

Ion exchange: Ion exchange is one of the conventional and frequently applied techniques for waste water treatment around the world. A reversible inter change of ions between the solid and liquid phases occurs in ion exchange process. An insoluble substance removes ions from solution and releases other ions of similar charge in a chemically equivalent amount without any structural change of the solid.[34-39] Ion exchange can be used to recover valuable metals from inorganic effluent. The metal can be recovered in a more concentrated form by elution with suitable reagents. Depending on the oxidation state of metal and the characteristics of the ion exchanger, heavy metal removal works effectively in acidic conditions. Ion exchange does not present any sludge disposal problems unlike chemical precipitation. This decreases the operational costs for the disposal of the metal sludge. Resins have certain ligands that can selectively bond with metal cations, making ion exchange limited for a few heavy metal ions. Other pollutants such as dissolved organics and nanomaterials are not removed by this method.

Electrodialysis (ED): Electrodialysis is a membrane separation in which ions are passed through an ion exchange membrane by applying an electric potential. When ionic species passes through the cell compartments, the cations migrate toward the cathode and the anions migrate toward the anode. The literature indicates that ED cannot effectively treat inorganic effluent with a higher metal concentration (1000 mg/L).[40,41] ED requires clean feed, careful operation, and periodic maintenance to prevent any damages to the stack since it is a membrane process.

Oxidation: Oxidation involves the treatment of waste water using different oxidizing agents. Generally, two types of oxidation viz. chemical oxidation and UV assisted oxidation are commonly used. Chlorine, hydrogen peroxide, ozone, fenton's reagent, or potassium permanganate is used for treating the effluents.[42-45] Advanced oxidation process involves combination of chemical and UV treatments.[44,46,47] It is known that pH and catalysts play an important role in oxidation process. Formation of side products, high cost of oxidising agents are main limitations of this process. Various water treatment techniques and their advantages and limitations are summarised below.

Table 1.1. Comparison of Different water treatment techniques

Technique	**Advantage**	**Challenge**
Coagulation & flocculation	Simple, economically feasible	High sludge production and disposal problem
Biodegradation	Efficient and cost effective	Slow process, necessary to create favourable environment, maintenance and nutrition requirements
Adsorption on activated carbon	An effective adsorbent, great, capacity, produce a high quality treated effluent	Ineffective against some organics, regeneration is expensive and result in loss of the adsorbent, non-destructive process
Membrane separations	Removes all dye types, produce high quality treated effluent	High pressure, expensive, incapable of treating large volumes
Ion exchange	Simple method and easy regeneration	Not effective for all kinds of dyes, not economical
Chemical oxidation	Rapid and efficient process	High energy cost, chemicals required, by products formation
Reverse osmosis	Efficient and removes most of the pollutants	High pressures, membrane fouling, expensive
Advanced oxidation process	No sludge production, little or no consumption of chemicals	Economically unfeasible, formation of by products, technical constraints
Selective bioadsorbents	Economically attractive, regeneration may not necessary, high selectivity	Requires chemical modification, non-destructive process
Biomass	Low operating cost, good efficiency and selectivity, no toxic effect on microorganisms	Slow process, performance depends on some external factors (pH, ionic strength)

1.4. Adsorption: biowaste as novel adsorbent

Adsorption is a mass transfer process in which a pollutant is transferred from the liquid phase to the solid surface and bound by physical and/or chemical interactions. Adsorption method for water purification is becoming popular because of its capability to remove both organic and inorganic pollutants and its simple operational procedures.[48-51] Several biological materials have been screened for this purpose with good results. Most of the biological materials have an affinity for metal ions and other pollutants. The variety of biomass available for biosorption purposes is enormous. Microbial, plant and animal biomass and their derived products have various biological and industrial applications. Feasibility studies for industrial applications have shown that biosorption processes using non-living biomass is in fact more practical than the bioaccumulative processes that involve living microorganisms, since the microorganisms require complicated bioreactor systems and nutrient supply.[52,53] In addition, maintenance of a healthy microbial population is difficult due to toxicity of the pollutants being extracted, environmental factors such as pH and temperature of the waste solution being treated. Recovery of valuable metals is also not efficient in living cells since these may be bound intracellularly[52] so attention has been focused on the use of non-living biomass as biosorbents. It is demonstrated that adsorption using low-cost adsorbents derived from agricultural wastes is an effective and economic method for water decontamination due to its ecofriendly nature, low cost, biodegradability, large scale availability throughout the world and efficiency towards different pollutants. Agricultural waste materials are composed of lignin and cellulose as the vital constituents. Other components are lipids, proteins, hemicellulose, simple sugars, starches, water, hydrocarbons and many other compounds with different functional groups present in the bidding process.[54,55] Hemicellulose is a heteropolymer of xylose with β-1,4-glycosidic linkage with other substances of acetyl and glycouronyl groups. Cellulose is a polymer of glucose with β-1,4-glycosidic linkage and intra-molecular and intermolecular hydrogen bonds. Lignin is a three dimensional polymer of aromatic compounds covalently linked with xylans.[56-58] The different functional groups present in biomass molecules are amido, amino, sulphydryl,

carbonyl, phenolic, polysaccharides, carboxyl groups alcohols and esters.[59] These groups have the affinity for different metal ions, dyes and phenolic compounds. Some biosorbents are non-selective and can bind to a wide range of heavy metals and organics with no specific priority, whereas others have specificity for certain types of metals depending upon their chemical composition.

Different biomass types have been tested for their biosorptive capacities under various conditions. Many review papers quantitatively compared biosorptive capacities of various biomass materials. Crini reviewed the use of plant based materials as adsorbents,[60] while O'Connell et al. reviewed cellulose based materials.[61] A brief comparison of biosorptive efficiencies of various types of bacterial species was done by Malik, Veglio and Beolchini, Vijayaraghavan and Holan.[62-65] Mehta and Gaur compared heavy metal removal by algae.[66,67] biosorptive capacities of chitin/chitosan and its many derivatives was summarized by Varma et al. and Gerente et al.[68,69] Other researchers compared the biosorptive capacities of agricultural wastes for heavy metals.[70-74] Recovery of precious metals such as gold, platinum, and palladium using biosorbents was reviewed by Mack et al.[75-77] Andrès et al. reviewed microbial biosorbents for concentrating rare earth elements like europium, lanthanum, scandium, and ytterbium.[78]

The type and origin of the biomass is very important. For example freely-suspended biomass, immobilized preparations, living biofilms, physical and chemical treatments such as drying, boiling, autoclaving and mechanical disruption will affect binding properties while chemical treatments often improve biosorption capacity. Pollutant adsorption can involve various types of biosorption processes that will be affected by different physical and chemical factors. These factors are responsible for the overall biosorption performance of the biosorbent. Hence the first step of biosorption process is to examine the individual or cooperative effects of various factors involved in biosorption. In case of batch biosorption processes, the important factors include solution pH, temperature, ionic strength, initial pollutant concentration,

biosorbent dosage, biosorbent size, agitation speed, and also the coexistence of other pollutants.

1.5. Biopeels as efficient adsorbents

Use of biopeels as adsorbents may be viable for industrial applications. These vegetable or fruit peels contain fibrous structures with sufficient mechanical strength that can withstand the water flow. Chemical modification on these peels will not cause any damage to the adsorbent. Column packing, loading and washing procedures will be easy by choosing right size of the adsorbent. Suitable washing can reduce the release of organics into water significantly. Adsorbent must be stable for the elution of pollutants in desorption process. These advantages attracted many researchers to evaluate the adsorption efficiency of different biopeels towards pollutants. Some of them are mentioned in table 1.2.

Table 1.2. List of biopeels (Fruit & vegetable) used for adsorption of different pollutants

Biopeel used	Pollutants	Reference
Banana peel	Dyes, heavy metals ions, pesticides	79-82
Pineapple leaf	Heavy metal ions	98
Rice husk	Dyes, heavy metals ions, pesticides	83-109
Orange peel	Dyes, heavy metals ions, pesticides	82,110-117
Corn cob	Dyes, heavy metals ions, pesticides	118-124
Durain, Pummelo	Heavy metals ions	125
Maize leaf	Heavy metals ions	126
Papaya peel	Heavy metals ions	265
Tamarind	Heavy metals ions	127,128
Potato	Heavy metals ions	266
Water melon shell	Heavy metals ions	267
Papaya wood	Heavy metals ions	129
Tree fern	Heavy metals ions	130-132
Neem leaf	Dyes, Heavy metals ions	133,134
Grape stalk	Heavy metals ions	135
Peanut husk / shell	Heavy metals ions	136-149
Wheat straw/ bran	Dyes, Heavy metals ions	150-160
Mango peel/ bark	Heavy metals ions	161
Jute fibers	Heavy metals ions	162
Sugarcane bagase	Dyes, heavy metals	163,164
Carrot residues	Heavy metals ions	165
Coconut coir/shell	Dyes, Heavy metals ions	166-174
Tea leaves	Heavy metals ions	175-179
Sunflower	Heavy metals ions	91,180,181
Soybean hull	Heavy metals ions	182-185

Palm fruit bunch	Dyes	268
Yellow passion fruit	Dyes	186
Guava leaf	Dyes	187
Hazelnut	Heavy metals ions	118,189
Oil palm trunk fibers	Dyes, heavy metal ions	190,191
Eucalyptus bark	Dyes, heavy metal ions	192.193
Black gram husk	Heavy metals ions	194-196
Peels of peas, broad bean, medlar and fig leaves	Heavy metals ions	197
Onion, garlic	Heavy metals ions	198
Sesame hull	Dyes	199
Tomato peel	Dyes, heavy metals ions, pesticides	200

1.6. Factors effecting biosorption

pH studies provide information on the chemical nature of the functional group present on the adsorbent. Basic pH enhances biosorptive removal of cationic pollutants, but reduces the adsorption of anionic pollutants.[201] Higher temperature usually enhances the adsorption capacity of many adsorbents by increasing surface activity and kinetic energy of the adsorbate, but increase in temperature may damage physical structure of biosorbent. Increase in ionic strength reduces biosorptive removal of many pollutants by competing with the adsorbate for binding sites of biosorbent. Initial pollutant concentration has significant effect on removal efficiency.[202,203] Higher pollutant concentration increases the adsorption capacity (quantity of biosorbed pollutant per unit weight of biosorbent), but decreases its removal efficiency. Biosorbent dosage affects the removal efficiency in reverse manner to pollutant concentration. Increase in adsorbent dosage decreases the quantity of biosorbed pollutant per unit weight of biosorbent, but increases its removal efficiency.[204] Biosorbent size is important parameter in industrial applications. Smaller size is favourable for batch process due to higher surface area of the biosorbent, but not for column process due to its poor mechanical strength and clogging of the column. Agitation speed has slightly less impact on adsorption behaviour. Generally higher agitation speed enhances biosorptive removal rate of adsorptive pollutant by minimizing its mass transfer resistance, but may damage physical structure of the biosorbent. Presence of other pollutant competes with a target pollutant for binding sites or forms complex with it.[205] Waste water is a mixture of different pollutant so it is worth to study

adsorption behaviour of adsorbents in presence of a mixture of pollutants. Generally higher concentration of other pollutants will reduce biosorptive removal of the target pollutant.

1.7. Mechanism of biosorption

The interaction between pollutant and adsorbent can be understood by adsorption-desorption cycles. This information is crucial for understanding the biosorption process as it can serve as a basis for selecting suitable isotherms, kinetics and mathematical models. Different binding mechanisms have been postulated to be active in biosorption including complexation, coordination and chemisorption by ion exchange, chelation, physical adsorption and microprecipitation.[206-213] Complexation is defined as the formation of a species by the association of two or more species. When one of the species is a metal ion, the resulting entity is known as a metal complex. Ligands are molecules with electron rich functional groups to interact with the central metal atom. Some ligands are attached to a metal atom by more than one donor atom in such a manner as to form a heterocyclic ring which is considered as chelation. Ion exchange is the interchange of ions where bivalent metal ions exchange with counter ions from active groups of bioadsorbent. Adsorption is a process by which molecules or ions adhere to solid surfaces. Adsorption is a surface phenomenon hence the actual process may involve either physical or chemical binding forces. Physical adsorption is non-specific and relatively weak. Chemisorption is specific and involves forces much stronger than physical adsorption. The strength of physical adsorption decreases rapidly with increase in temperature and is generally very small above the critical temperature of the adsorption. According to Langmuir, the adsorbed molecules are held to the surface by valence forces of the same type as those occurring between atoms in molecules. Examples of chemisorption are metal complexation and chelation.

The chemical nature of biological materials is complex and a variety of mechanisms may be operative simultaneously under the given conditions. Precipitations, where bound metal / pollutant species can act as loci for subsequent deposition can lead to very high uptake capacities but this may

inhibit desorption. The variety of structural components present in biopeels means that different functional groups are able to interact with pollutants. For example carboxyl, phosphate, hydroxyl, amino, thiols are common functional groups present in varying degrees and are affected by physicochemical factors. The diversity of chemical structure encountered in organic pollutants (molecular size, charge, solubility, hydrophobicity, and reactivity), the type of biosorbent and wastewater composition affect biosorption as well. It is likely that the various mechanisms involved in biosorption can operate simultaneously to varying degrees.[50,65,71,214-222] There are various reports describing the binding mechanism of different cationic pollutants to various biopeels but mechanisms of anion biosorption have not been investigated in detail, although this can be markedly affected by chemical conditions such as pH.

1.8. Isotherms

Batch adsorption studies can give useful information on relative biosorbent efficiencies and important physicochemical factors that affect biosorption, although they do not provide significant insights about mechanisms.[223-228]A variety of models ranging from single component (Langmuir and Freundlich) to multicomponent models have been used to validate biosorption. Interpretation of these models has some use in comparing different biosorbent systems. Most of these models are proposed based on assumptions that are relatively simple for biological systems. These assumptions were derived for the adsorption of gases in monolayers of activated carbon. Some of the assumptions, such as binding sites having the same affinity, do not often apply to biopeels. Biosorbents have multiple binding sites such as carbonyl, thiol, amine, carboxyl, hydroxyl and phosphate groups. Such functional groups have different affinities for sorbate species, and can be easily affected by changes in pH and solution chemistry. Some models which reflect multilayer adsorption such as the Brunauer–Emmett–Teller (BET) isotherms also have been reported. Many biosorption models have now been described for different biopeels but only the most common will be described here. The Freundlich isotherm defines adsorption to heterogeneous surfaces. It means surfaces possess adsorption sites of varying affinities. The Freundlich isotherm equation[229,230] is:

$$q_e = KC^{\beta} \qquad (1.1)$$

where q_e is the equilibrium value of sorbate uptake by the sorbent, C is the equilibrium sorbate concentration, K is an affinity parameter and β is a dimensionless heterogeneity parameter: the smaller the value of β, the greater the heterogeneity. The Freundlich equation reduces to a linear adsorption isotherm when β = 1. This equation is often used over a wide range of concentrations even though it is strictly valid for metal adsorption at low concentrations. Data are usually fitted to the logarithamic form of the equation:

$$\log q_e = \log K + \beta \log C \qquad (1.2)$$

which should give a straight line by plotting log q_e versus log C of slope β and an intercept of log K. The Langmuir isotherm was derived originally from studies on gas adsorption to activated carbon. This model based on few assumptions which include that (a) adsorption is limited to formation of a monolayer, (b) all binding sites possess an equal affinity for the adsorbate and (c) the number of adsorbed species does not exceed the total number of surface sites which means there is a 1: 1 stoichiometry between surface adsorption sites and adsorbate.

The Langmuir adsorption isotherm[223,231-233] is represented as:

$$q_e = \frac{Q^0 KC}{1 + KC} \qquad (1.3)$$

Where Q˚ is the maximum adsorption of sorbate per unit mass sorbent, K is an affinity parameter related to the bonding energy of the sorbate species to the surface and other symbols are as previously described. The Langmuir isotherm assumes a finite number of uniform adsorption sites and overlooked the lateral interactions between adsorbed species. Biological materials are more complex containing different adsorption sites so these assumptions are clearly invalid for such adsorbents. In addition, the Langmuir isotherm is only able to describe adsorption at low sorbate concentrations (1. 3). A multisite Langmuir adsorption isotherm allows for more than one type of binding site. The multisite Langmuir adsorption isotherm is:

$$q_e = \sum_{i=1}^{n} \frac{Q^0{}_i K_i C}{1 + K_i C} \qquad (1.4)$$

where n is the number of types of surface sites. This isotherm is expected to provide a better fit to metal adsorption data than the single Langmuir isotherm. The BET is another isotherm with multilayer adsorption at the adsorbent surface and assumes that a Langmuir equation is applicable to each layer. Further a given layer may not need to be completely formed before the next layer forms. The BET equation is:

$$q_e = \frac{BCQ^0}{(C_s - C)[1 + (B-1)\left(\frac{C}{C_s}\right)]} \qquad (1.5)$$

Where C_s is the saturation concentration of the solute, B is a constant relating to the energy of interaction with the surface, and other symbols are as previously described. A plot of $C/(C_s - C)$ qe against C/C_s gives a straight line for data conforming to the BET isotherm of slope $(B-1)/B\ Q^{\circ}$ and intercept $1/B\ Q^{\circ}$. There will not be any significant information regarding the mechanism by fitting biosorption data to adsorption isotherm equations and should be considered simply as numerical relationships used to fit data. Experimental evidence is important before any chemical significance can be attributed to isotherm equation parameters. Further, these parameters are valid only for the chemical conditions under which the experiment was conducted. Use of these equations for prediction of pollutant adsorption behaviour under different pH, ionic strength, and pollutant concentration is not straight forward.

1.9. Kinetics

Batch kinetic modelling is necessary to describe the response of the biosorption system to changes caused by variations in the experimental conditions and the properties of biosorbents. The model results can be affected by the maximum uptake capacity of biosorbent, mass transfer coefficients, biosorbent size, initial pollutant con-centration, and solute diffusivity. Thus, kinetics studies give detailed information on adsorbate uptake rates and on rate controlling steps such as intraparticle mass transfer, external mass transfer and

biosorptive reactions.[224,228,234-243] Intra-particle diffusion has often shown to be an important factor in determining the attainment of equilibrium in immobilized biosorbents. To identify these processes, batch kinetic data is fitted to an intra-particle diffusion plot as suggested by Morris.[244] If this plot passes through the origin then intra-particle diffusion is the rate determining step. There are various intra or extra mass transfer models in biosorption studies that have been reported in the literature.[245] Around 25 models have been introduced in attempts to quantitatively describe kinetic behaviour during the adsorption process, but every model has its own limitations. Derivation of these equations and their physical meaning has been summarized in the literature.[246] In most cases, both pseudo-first- and second-order kinetic equations have been commonly employed in parallel, and one was often claimed to be better than the other, according to marginal differences in the correlation coefficient. In general, the pseudo-second-order equation has been successfully applied to the biosorption of metal ions, dyes, and organic substances from aqueous solutions. Due to the complexity of the biosorption mechanism, however, in theory, the order of a biosorption process must be determined by the general rate law equation, rather than preset-order kinetic equations.

The criteria for choosing the isotherm or kinetic equation for biosorption data is generally based on the goodness of curve fitting which is often evaluated by statistical analysis. However, good curve fitting in the sense of statistical evaluation may not necessarily imply that this curve fitting has true physical meaning. That means if a set of biosorption data is analyzed by different isotherm or kinetic equations, the best fit equation may not be the one reflecting the biosorption mechanism.[247,248] Therefore most of the isotherm and kinetic studies about biosorption process are simple mathematical exercises. It has been stated that selection of kinetic equations should be based on the mechanisms. Strong theoretical characteristics are needed to formulate a mathematical expression of biosorption rather than simple curve fitting.

1.10. Modification of biopeels

Advantages of using raw biopeels for waste water treatment include low cost, easy availability, fast regeneration, requires little processing, selective adsorption of heavy metal ions and good adsorption capacity. However, some of the limitations include high chemical oxygen demand (COD) and biological chemical demand (BOD) as well as increase in total organic carbon (TOC) due to release of soluble organic compounds contained inside the biopeels.[249] The increase of the COD, BOD and TOC can cause decrease of oxygen content in water and can threaten the aquatic life. Hence plant wastes need modification or treatment before being used for water treatment. Immobilisation of the biomass on solid structures creates a material with the right size, mechanical strength, rigidity and porosity necessary for use in columns. Immobilisation can also yield beads or granules that can be reused many times similar to ion exchange resins.[250,251] The possibility of using the biosorbent material in subsequent adsorption desorption cycles would improve the economics of biomass technical applications. Pre-treatment of plant wastes can extract soluble organic compounds and improve binding efficiency.[74] Pre-treatment methods include different kinds of modifying agents such as base solutions (calcium hydroxide, sodium hydroxide, sodium carbonate), acid solutions (hydrochloric acid, sulfuric acid, nitric acid, citric acid, tartaric acid, thioglycollic acid), organic compounds (methanol, ethylenediamine, epichlorohydrin, formaldehyde, isopropanol), oxidizing agent (hydrogen peroxide), dye (Reactive Orange 13) and others.[51,97-103]

Surface modification can greatly alter the biosorptive capacity of the biomass as biosorption is a surface process. A number of chemical, physical, and other modification methods are reported in literature. Generally, physical modification is very simple and inexpensive, but is generally less efficient than chemical modification. In some cases, biosorption mechanism connected with target chemical group in a form of biomass can be characterized by chemical modification of that group. Among various chemical modification methods, washing with different chemicals has been preferred due to its simplicity and efficiency. For example, acid washing can enhance the capacity of biosorbents for cationic metals or basic dyes in many cases, through extraction of soluble organic or inorganic components from raw biomass and

by changing its biochemistry. However, some chemicals may cause mass losses of the biosorbent via structural damage and decrease in the biosorptive capacity. Modification of its functional groups facilitates significant improvements in the adsorptive efficiency of a biosorbent. Amine, carboxyl, hydroxyl, sulfonate, thiol, and phosphonate groups are known to be good binding sites for metals or dyes. Hence, these functional groups can be formed, modified or transformed to enhance biosorptive capacity. Raw biomass may have certain groups that inhibit biosorption of a target pollutant; thus, chemical elimination of the inhibiting groups will also produce a better biosorbent. Grafting of long polymer chains onto the surface of raw biomass is another efficient way to introduce binding groups onto the surface of a biosorbent. Various monomers, such as acrylic acid, acrylamide, acrylonitrile, ethylenediamine, hydroxylamine, glycidyl monomers, and urea are reported in literature for surface grafting.[253,259-263] Table 1.3 summarises various modification methods currently in practice for the preparation of better biosorbents.

Table 1.3. Different approaches to modify of biopeels for applications in water treatment.

Method	**Purpose**	**Process involved**
Physical modification	Pre-treatment	Cutting, grinding, autoclaving, steam, thermal drying, lyophilisation,
Chemical modification	Pre-treatment (washing)	Acids(HCl,H_2SO_4,HNO_3,H_3PO_4,citric acid, etc), Alkalis(NaOH,KOH,NH_4OH,$Ca(OH)_2$, etc), organic solvents(methanol, ethanol, acetone, tolune, formaldehyde, epichlorohydrin, salicylic acid, NTA,EDTA,SDS,L-cysteine,Triton X-100, tec) and other chmicals (NaCl, $CaCl_2$, $ZnCl_2$,Na_2CO_3,$NaHCO_3$,K_2CO_3, $(NH_4)_2SO_4$,H_2O_2,NH_4CH_3COO, etc)
	Enhancement of binding groups	Amination of hydroxyl groups, carboxylation of hydroxyl group, phosphorylation of hydroxyl group, carboxylation of amine group, amination of carboxyl group, saponification of ester groups, sulfonation, xanthanation. Thiolation, halogenation, oxidation, etc.
	Elimination of	Decarboxylation/elimination of carboxyl group, deamination/elimination of amine

	inhibiting groups	group
	Graft polymerization	High energy radiation grafting(using gama irradiation, microwave radiation, electro-magnetic radiation, etc) photochemical grafting(with/without sensitizers like benzon ethyl ether, acrylated azo dye and aromatic ketones under UV light) and chemical initiation grafting(using ceric ion, permanganate ion, ferrous ammonium nitrate/H_2O_2,$KMnO_4$/citric acid, etc)
	Culture optimisation	Optimisation of culture conditions for enhancing biosorptive capacity of cells
	Genetic engineering	Over expression of cysteine rich peptide (glutathione, phytochelatins, metallothioneins, etc) and expression of hybrid proteins on the surface of cells

1.11. Challenges

The application of untreated plant wastes as adsorbents may involve serious release of soluble organic compounds into water, which then increase the COD, BOD and TOC. It is important to consider such issues when screening raw biomass for potential use in biosorption processes. Generally, biomass and biomass driven biosorbents show low stability due to degradation. This property may be a serious limitation for long term applications in water treatment facilities. The low thermal stability of biomass and its degradation resulting from desorbing agents are other important criteria that need to be taken into account. Further, the continuous supply of biomass should be considered, which has a huge impact on its successful application in real applications. Many researchers reported the use of microbial biomass systems without adequately considering this point. Factors other than the availability and low cost of biomass, especially the biosorptive capacity need to be considered towards the selection of appropriate material. Most studies reported the use of particular biopeel for the extraction of a single pollutant. Reports on the use of single biopeel for the extraction of various pollutants including heavy metal ions, dyes, pesticide and nanocontaminants are rare. We aim to develop novel adsorbents and investigate the efficiency for water treatment.

1.12. Scope and outline of the thesis

The main purpose of this study was to develop an efficient and stable adsorbent for water treatment. The specific objectives of this research are

- To identify potential adsorbents among available vegetable and fruit peels
- To investigate adsorption efficiency of biopeels such as tomato and apple peels towards different non bio pollutants
- To design chemically modified peels for the removal of various anionic pollutants
- To synthesize highly stable and robust metal oxides for removal of nanoparticle from water using biowaste
- To demonstrate the usage of biomass for synthesizing efficient catalyst for different organic reactions

A few viable vegetable and fruit peels were selected and screened for removal of pollutants. Chapter 2 of the thesis describes materials and synthetic procedures used in the present study. We investigated the removal efficiencies of different working peels (Longan, kiwi, avocado, hami melon and dragon fruit) against various pollutants including heavy metal ions, pesicides and nanoparticles and discussed in chapter 3. Chapter 4 describes the investigation of the adsorption efficiencies of tomato and apple peel against different cationic pollutants. The results showed that raw biopeels can extract cations more efficiently than anions. Zr cation immobilized apple peels were prepared and investigated the adsorption capacity towards different anionic pollutants. Robust and stable metal oxides were prepared using Eggshell membrane as template. These metal oxides were employed as adsorbents to remove nanoparticle from water. Biotemplated Mn_3O_4 was synthesised and used for the removal of dyes from water. Chapter 7 describes the use of Mn_3O_4 for the extraction of other pollutants along with dyes. Efficient and viable catalysts were prepared by using eggshell membrane as template. Catalytic activity was investigated against two organic reactions and discussed in Chapter 8. Overall the thesis describe attempts to use bioadsorbent for multiple applications, predominantly for water purification.

1.13. References

(1) Järup, L. *British Medical Bulletin* **2003**, *68*, 167.

(2) Rajaganapathy, V.; Xavier, F.; Sreekumar, D.; Mandal, P. K. *Journal of Environmental Science and Technology* **2011**, *4*, 234.

(3) Lapworth, D. J.; Baran, N.; Stuart, M. E.; Ward, R. S. *Environmental Pollution* **2012**, *163*, 287.

(4) Mitchell, E.; Frisbie, S.; Sarkar, B. *Metallomics* **2011**, *3*, 874.

(5) Tünay, O. *Water Science and Technology* **2004**, *48*, 43.

(6) Benefield, L. D.; Morgan, J. M. *Water Quality and Treatment* **1999**, 10.1.

(7) Wang, L. K.; Vaccari, D. A.; Li, Y.; Shammas, N. K. *Physicochemical Treatment Processes* **2004**, *3*, 141.

(8) Shammas, N. K. *Physicochemical Treatment Processes* **2004**, *3*, 103.

(9) Charerntanyarak, L. *Water Science and Technology* **1999**, *39*, 135.

(10) Venkata Mohan, S.; Sailaja, P.; Srimurali, M.; Karthikeyan, J. *Environ. Eng. Policy* **1999**, *1*, 149.

(11) Ayoub, G. M.; Semerjian, L.; Acra, A.; El Fadel, M.; Koopman, B. *Journal of Environmental Engineering* **2001**, *127*, 196.

(12) Lee, J. W.; Choi, S. P.; Thiruvenkatachari, R.; Shim, W. G.; Moon, H. *Dyes and Pigments* **2006**, *69*, 196.

(13) Zabel, T. *The Scientific Basis of Flotation* **1984**, 349.

(14) Rubio, J.; Tessele, F. *Minerals Engineering* **1997**, *10*, 671.

(15) Zouboulis, A. I.; Matis, K. A. *Critical Reviews in Environmental Science and Technology* **1997**, *27*, 195.

(16) Matis, K. A.; Zouboulis, A. I.; Lazaridis, N. K.; Hancock, I. C. *International Journal of Mineral Processing* **2003**, *70*, 99.

(17) Matis, K. A.; Zouboulis, A. I.; Gallios, G. P.; Erwe, T.; Blöcher, C. *Chemosphere* **2004**, *55*, 65.

(18) Zouboulis, A. I.; Lazaridis, N. K.; Matis, K. A. *International Journal of Environment and Pollution* **2008**, *32*, 29.

(19) Juang, R. S.; Shiau, R. C. *Journal of Membrane Science* **2000**, *165*, 159.

(20) Van der Bruggen, B.; Vandecasteele, C. *Desalination* **2002**, *143*, 207.

(21) Blöcher, C.; Dorda, J.; Mavrov, V.; Chmiel, H.; Lazaridis, N. K.; Matis, K. A. *Water Research* **2003**, *37*, 4018.

(22) Lin, S. H.; Hsiao, R. C.; Juang, R. S. *Journal of Hazardous Materials* **2006**, *135*, 134.

(23) Marcucci, M.; Nosenzo, G.; Capannelli, G.; Ciabatti, I.; Corrieri, D.; Ciardelli, G. *Desalination* **2001**, *138*, 75.

(24) Kryvoruchko, A.; Yurlova, L.; Kornilovich, B. *Desalination* **2002**, *144*, 243.

(25) Saffaj, N.; Loukili, H.; Younssi, S. A.; Albizane, A.; Bouhria, M.; Persin, M.; Larbot, A. *Desalination* **2004**, *168*, 301.

(26) Sablani, S.; Goosen, M.; Al-Belushi, R.; Wilf, M. *Desalination* **2001**, *141*, 269.

(27) Van Der Bruggen, B.; Vandecasteele, C. *Environmental Pollution* **2003**, *122*, 435.

(28) Mohammad, A. W.; Othaman, R.; Hilal, N. *Desalination* **2004**, *168*, 241.

(29) Chakraborty, S.; De, S.; Basu, J. K.; DasGupta, S. *Desalination* **2005**, *174*, 73.

(30) Slater, C. S.; Ahlert, R. C.; Uchrin, C. G. *Desalination* **1983**, *48*, 171.

(31) Potts, D. E.; Ahlert, R. C.; Wang, S. S. *Desalination* **1981**, *36*, 235.

(32) Benito, Y.; Ruíz, M. L. *Desalination* **2002**, *142*, 229.

(33) Ozaki, H.; Sharma, K.; Saktaywin, W. *Desalination* **2002**, *144*, 287.

(34) Thomas, H. C. *Journal of the American Chemical Society* **1944**, *66*, 1664.

(35) Rao, M. G.; Gupta, A. K. *The Chemical Engineering Journal* **1982**, *24*, 181.

(36) Clifford, D. A. *Water Quality and Treatment* **1999**, 9.1.

(37) Karcher, S.; Kornmüller, A.; Jekel, M. *Water Research* **2002**, *36*, 4717.

(38) Liu, C. H.; Wu, J. S.; Chiu, H. C.; Suen, S. Y.; Chu, K. H. *Water Research* **2007**, *41*, 1491.

(39) Wu, J. S.; Liu, C. H.; Chu, K. H.; Suen, S. Y. *Journal of Membrane Science* **2008**, *309*, 239.

(40) Tzanetakis, N.; Taama, W. M.; Scott, K.; Jachuck, R. J. J.; Slade, R. S.; Varcoe, J. *Separation and Purification Technology* **2003**, *30*, 113.

(41) Marder, L.; Bernardes, A. M.; Zoppas Ferreira, J. *Separation and Purification Technology* **2004**, *37*, 247.
(42) Gregor, K. H. *Chemical Oxidation* **1992**, *2*, 161.
(43) Von Gunten, U. *Water Research* **2003**, *37*, 1443.
(44) Doğan, D.; Türkdemir, H. *Journal of Chemical Technology and Biotechnology* **2005**, *80*, 916.
(45) Maezawa, A.; Nakadoi, H.; Suzuki, K.; Furusawa, T.; Suzuki, Y.; Uchida, S. *Ultrasonics Sonochemistry* **2007**, *14*, 615.
(46) Alnaizy, R.; Akgerman, A. *Advances in Environmental Research* **2000**, *4*, 233.
(47) Arslan-Alaton, I. *Coloration Technology* **2003**, *119*, 345.
(48) Hu, Q. H.; Qiao, S. Z.; Haghseresht, F.; Wilson, M. A.; Lu, G. Q. *Industrial and Engineering Chemistry Research* **2006**, *45*, 733.
(49) Xiaoli, C.; Youcai, Z. *Journal of Hazardous Materials* **2006**, *137*, 410.
(50) Wan Ngah, W. S.; Teong, L. C.; Hanafiah, M. A. K. M. *Carbohydrate Polymers* **2011**, *83*, 1446.
(51) Senthil Kumar, P.; Ramalingam, S.; Abhinaya, R. V.; Kirupha, S. D.; Murugesan, A.; Sivanesan, S. *Clean - Soil, Air, Water* **2012**, *40*, 188.
(52) Wang, J. L.; Han, Y. J.; Qian, Y. *Microbiology* **2000**, *27*, 449.
(53) Gadd, G. M. *Experientia* **1990**, *46*, 834.
(54) Young, R. A. *Cellulose: Structure, Modification and Hydrolysis* **1986**, 91.
(55) Timell, T. E. *Wood Science and Technology* **1967**, *1*, 45.
(56) Annadurai, G.; Juang, R. S.; Lee, D. J. *Journal of Hazardous Materials* **2002**, *92*, 263.
(57) Garcia-Valls, R.; Hatton, T. A. *Chemical Engineering Journal* **2003**, *94*, 99.
(58) Demirbas, A. *Journal of Hazardous Materials* **2004**, *109*, 221.
(59) Volesky, B. *Water Research* **2007**, *41*, 4017.
(60) Crini, G. *Bioresource Technology* **2006**, *97*, 1061.
(61) O'Connell, D. W.; Birkinshaw, C.; O'Dwyer, T. F. *Bioresource Technology* **2008**, *99*, 6709.
(62) Malik, A. *Environment International* **2004**, *30*, 261.
(63) Kaushik, P.; Malik, A. *Environment International* **2009**, *35*, 127.

(64) Veglio, F.; Beolchini, F.; Gasbarro, A. *Process Biochem.*

(65) Veglio, F.; Beolchini, F. *Hydrometallurgy* **1997**, *44*, 301.

(66) Mehta, S. K.; Gaur, J. P. *Critical Reviews in Biotechnology* **2005**, *25*, 113.

(67) Wilde, E. W.; Benemann, J. R. *Biotechnology Advances* **1993**, *11*, 781.

(68) Varma, A. J.; Deshpande, S. V.; Kennedy, J. F. *Carbohydrate Polymers* **2004**, *55*, 77.

(69) Gerente, C.; Lee, V. K. C.; Le Cloirec, P.; McKay, G. *Critical Reviews in Environmental Science and Technology* **2007**, *37*, 41.

(70) Demirbas, A. *Journal of Hazardous Materials* **2008**, *157*, 220.

(71) Johnson, T. A.; Jain, N.; Joshi, H. C.; Prasad, S. *Journal of Scientific and Industrial Research* **2008**, *67*, 647.

(72) Mahvi, A. H. *International Journal of Environmental Science and Technology* **2008**, *5*, 275.

(73) Ahluwalia, S. S.; Goyal, D. *Bioresource Technology* **2007**, *98*, 2243.

(74) Wan Ngah, W. S.; Hanafiah, M. A. K. M. *Bioresource Technology* **2008**, *99*, 3935.

(75) Lodeiro, P.; Herrero, R.; Vicente, M. E. S. d. *Journal of Hazardous Materials* **2006**, *137*, 244.

(76) Mack, C.; Wilhelmi, B.; Duncan, J. R.; Burgess, J. E. *Biotechnology Advances* **2007**, *25*, 264.

(77) Mack, C. L.; Wilhelmi, B.; Duncan, J. R.; Burgess, J. E. *Minerals Engineering* **2008**, *21*, 31.

(78) Andrès, Y.; Texier, A. C.; Le Cloirec, P. *Environmental Technology* **2003**, *24*, 1367.

(79) Namasivayam, C.; Prabha, D.; Kumutha, M. *Bioresource Technology* **1998**, *64*, 77.

(80) Namasivayam, C.; Kanchana, N.; Yamuna, R. T. *Waste Management* **1993**, *13*, 89.

(81) Low, K. S.; Lee, C. K.; Leo, A. C. *Bioresource Technology* **1995**, *51*, 227.

(82) Annadurai, G.; Juang, R. S.; Lee, D. J. *Water Science and Technology* **2003**, *47*, 185.

(83) Gao H Fau - Liu, Y.; Liu Y Fau - Zeng, G.; Zeng G Fau - Xu, W.; Xu W Fau - Li, T.; Li T Fau - Xia, W.; Xia, W.

(84) Wong, K. K.; Lee, C. K.; Low, K. S.; Haron, M. J. *Chemosphere* **2003**, *50*, 23.

(85) Williams, P. T.; Nugranad, N. *Energy* **2000**, *25*, 493.

(86) Teixeira Tarley, C. R.; Costa Ferreira, S. L.; Zezzi Arruda, M. A. *Microchemical Journal* **2004**, *77*, 163.

(87) Sumanjit; Prasad, N. *Indian Journal of Chemistry - Section A Inorganic, Physical, Theoretical and Analytical Chemistry* **2001**, *40*, 388.

(88) Srinivasan, K.; Balasubramanian, N.; Ramakrishna, T. V. *Indian Journal of Environmental Health* **1988**, *30*, 376.

(89) Singh, D. K.; Srivastava, B. *Indian Journal of Chemical Technology* **2001**, *8*, 133.

(90) Ong, S. A.; Seng, C. E.; Lim, P. E. *Electronic Journal of Environmental, Agricultural and Food Chemistry* **2007**, *6*, 1764.

(91) Nakbanpote, W.; Thiravetyan, P.; Kalambaheti, C. *Minerals Engineering* **2000**, *13*, 391.

(92) Mohamed, M. M. *Journal of Colloid and Interface Science* **2004**, *272*, 28.

(93) Mahvi, A. H.; Maleki, A.; Eslami, A. *Am. J. Appl. Sci.* **2004**, *1*, 321.

(94) Mahvi, A. H.; Alavi, N.; Maleki, A. *Pakistan J. Biol. Sci* **2005**, *8*, 721.

(95) Low, K. S.; Lee, C. K. *Bioresource Technology* **1997**, *61*, 121.

(96) Lee, C. K.; Low, K. S.; Liew, S. C.; Choo, C. S. *Environmental Technology* **1999**, *20*, 971.

(97) Kumar, U.; Bandyopadhyay, M. *Bioresource Technology* **2006**, *97*, 104.

(98) Khalid, N.; Ahmad, S.; Toheed, A.; Ahmed, J. *Applied Radiation and Isotopes* **2000**, *52*, 31.

(99) Khalid, N.; Ahmad, S.; Toheed, A.; Ahmad, J. *Applied Radiation and Isotopes* **2000**, *52*, 30.

(100) Khalid, N.; Ahmad, S.; Kiani, S. N.; Ahmed, J. *Separation Science and Technology* **1998**, *33*, 2349.

(101) Hayashi, H.; Nakashima, S. *Clay Science* **1992**, *8*, 181.

(102) Gou, Y.; Yang, S.; Fu, W.; Qi, J.; Li, R.; Wang, Z.; Xu, H. *Dyes and Pigments* **2003**, *56*, 219.

(103) Daifullah, A. A. M.; Girgis, B. S.; Gad, H. M. H. *Materials Letters* **2003**, *57*, 1723.

(104) Dadhich, A. S.; Beebi, S. K.; Kavitha, G. V. *Indian Journal of Environmental Health* **2004**, *46*, 179.

(105) Chuah, T. G.; Jumasiah, A.; Azni, I.; Katayon, S.; Thomas Choong, S. Y. *Desalination* **2005**, *175*, 305.

(106) Bishnoi, N. R.; Bajaj, M.; Sharma, N.; Gupta, A. *Bioresource Technology* **2004**, *91*, 305.

(107) Bakircioglu, Y.; Bakircioglu, D.; Akman, S. *Journal of Trace and Microprobe Techniques* **2003**, *21*, 467.

(108) Akhtar, M.; Bhanger, M. I.; Iqbal, S.; Hasany, S. M. *Journal of Hazardous Materials* **2006**, *128*, 44.

(109) Ajmal, M.; Ali Khan Rao, R.; Anwar, S.; Ahmad, J.; Ahmad, R. *Bioresource Technology* **2003**, *86*, 147.

(110) Sivaraj, R.; Namasivayam, C.; Kadirvelu, K. *Waste Management* **2001**, *21*, 105.

(111) Pérez-Marín, A. B.; Zapata, V. M.; Ortuño, J. F.; Aguilar, M.; Sáez, J.; Lloréns, M. *Journal of Hazardous Materials* **2007**, *139*, 122.

(112) Namasivayam, C.; Muniasamy, N.; Gayatri, K.; Rani, M.; Ranganathan, K. *Bioresource Technology* **1996**, *57*, 37.

(113) Ghimire, K. N.; Inoue, K.; Makino, K.; Miyajima, T. *Separation Science and Technology* **2002**, *37*, 2785.

(114) Dhakal, R. P.; Ghimire, K. N.; Inoue, K. *Hydrometallurgy* **2005**, *79*, 182.

(115) Brahimi-Horn, M. C.; Lim Liany, S. L.; Mou, D. G. *J. Ind. Microbiol.* **1992**, *10*, 245.

(116) Biswas, B. K.; Inoue, K.; Ghimire, K. N.; Ohta, S.; Harada, H.; Ohto, K.; Kawakita, H. *Journal of Colloid and Interface Science* **2007**, *312*, 214.

(117) Biswas, B. K.; Inoue, J.-i.; Inoue, K.; Ghimire, K. N.; Harada, H.; Ohto, K.; Kawakita, H. *Journal of Hazardous Materials* **2008**, *154*, 1066.

(118) Wu, F. C.; Tseng, R. L.; Juang, R. S. *Environmental Technology* **2001**, *22*, 205.

(119) Vaughan, T.; Seo, C. W.; Marshall, W. E. *Bioresource Technology* **2001**, *78*, 133.

(120) Robinson, T.; Chandran, B.; Nigam, P. *Environment International* **2002**, *28*, 29.

(121) Kweon, D. K.; Choi, J. K.; Kim, E. K.; Lim, S. T. *Carbohydrate Polymers* **2001**, *46*, 171.

(122) Hawrhorne-Costa, E. T.; Winkler Hechenleitner, A. A.; Gomez-Pineda, E. A. *Sep. Sci. Technol.* **1995**, *30*.

(123) El-Hendawy, A. N. A.; Samra, S. E.; Girgis, B. S. *Colloids and Surfaces A: Physicochemical and Engineering Aspects* **2001**, *180*, 209.

(124) Bosinco, S.; Roussy, J.; Guibal, E.; Le Cloirec, P. *Environmental Technology* **1996**, *17*, 55.

(125) Saikaew, W.; Kaewsarn, P. *Songklanakarin Journal of Science and Technology* **2009**, *31*, 547.

(126) Singh, K. K.; Talat, M.; Hasan, S. H. *Bioresource Technology* **2006**, *97*, 2124.

(127) Verma, A.; Chakraborty, S.; Basu, J. K. *Separation and Purification Technology* **2006**, *50*, 336.

(128) Agarwal, G. S.; Bhuptawat, H. K.; Chaudhari, S. *Bioresource Technology* **2006**, *97*, 949.

(129) Saeed, A.; Akhter, M. W.; Iqbal, M. *Separation and Purification Technology* **2005**, *45*, 25.

(130) Ho, Y. S.; Huang, C. T.; Huang, H. W. *Process Biochemistry* **2002**, *37*, 1421.

(131) Ho, Y. S.; Chiang, T. H.; Hsueh, Y. M. *Process Biochemistry* **2005**, *40*, 119.

(132) Ho, Y. S. *Water Research* **2003**, *37*, 2323.

(133) Venkateswarlu, P.; Ratnam, M. V.; Rao, D. S.; Rao, M. V. *Int. J. Phys. Sci.* **2007**, *2*, 188.

(134) Bhattacharyya, K. G.; Sarma, A. *Dyes and Pigments* **2003**, *57*, 211.

(135) Fiol, N.; Escudero, C.; Poch, J.; Villaescusa, I. *Reactive and Functional Polymers* **2006**, *66*, 795.

(136) Wilson, K.; Yang, H.; Seo, C. W.; Marshall, W. E. *Bioresource Technology* **2006**, *97*, 2266.

(137) Wafwoyo, W.; Seo, C. W.; Marshall, W. E. *Journal of Chemical Technology and Biotechnology* **1999**, *74*, 1117.

(138) Romero, L. C.; Bonomo, A.; Gonzo, E. E. *Adsorption Science and Technology* **2004**, *22*, 237.

(139) Randall, J. M.; Reuter, F. W.; Waiss, A. C. *J. Appl. Polym. Sci.* **1975**, *19*.

(140) Randall, J. M.; Reuter, F. C.; Waiss, A. C. *J. Appl. Polym. Sci.* **1974**, *19*, 156.

(141) Randall, J. M.; Hautala, E.; McDonald, G. *Journal of Applied Polymer Science* **1978**, *22*, 379.

(142) Periasamy, K.; Namasivayam, C. *Chemosphere* **1996**, *32*, 769.

(143) Periasamy, K.; Namasivayam, C. *Sep. Sci. Technol.* **1995**, *30*, 2223.

(144) Periasamy, K.; Namasivayam, C. *Waste Management* **1995**, *15*, 63.

(145) Namasivayam, C.; Periasamy, K. *Water Research* **1993**, *27*, 1663.

(146) Johnson, P. D.; Watson, M. A.; Brown, J.; Jefcoat, I. A. *Waste Management* **2002**, *22*, 471.

(147) Hashem, A.; Abdel-Halim, E. S.; El-Tahlawy, K. F.; Hebeish, A. *Adsorption Science and echnology* **2005**, *23*, 367.

(148) Chamarthy, S.; Seo, C. W.; Marshall, W. E. *Journal of Chemical Technology and Biotechnology* **2001**, *76*, 593.

(149) Brown, P.; Atly Jefcoat, I.; Parrish, D.; Gill, S.; Graham, E. *Advances in Environmental Research* **2000**, *4*, 19.

(150) Sun, R. C.; Mark Lawther, J.; Banks, W. B. *Wood and Fiber Science* **1998**, *30*, 56.

(151) Singh, K. K.; Singh, A. K.; Hasan, S. H. *Bioresource Technology* **2006**, *97*, 994.

(152) Robinson, T.; Chandran, B.; Nigam, P. *Water Research* **2002**, *36*, 2824.

(153) Ravat, C.; Monteil-Rivera, F.; Dumonceau, J. *Journal of Colloid and Interface Science* **2000**, *225*, 329.

(154) Gough, B. M.; Pybus, J. N.; St, A. *Die Stärke* **1968**, *20*, 108.

(155) Farajzadeh, M. A.; Monji, A. B. *Separation and Purification Technology* **2004**, *38*, 197.

(156) Dupont, L.; Guillon, E. *Environmental Science and Technology* **2003**, *37*, 4235.

(157) Dupont, L.; Bouanda, J.; Dumonceau, J.; Aplincourt, M. *Journal of Colloid and Interface Science* **2003**, *263*, 35.

(158) Camire, A. L.; Clydesdale, F. M. *J Food Sci* **1981**, *46*, 548.

(159) Bouanda, J.; Dupont, L.; Dumonceau, J.; Aplincourt, M. *Analytical and Bioanalytical Chemistry* **2002**, *373*, 174.

(160) Basci, N.; Kocadagistan, E.; Kocadagistan, B. *Desalination* **2004**, *164*, 135.

(161) Reddy, B. R.; Mirghaffari, N.; Gaballah, I. *Resources, Conservation and Recycling* **1997**, *21*, 227.

(162) Shukla, S. R.; Pai, R. S. *Bioresource Technology* **2005**, *96*, 1430.

(163) Peternele, W. S.; Winkler-Hechenleitner, A. A.; Gómez Pineda, E. A. *Bioresource Technology* **1999**, *68*, 95.

(164) Khattri, S. D.; Singh, M. K. *Adsorption Science and Technology* **1999**, *17*, 269.

(165) Nasernejad, B.; Zadeh, T. E.; Pour, B. B.; Bygi, M. E.; Zamani, A. *Proc Biochem* **2005**, *40*, 4.

(166) Tan, W. T.; Ooi, S. T.; Lee, C. K. *Environmental Technology* **1993**, *14*, 277.

(167) Prasad, S. C.; Dubey, R. B. *J. Inst. Engr (India), Environ. Engng. Div.* **1995**, *75*, 36.

(168) Pino, G. H.; Souza De Mesquita, L. M.; Torem, M. L.; Pinto, G. A. S. *Minerals Engineering* **2006**, *19*, 380.

(169) Pino, G. H.; De Mesquita, L. M. S.; Torem, M. L.; Pinto, G. A. S. *Separation Science and Technology* **2006**, *41*, 3141.

(170) Parimala, V.; Krishnani, K. K.; Gupta, B. P.; Jayanthi, M.; Abraham, M. *Bulletin of Environmental Contamination and Toxicology* **2004**, *73*, 31.

(171) Low, K. S.; Lee, C. K.; Wong, S. L. *Environmental Technology* **1995**, *16*, 877.

(172) Baes, A. U.; Umali, S. J. P.; Mercado, R. L. *Water Science and Technology* **1996**, *34*, 193.

(173) Babarinde, N. A. A. *J. Pure Appl. Sci.* **2002**, *5*, 81.

(174) Alaerts, G. J.; Jitjaturunt, V.; Kelderman, P. *Water Science and Technology* **1989**, *21*, 1701.

(175) Tee, T. W.; Khan, A. R. M. *Environmental Technology Letters* **1988**, *9*, 1223.

(176) Malkoc, E.; Nuhoglu, Y. *Journal of Hazardous Materials* **2005**, *127*, 120.

(177) Mahvi, A. H.; Naghipour, D.; Vaezi, F.; Nazmara, S. *Am. J. Appl. Sci.* **2005**, *2*, 372.

(178) Çay, S.; Uyanik, A.; Özaşik, A. *Separation and Purification Technology* **2004**, *38*, 273.

(179) Ahluwalia, S. S.; Goyal, D. *Engineering in Life Sciences* **2005**, *5*, 158.

(180) Sun, G.; Shi, W. *Industrial and Engineering Chemistry Research* **1998**, *37*, 1324.

(181) Hashem, A. *Polymer - Plastics Technology and Engineering* **2006**, *45*, 35.

(182) Marshall, W. E.; Wartelle, L. H.; Boler, D. E.; Johns, M. M.; Toles, C. A. *Bioresource Technology* **1999**, *69*, 263.

(183) Laszlo, J. A.; Dintzis, F. R. *Journal of Applied Polymer Science* **1994**, *52*, 531.

(184) Daneshvar, N.; Salari, D.; Aber, S. *Journal of Hazardous Materials* **2002**, *94*, 49.

(185) Bankar, D. B.; Dara, S. S. *Proc. Nation. Semin. Pollut. Cont. Environ. Manage.* **1985**, *1*, 121.

(186) Pavan Fa Fau - Lima, E. C.; Lima Ec Fau - Dias, S. L. P.; Dias Sl Fau - Mazzocato, A. C.; Mazzocato, A. C.

(187) Ponnusami V Fau - Vikram, S.; Vikram S Fau - Srivastava, S. N.; Srivastava, S. N.

(188) Cimino, G.; Passerini, A.; Toscano, G. *Water Research* **2000**, *34*, 2955.

(189) Altun, T.; Pehlivan, E. *CLEAN – Soil, Air, Water* **2007**, *35*, 601.

(190) Guo, J.; Lua, A. C. *J. Oil Palm Res.* **2000**, *12*, 64.

(191) Chu, K. H.; Hashim, M. A. *Journal of Chemical Technology and Biotechnology* **2002**, *77*, 685.

(192) Sarin, V.; Pant, K. K. *Bioresource Technology* **2006**, *97*, 15.

(193) Morais, L. C.; Freitas, O. M.; Gonçalves, E. P.; Vasconcelos, L. T.; González Beça, C. G. *Water Research* **1999**, *33*, 979.

(194) Saeed, A.; Iqbal, M.; Akhtar, M. W. *Journal of Hazardous Materials* **2005**, *117*, 65.

(195) Saeed, A.; Iqbal, M. *Water Research* **2003**, *37*, 3472.

(196) Saeed, A.; Akhtar, M. W.; Iqbal, M. *Fresenius Environmental Bulletin* **2005**, *14*, 219.

(197) Benaissa, H.

(198) Negi, R.; Satpathy, G.; Tyagi, Y. K.; Gupta, R. K. *International Journal of Environment and Pollution* **2012**, *49*, 179.

(199) Feng, Y.; Yang, F.; Wang, Y.; Ma, L.; Wu, Y.; Kerr, P. G.; Yang, L. *Bioresource Technology* **2011**, *102*, 10280.

(200) Mallampati, R.; Valiyaveettil, S. *RSC Advances* **2012**, *2*, 9914.

(201) Zhou, J. L.; Huang, P. L.; Lin, R. G. *Environmental Pollution* **1998**, *101*, 67.

(202) Voerman, S.; Tammes, P. M. L. *Bulletin of Environmental Contamination and Toxicology* **1969**, *4*, 271.

(203) Vachoud, L.; Zydowicz, N.; Domard, A. *International Journal of Biological Macromolecules* **2001**, *28*, 93.

(204) Mittal, A. K.; Venkobachar, C. *Journal of Environmental Engineering* **1993**, *119*, 366.

(205) Kuyucak, N.; Volesky, B. *Biotechnol Bioeng* **1989**, *33*, 815.

(206) Zhang, A.; Asakura, T.; Uchiyama, G. *Reactive and Functional Polymers* **2003**, *57*, 67.

(207) Schmidt, G. T.; Vlasova, N.; Zuzaan, D.; Kersten, M.; Daus, B. *Journal of Colloid and Interface Science* **2008**, *317*, 228.

(208) Sakkayawong, N.; Thiravetyan, P.; Nakbanpote, W. *Journal of Colloid and Interface Science* **2005**, *286*, 36.

(209) Park, S. J.; Jang, Y. S. *Journal of Colloid and Interface Science* **2002**, *249*, 458.

(210) Mohapatra, D.; Mishra, D.; Chaudhury, G. R.; Das, R. P. *Korean Journal of Chemical Engineering* **2007**, *24*, 426.

(211) Métivier-Pignon, H.; Faur-Brasquet, C.; Le Cloirec, P. *Separation and Purification Technology* **2003**, *31*, 3.

(212) Aoki, T.; Munemori, M. *Water Research* **1982**, *16*, 793.

(213) Al-Ghouti, M. A.; Khraisheh, M. A. M.; Allen, S. J.; Ahmad, M. N. *Journal of Environmental Management* **2003**, *69*, 229.

(214) Wang, J.; Chen, C. *Biotechnology Advances* **2006**, *24*, 427.

(215) Sud, D.; Mahajan, G.; Kaur, M. P. *Bioresource Technology* **2008**, *99*, 6017.

(216) Pollard, S. J. T.; Fowler, G. D.; Sollars, C. J.; Perry, R. *Science of the Total Environment* **1992**, *116*, 31.

(217) Lin, S. H.; Juang, R. S. *Journal of Environmental Management* **2009**, *90*, 1336.

(218) Ioannidou, O.; Zabaniotou, A. *Renewable and Sustainable Energy Reviews* **2007**, *11*, 1966.

(219) Gupta, V. K.; Suhas *Journal of Environmental Management* **2009**, *90*, 2313.

(220) Fu, F.; Wang, Q. *Journal of Environmental Management* **2011**, *92*, 407.

(221) Forgacs, E.; Cserháti, T.; Oros, G. *Environment International* **2004**, *30*, 953.

(222) Bailey, S. E.; Olin, T. J.; Bricka, R. M.; Adrian, D. D. *Water Research* **1999**, *33*, 2469.

(223) Ahmaruzzaman, M. *Advances in Colloid and Interface Science* **2008**, *143*, 48.

(224) Tempkin, M. J.; Pyzhev, V. *Acta Physiochim. URSS* **1940**, *12*, 217.

(225) Liu, Y.; Liu, Y. J. *Separation and Purification Technology* **2008**, *61*, 229.

(226) Limousin, G.; Gaudet, J. P.; Charlet, L.; Szenknect, S.; Barthès, V.; Krimissa, M. *Applied Geochemistry* **2007**, *22*, 249.

(227) Al-Asheh, S.; Banat, F.; Al-Omari, R.; Duvnjak, Z. *Chemosphere* **2000**, *41*, 659.

(228) Aksu, Z.; Açikel, Ü.; Kutsal, T. *Journal of Chemical Technology and Biotechnology* **1997**, *70*, 368.

(229) Abdullah, M. A.; Chiang, L.; Nadeem, M. *Chemical Engineering Journal* **2009**, *146*, 370.

(230) Freundlich, H. *Z. Phys. Chem.* **1906**, *57*, 385.

(231) Freundlich, H. *Phys. Chem. Soc.* **1906**, *40*, 1361.

(232) Liu, Y. *Colloids and Surfaces A: Physicochemical and Engineering Aspects* **2006**, *274*, 34.

(233) Langmuir, I. *The Journal of the American Chemical Society* **1918**, *40*, 1361.

(234) Langmuir, I. *The Journal of the American Chemical Society* **1916**, *38*, 2221.

(235) Zogorski, J. S.; Faust, S. D.; Haas Jr, J. H. *Journal of Colloid and Interface Science* **1976**, *55*, 329.

(236) Young Hee, Y.; Nelson, J. H. *American Industrial Hygiene Association Journal* **1984**, *45*, 509.

(237) Weber, W. J.; Morris, J. C. *J. Sanit. Eng. Div. Am. Soc. Civ. Eng.* **1963**, *89*, 31.

(238) Walker, G. M.; Weatherley, L. R. *Water Research* **1999**, *33*, 1895.

(239) Vasudevan, P.; Padmavathy, V.; Dhingra, S. C. *Bioresource Technology* **2003**, *89*, 281.

(240) Sarkar, M.; Acharya, P. K.; Bhattacharya, B. *Journal of Colloid and Interface Science* **2003**, *266*, 28.

(241) Palanichamy, M. S.; Joseph, B.; Chandran, S. *Indian J. Env. Prot.* **1994**, *14*, 591.

(242) Özcan, A.; Öncü, E. M.; Özcan, A. S. *Colloids and Surfaces A: Physicochemical and Engineering Aspects* **2006**, *277*, 90.

(243) Ho, Y. S.; Ng, J. C. Y.; McKay, G. *Separation and Purification Methods* **2000**, *29*, 189.

(244) Ho, Y. S.; McKay, G. *Water Research* **2000**, *34*, 735.

(245) Weber Jr, W. J.; Liu, K. T. *Chemical Engineering Communications* **1980**, *6*, 49.

(246) Weber Jr, W. J. *Journal of Environmental Engineering* **1984**, *110*, 899.

(2247) Mattson, J. A.; Mark Jr, H. B.; Malbin, M. D.; Weber Jr, W. J.; Crittenden, J. C. *Journal of Colloid and Interface Science* **1969**, *31*, 116.

(248) Bose, P.; Aparna Bose, M.; Kumar, S. *Advances in Environmental Research* **2002**, *7*, 179.

(249) Gupta, V. K.; Carrott, P. J. M.; Ribeiro Carrott, M. M. L.; Suhas *Critical Reviews in Environmental Science and Technology* **2009**, *39*, 783.

(250) Park, D.; Yun, Y. S.; Park, J. M. *Biotechnology and Bioprocess Engineering* **2010**, *15*, 86.

(251) Brierley, C. L.; Brierley, J. A. *Biohydrometallurgical Technologies* **1993**, *2*, 35.

(252) Bedell, G. W.; Darnall, D. W. *Biosorption of Heavy Metals* **1990**, 313.

(253) Roberts, E. J.; Rowland, S. P. *Environmental Science and Technology* **1973**, *7*, 552.

(254) Maniruzzaman, M.; Rahman, M. A.; Gafur, M. A.; Fabritius, H.; Raabe, D. *Journal of Composite Materials* **2012**, *46*, 79.

(255) Lasheen, M. R.; Ammar, N. S.; Ibrahim, H. S. *Solid State Sciences* **2012**, *14*, 202.

(256) Jianlong, W. *Process Biochemistry* **2002**, *37*, 847.

(257) Feng, N.; Guo, X.; Liang, S.; Zhu, Y.; Liu, J. *Journal of Hazardous Materials* **2011**, *185*, 49.

(258) Azlan, K.; Wan Saime, W. N.; Lai Ken, L. *Journal of Environmental Sciences* **2009**, *21*, 296.

(259) Abia, A. A.; Horsfall Jr, M.; Didi, O. *Bioresource Technology* **2003**, *90*, 345.

(260) Martel, B.; Le Thuaut, P.; Crini, G.; Morcellet, M.; Naggi, A. M.; Maschke, U.; Bertini, S.; Vecchi, C.; Coqueret, X.; Torri, G. *Journal of Applied Polymer Science* **2000**, *78*, 2166.

(261) Le Thuaut, P.; Martel, B.; Crini, G.; Maschke, U.; Coqueret, X.; Morcellet, M. *Journal of Applied Polymer Science* **2000**, *77*, 2118.

(262) Hashem, A.; Abou-Okeil, A.; El-Shafie, A.; El-Sakhawy, M. *Polymer - Plastics Technology and Engineering* **2006**, *45*, 135.

(263) Chen, S.; Wang, Y. *Journal of Applied Polymer Science* **2001**, *82*, 2414.

(264) Chao, A. C.; Shyu, S. S.; Lin, Y. C.; Mi, F. L. *Bioresource Technology* **2004**, *91*, 157.

(265) Manjusha1, A.; Gandhi, N.; Sirisha, D. *International Journal of Pharma world research* **2012**, *2*, 1.

(266) Devi Prasad, A.G.; Mohammed abdul salam Abdullah, *Journal of Applied Sciences in Environmental Sanitation* **2009**, *4*, 273.

(267) Koel Banerjee, S. T.; Ramesh, R.; Gandhimathi, P. V.; Bharathi, K.S. *Iranica Journal of Energy & Environment* **2012**, *3***,** 143.

(268) Nassar, M. M.; Hamoda, M. F.; Radwan, G. H. *Water Science and Technology* **1995**, *32*, 27.

CHAPTER 2

MATERIALS AND METHODS

Introduction

This chapter provides a brief summary of materials and synthetic methods employed in this thesis.

2.1. Commercially purchased chemicals:

All inorganic salts: zinc nitrate ($Zn(NO_3)_2$), cobalt nitrate ($Co(NO_3)_2.6H_2O$), ammonium cerium (IV) nitrate ($(NH_4)_2Ce(NO_3)_6$), copper nitrate hexahydrate ($Cu(NO_3)_2.6H_2O$), nickel nitrate hexahydrate ($Ni(NO_3)_2.6H_2O$), silver nitrate ($AgNO_3$), hydrogen tetrachloroaurate trihydrate ($HAuCl_4.3H_2O$), sodium borohydride ($NaBH_4$) and polyvinylpyrrolidone (PVP), 2,4,6 - trichlorophenol (TCP), *p* - chlorophenol (PCP), phenol and *p* - nitrophenol (PNP), Alcian blue (AB), coomassie brilliant blue G - 250 (BB), neutral red (NR) and methylene blue (MB), sodium arsenite ($NaAsO_2$), potassium dichromate ($K_2Cr_2O_7$), lead nitrate ($Pb(NO_3)_2$) and nickel nitrate hexahydrate ($Ni(NO_3)_2.6H_2O$), manganese nitrate tetrahydrate ($Mn(NO_3)_2.4H_2O$), hydrochloric acid (HCl), methanol (CH_3OH), Sodium hydroxide (NaOH), sodium citrate, victoria blue and bromophenol blue were purchased from Sigma-Aldrich and used without further purification. Deionized water was used for all syntheses. Stock solutions were prepared by dissolving stoichiometric amounts of corresponding chemical.

2.2. Synthesis of materials

2.2.1. Preparation of biopeel adsorbent

Apple, tomato, kiwi, longan, hamimelon, avacado and dragon fruits were bought from local supermarket and the outer layer was carefully peeled off and cut into small pieces of around 0.04 cm^2 in size. Raw peels were saponified with NaOH to cleave ester bonds and generate more hydoxyl groups. Deionized water washings were given to remove excess base. Washed peels were then sonicated in 2-propanol to extract leachable organics. The resulting adsorbent was washed with water and dried.

2.2.2. Immobilization of apple peel

Zr(IV) (0.1 M) solution was prepared by dissolving $ZrOCl_2.8H_2O$ (3.22g) in deionised water (100 mL). Dried apple peel (5 g) was added to Zr solution (100 mL, 0.1 M) and left it for 6 h at room temperature at neutral pH. The Zr-loaded apple peel was then washed with copious amounts of water to remove excess ions from the surface. The peel was dried and used for characterizations and adsorption studies. This study was focused on the water treatment using Zr immobilized apple peels. All chemicals and reagents used were AR grade and purchased from Sigma Aldrich.

2.2.3. Synthesis of gold and silver nanoparticles

Stable gold and silver nanoparticles in aqueous solution were prepared by reduction of corresponding salts with $NaBH_4$. PVP / trisodiumcitrate (100 mg) dissolved in water (3 mL) and $HAuCl_4.3H_2O$ / $AgNO_3$ (500µl of 100 mM) solution was added to water (50 ml) under magnetic stirring at room temperature. $NaBH_4$ (10 mg) dissolved in water (3 ml) was added drop wise to the stirring solution. The initial colourless solution became dark red in case of Au, grey for Ag respectively, which indicated the formation of nanoparticles. The solution was left to stir for a day before it was being diluted to 200ml to make the concentration of nanoparticle solution $2.5x10^{-4}$ M. Same concentration ($2.5x10^{-4}$ M) of citrate capped nanoparticles were prepared in the similar manner.

2.2.4. Synthesis of Eggshell membrane (ESM) composites

Fresh eggs from local supermarket were gently broken and washed with water to remove the albumin and yolk. The membrane was carefully peeled from eggshells and cleaned with deionized water. The clean ESM (100 mg) was dried in air at ambient conditions, cut into small pieces and immersed in $HAuCl_4$ or $AgNO_3$ (10.0 mL, 5 mM) solution for 2 h. It is conceivable that the reaction was initiated by adsorption of the charged Au (III) or Ag (I) ions onto the surface of ESM followed by the reduction of metal ions to Au or Ag atoms and deposited as NPs on the ESM surface. The yellow $HAuCl_4$ solution was slowly decolorized and the

white ESM was turned to light red colour in case of gold and grey colour for silver. Ag ions require relatively longer time (48 h) for reduction on ESM surface. The NP immobilized ESMs (NP-ESMs) were removed from the solutions after 12 h and rinsed with copious amounts of deionised water to remove excess non-reduced metal salts. The NP-ESMs were air-dried at ambient conditions for further characterization.

2.2.5. Synthesis of metal oxides

Preparation of metal oxides using ESM template: Fresh eggs from local supermarket were gently broken and washed with water to remove the egg white and yolk. The eggshell membrane (ESM) was carefully removed by immersing eggshells in HCl (100 mL, 2 M) and rinsed with deionized water. The ESM was immersed in metal salt solutions (10 mL, 0.02 M) for about 12 h at room temperature. The ESM composites were taken out, rinsed with deionized water and dried at room temperature. Certain amount of ESM composites were placed in porcelain crucible and calcined at a heating rate of 0.5 °C / min upto 750 °C for 3 hr. The resulting powders (metal oxides) were stored at room temperature and used for further characterization.

2.3. Characterization methods

X-ray diffraction (XRD) pattern of the samples were recorded using Bruker - AXS: D8 DISCOVER with GADDS Powder X-ray diffractometer with Cu-K_α (λ = 1.5418 Å) at 40 kV and 40 mA over a range of 2θ angle 2° to 80° using a step size of 1°. Surface structures of the peel were captured using Field Emission Scanning Electron Microscopy (JEOL JSM-6701F). Dried apple peels were coated with platinum metal before SEM analysis to make the surface conductive. Energy dispersive X-Ray spectroscopy (EDS) was done in conjunction with SEM to investigate the chemical composition of the apple peel. The IR spectra were recorded in the range of 4000 - 400 cm^{-1} using a Bruker ALPHA FT-IR Spectrophotometer with a resolution of 4.0 cm^{-1}. Specimens were first mixed with KBr powder and then grounded in an agate mortar. The mixture was pressed at 10

tons for 5 min to form a 100 mg disk using a KBr press model MP-15. 20 scans were used for each spectrum. Thermogravimetric analysis (TGA) and differential thermal analysis (DTA) were conducted on TA - SDT 2960 thermal analysis system with a heating rate of 5 °C/min in N_2 atmosphere.The concentrations of pollutants of experimental and control samples were analysed using inductively coupled plasma optical emission spectroscopy (ICP-OES), which was carried out using the Dual-view Optima 5300 DV ICP-OES system, for arsenic (III, V) and chromium (VI). The ion-exchange chromatography was employed using the 818 IC Pump, 820 Separation Center, 830 Interface, 833 Liquid handling Unit, 732 Detector and 813 Compact auto sampler for phosphate. Surface elements of the peels were identified using X-ray photo electron spectroscopy (XPS) with a spatial resolution of 30 µm (Kratos XPS system– Axis His –165 Ultra, Shimadzu, Japan). The C1s signal of an adventitious carbon was used as reference to compensate for charging effect at a binding energy (BE) of 284.8 eV. The XPS results were collected in binding energy form and fit using a non-linear least-square curve fitting program (XPSPEAK41 Software). The peak's full-width-at-half-maximum (FWHM) was fixed during the fitting. NPs were observed with JEOL 2010-F Field Emission Transmission Electron Microscope (FETEM). Size and zeta potential measurements of synthesized NPs were done using Malvern Zetasizer Nano-ZS90. The quantitative measurements of NPs were carried out using a UV-Vis spectrophotometer (Shimadzu-1601 PC spec-trophotometer). The amount of pollutant in the spiked solution before and after adsorption was quantified by HPLC-UV (Agilent 1200) with C18 inverse phase (3.9 x 150mm) column. Mobile phase was a mixture of water/methanol (60:40) injected in at a rate of 0.7ml/min. Carbon, Hydrogen, Nitrogen and Sulphur (CHNS) Analysis: Instrumentation includes includes Elementar Vario Micro Cube.

2.4. Batch adsorption studies

2.4.1. Effect of initial adsorbate concentration and time

Adsorbent (0.1g) was added to solutions (10 mL) of different concentrations of pollutants. All adsorption experiments were carried at 30 °C using an orbital

shaker at 200 rpm. The residual concentration of pollutants were analysed after predetermined interval of time until the system reached equilibrium. The pollutant adsorbed at equilibrium q_e (mg/g) was calculated by using the following equation

$$q_e = (C_0 - C_e)\, V/M \qquad (2.\ 1)$$

Where C_0 and C_e (mg / L) are concentrations of pollutant at initial stage and equilibrium conditions respectively, V (L) is volume of the pollutant solution and M (g) is the mass of the adsorbent used. The initial concentrations of pollutant solution tested were 5, 10, 20, 40, 70, 100 and 200 mg / L and the experiments were carried out at 303 K for 24 h.

2.4.2. Kinetic and isotherm studies

Samples consisting of a portion (0.1 g) of the adsorbent material and various initial pollutant concentrations of 5 - 200 mg / L were taken in the conical reaction flask. Flasks were agitated using an orbital shaker at 200 rpm at 30 °C. The time required to reach equilibrium was maintained as determined by equilibrium studies. The equilibrium adsorption isotherms and kinetics for all pollutants were studied using Langumir and Freundlich models. The adsorption mechanism of different pollutants onto the adsorbent was proposed by studying kinetics of adsorption.

2.4.3. Effect of solution pH

The solution pH effect on pollutant removal was studied by varying the pH from 2 to 12, where the pH was adjusted by adding either 0.01N HCl or 0.01N NaOH. The initial concentration used was 100 mg / L for TCP, PCP, phenol, AB, Pb^{+2} and Ni^{+2}, 20 mg / L for PNP, As^{+3}, Cr^{+6}, BB, NR and MB. Other parameters like adsorbent dosage, agitation speed and solution temperature were kept constant. The percentage removal of pollutant was calculated as:

$$\text{Removal}\,\% = \left(\frac{C_i - C_f}{C_i}\right) 100 \qquad (2.\ 2)$$

Where C_i and C_f (mg/ L) are initial and final concentration of pollutants in the water respectively

2.4.4. Desorption studies

Samples were prepared by adding adsorbent (0.01g) to solution (10 mL) of double distilled water. The solutions were equilibrated for different time periods and stirred constantly. Desorption studies were conducted at different pH and samples were analysed at different time intervals. The concentrations of organic pollutants were measured with a UV-Vis spectrophotometer and that of heavy metal ions with ICP-OES. Each experiment was repeated under identical conditions to check reproducibility.

CHAPTER 3

EVALUATION OF BIOPEELS AS EFFICIENT ADSORBENTS AGAINST VARIOUS POLLUTANTS

3.1. Introduction

A major problem that is faced by many countries around the world is the lack of safe and clean drinking water. Although there has been improvement to the access of safe drinking water in the world, there are still approximately one billion people who suffer deprivation.[1] Water is an essential part of life, without which humans cannot sustain life. In addition, aquatic life is also severely affected by the absence of clean water. With the increase in industrial activities due to urbanization, industrial waste water effluents containing pollutants such as heavy metal ions like Pb^{2+}, Ni^{2+} and $Cr_2O_7^{2-}$ are discharged to the ecosystem. This intensifies the condition of environmental pollution which poses potential hazard to human health when consumed.[2-4] Moreover, dissolved organic pollutants such as dyes are also of concern because of their toxicity which poses a serious threat to aquatic living organisms.[5,6] There are many industries such as dyestuff, textile, paper and plastics which actively use dyes in their products.[7,8] Since most of the dyes are organic molecules which are stable and not biodegradable, it is very difficult to eliminate them from waste water.[9] Thus there is a need to address this pressing issue which led to the development of various water purification methods such as chemical coagulation, precipitation, flocculation, activated sludge formation, membrane separation and ion exchange[2,4,10,11] with the aim of remediating polluted water. However till now, there is no single efficient method which can extract and remove all the pollutants from water. Compared to conventional water purification methods, biosorption shows great potential and advantages in removing pollutants. Due to the low cost, ready availability, environmental friendliness and effectiveness in removing pollutants, research has since moved towards discovering low-cost adsorbents including natural materials, biomembranes and biowaste.[5] In recent years, there have been many reports on low-cost adsorbents which are by-products from other processes and they showed good efficiency in removal of pollutants in water. Various bioadsorbents such as banana peel,[3] orange peel,[2,12,13] grape waste, rice husk,[10,14] tea waste,[15,16] maize corn cob, sugarcane bagasse[17] and pine bark[18] were developed from agro-wastes to remove heavy metal ions. Some of these bioadsorbents (corn cob, rice husk and bagasse) were also used in the removal of dyes.[5] These findings bring good news and hope for people living in

countries where they have to depend on contaminated water from rivers and lakes for their daily water consumption. Hence in bid of the continued effort in exploring low-cost adsorbents for the removal of pollutants from water and waste water, several peels such as sweet potato, malaysia putusan, snake gourd, chow chow, dragon fruit, rock melon , gold melons, corn fibers, dragon fruit, avocado peel, carrot peel, water chesnut, hami melon, luffa peel, red bean husk, green bean husk, beansprouts hull, potato, tomato, orange, papaya, apple and fish skin were selected as potential adsorbents for the extraction of different pollutants from water. We selected few biopeels based on their higher adsorption efficiency towards various contaminants and investigated different adsorption parameters in detail. Avacado (AV), hamimelon (HM), dragon fruit (DF), longan (LO) and kiwi (KW) were shortlisted based on some practical aspects such as easy availability, economic peel processing, stability and binding ability of different pollutants. These peels were investigated for their effectiveness in removing heavy metal ions and dissolved organic compounds from water.

Longan is a tropical fruit that belongs to the soapberry family to which also the lychee belongs. Apart from being eaten fresh, it is also often used in asian soups, snacks, desserts, and sweet-and-sour foods, either fresh or dried, sometimes canned with syrup in supermarkets. Kiwifruit is native to southern China where it has been declared a National Fruit of China. The fruit and skin contains vitamins, flavonoids and actinidain. Avocado fruit is commonly found in countries such as the United States of America, Mexico, Brazil, Chile and Indonesia. Due to its nutritional values, it can be found in many cuisines such as vegetarian food and in milk shakes, ice cream and sandwiches. The popularity of the fruit leads to the high consumption of it and thus a high portion of avocado peel is produced.[19] Avocado peel contains epicatechin as shown in Figure 3.1.

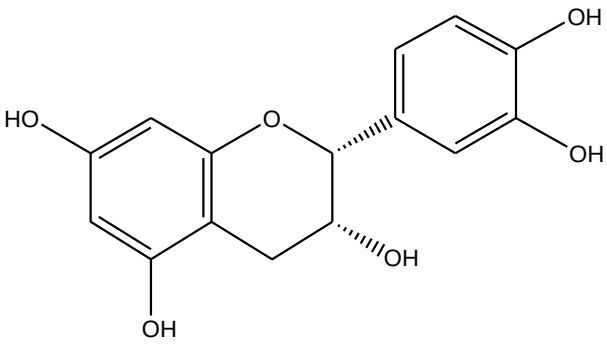

Figure 3.1. Structure of epicatechin

This implies that the avocado peel has functional groups such as -OH groups.[20] Carbonized avocado peels were used to reduce chemical oxygen demand and biological oxygen demand of waste water.[21] However, no reports exist on using avocado peels as adsorbents. Hamimelon belongs to the family of muskmelon. Muskmelon is one of the important crops which bring in economic benefits for the people living in northwestern China. Approximately four million tons of muskmelon are produced in the area every year.[22] Hamimelon is rich in nutrition, vitamins, calcium, phosphorus and iron. Due to its various health benefits, it has gained popularity in other parts of the world[23] leading to vast amounts of peels production. However there are yet to be reports on the characterization of the hamimelon peel, thus characterization of the functional groups and morphology of the peel was conducted by FT-IR and FESEM respectively. Dragon fruit is a fruit native to Mexico, Central America and South America. Currently the fruit is also cultivated in East Asia and Southeast Asia, in countries such as Indonesia, Thailand, Vietnam, Thailand, the Philippines and Sri Lanka. Dragon fruit is a well-liked fruit by many due to its high amount of Vitamin C and it is a good source of antioxidants.[24]It can also be processed into a variety of food products such as juice, jam, syrup, jelly and candy. Thus the waste dragon fruit peel becomes an attractive candidate as an adsorbent due to its low cost and availability. Its peel contains pectin with functional groups such as –OH and –COOH.[25] In addition to the free carboxyl groups, pectin also contains methylated ester groups in its polymeric chain.[26] These functional groups show great potential in binding the pollutants, especially the cationic ones. In order to test the effectiveness of the peels as adsorbents for pollutants, extractions of heavy

metal ions (Pb^{2+}, Ni^{2+} and $Cr_2O_7^{2-}$) and dyes (Alcian Blue, Methylene Blue, Neutral Red and Brilliant Blue) from water were investigated and analyzed.

3.2 Results and Discussion

3.2.1 Characterization of biosorbents

IN order to remove soluble components, raw peels were washed with water, NaOH and followed by isopropanol (Chapter 2). The chemical constituents of the five peels were studied using the FT-IR and the spectra of the all peels in the range of 4000 to 400 cm^{-1} are shown in Figure 3.2.

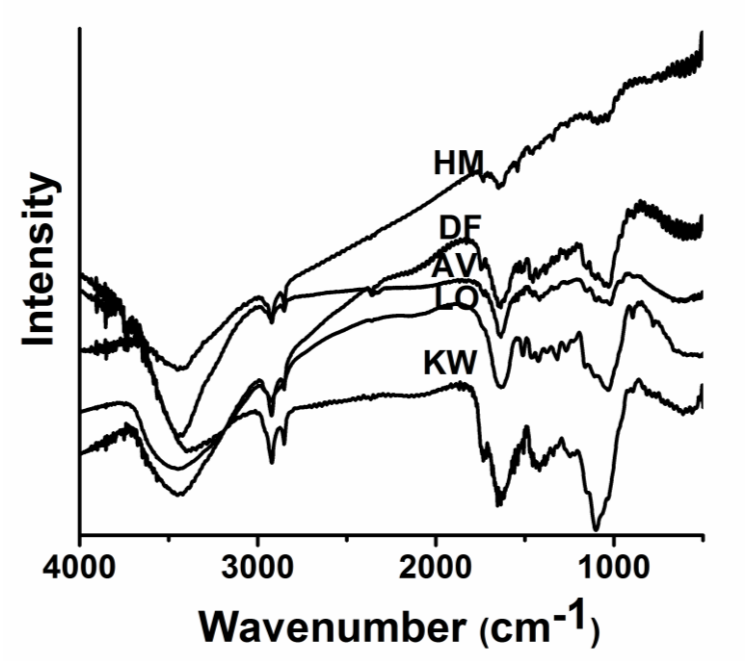

Figure 3.2. FT-IR spectra of avocado, hamimelon, dragon fruit, longan and kiwi peels.

The broad band observed in the range of 3200 – 3650 cm^{-1} for all five peels matches the O-H stretching of phenols which is usually in the range of 3200 and 3700 cm^{-1}. In addition, it corresponds to the O-H vibration of carboxylic acids which is in the range of 3400 and 2400 cm^{-1}. The sharp peaks at 2928 cm^{-1}, 2921 cm^{-1} and 2926 cm^{-1} observed in the spectra for biopeels correspond to the sp^3 C-H stretch. Sharp peaks at 1747 cm^{-1} for avocado peel and 1754 cm^{-1} for hamimelon peel were seen due to the C=O stretch in esters or carboxylic acids. The peaks in the ranges of 1680 – 1610 cm^{-1} correspond to the stretching of C=C bond in aromatic rings for all five peels. The absorptions in the range of 1300 – 1000 cm^{-1} due to angular deformation in the

plane of the C-H bonds of aromatic rings and in the range of 1200 – 1000 cm^{-1} due to the axial bonding of the C-O bond in phenols can be observed for avocado peel, kiwi and dragon fruit peel.

To elucidate the functional groups involved in the adsorption of pollutants, the FTIR spectra of a few peels were recorded after adsorption. We did not observe any significant differences in the positions of peaks in the spectrum when the spectra before and after adsorption of pollutants were compared (Figure 3.3). This is probably due to the complexity of bio peels which contain different chemical constituents including lignin, hemicellulose, cellulose, carbohydrates, proteins and other phenolic compounds. All these contain hydroxyl and carboxyl groups in majority which is responsible for the binding of different pollutants.

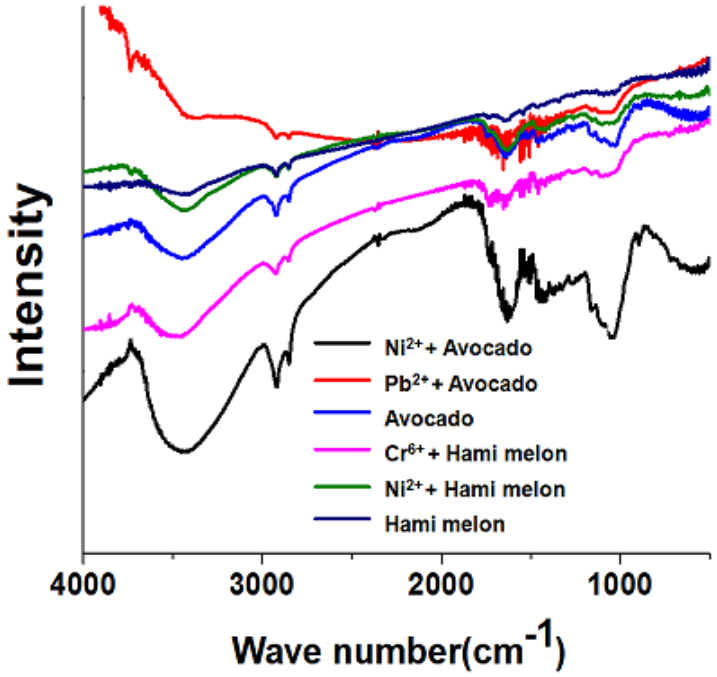

Figure 3.3. FT-IR spectra of avocado peel and hami melon peel before and after adsorption of pollutants.

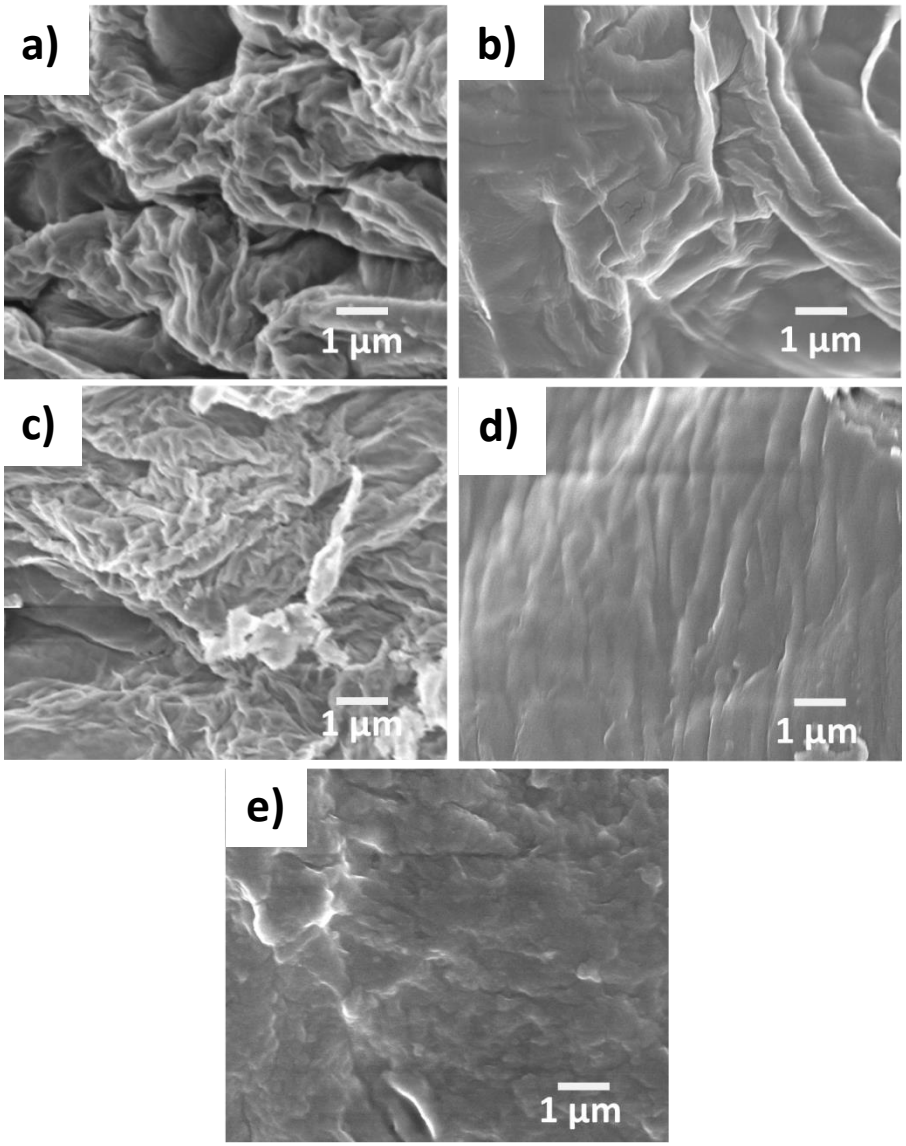

Figure 3.4. FESEM images of the surface of treated avocado (a), hami melon (b), dragon fruit (c), longan (d) and kiwi (e) peels.

Studies of the peel surface topography can aid in providing important information on the level of interfacial adhesion that could possibly exist between the peels and the pollutants. In the SEM images surfaces of the washed peels appear rough and irregular with fiber like morphologies (Figure 3.4). This rough texture is suitable for surface adsorption of the pollutants and fibers provide a higher surface area that aid in adsorption.[27] Further, the composition of all peels were evaluated using CHNS analyzer which has been provided in Table 3.1.

Table 3.1. CHNS analysis data of different biosorbents.

Bio peel	Carbon (wt %)	Hydrogen (wt %)	Nitrogen (wt %)	Sulphur (wt %)
Avocado	46.38	5.67	0.94	<0.50
Hami melon	39.35	5.14	<0.50	<0.50
Dragon fruit	33.14	4.66	1.29	0.58
Longan	33.60	4.06	<0.50	<0.50
Kiwi	44.05	5.46	0.82	<0.50

From Table 3.1, it can be observed that reasonable amounts of carbon (C) and hydrogen (H) were detected in peels and the amount of nitrogen (N) present was comparatively low. The observation is in line with the functional groups present in the treated peels, indicating that there are little or no amino groups present as seen in the IR analysis. These higher hydroxyl and carboxylic functionalities are responsible for binding pollutants. We can expect that these biopeels can adsorb cationic pollutants more efficiently than anions.

3.2.2. Effects of initial pollutant concentration and contact time

All biopeels were evaluated for their binding ability of different pollutants. Graphs of the adsorption uptake (q_t) against the contact time for the different pollutants for the five peels at room temperature are shown in Figure 3.5. From the plots, it is noted that the adsorption capacity of the pollutants in mg g^{-1} increased with increasing contact time up to 30 min and a plateau was observed, indicating equilibrium was reached. This implies that the adsorption process was rapid (30 min) and gradually decreased as time progress and finally attained saturation when equilibrium was reached.[28] High adsorption values were obtained for the adsorption of cationic dyes (Alcian blue and Methylene blue) and all five peels tend to bind cationic dyes more favorably than anionic (BB) and neutral dyes (NR). This might be due to the presence of phenoxide groups and carboxylate groups ($-COO^-$) which were obtained after

the alkaline wash of the peels. Electrostatic forces of attraction between the oppositely charged ions may be present which aid in the binding process. Similar observations were seen for the heavy metal ions where the cationic ions (Pb^{2+} and Ni^{2+}) showed higher adsorption values compared to the chromate ions. It is worth mentioning that all five peels showed good adsorption for Ni^{2+}. The adsorption values for chromium (VI) ions were rather high for avocado peel compared to other biopeels. Chromium (VI) exists as oxoanions in water. The adsorption might take place due to an esterification reaction between the functional groups of epicatechin found in avocado peel, specifically the 1,2-directing phenolic groups, and $HCrO_4^-$ ions.[29] This led to a higher amount of chromium(VI) ions being removed by the avocado peel. Also, adsorption of metal ions was faster than dyes which may be due to the higher mobility and charge density of metal cations. It was observed that the adsorption capacity for dragon fruit peel for the cationic pollutants was higher than other peels. In addition to the carboxylate ions present, this might be due to the methyl ester groups present in pectin of dragon fruit peel which underwent base hydrolysis with the sodium hydroxide solution during peel processing and gets converted into carboxylate groups.[26] The high percentage of carboxylate groups favoured the binding of cationic pollutants more than the anionic ones. Alcian blue is more cationic than other pollutants and showed highest adsorption on the surface of peels. This observation leads to the conclusion that adsorption of pollutants involve electrostatic interaction between adsorbent and adsorbate.

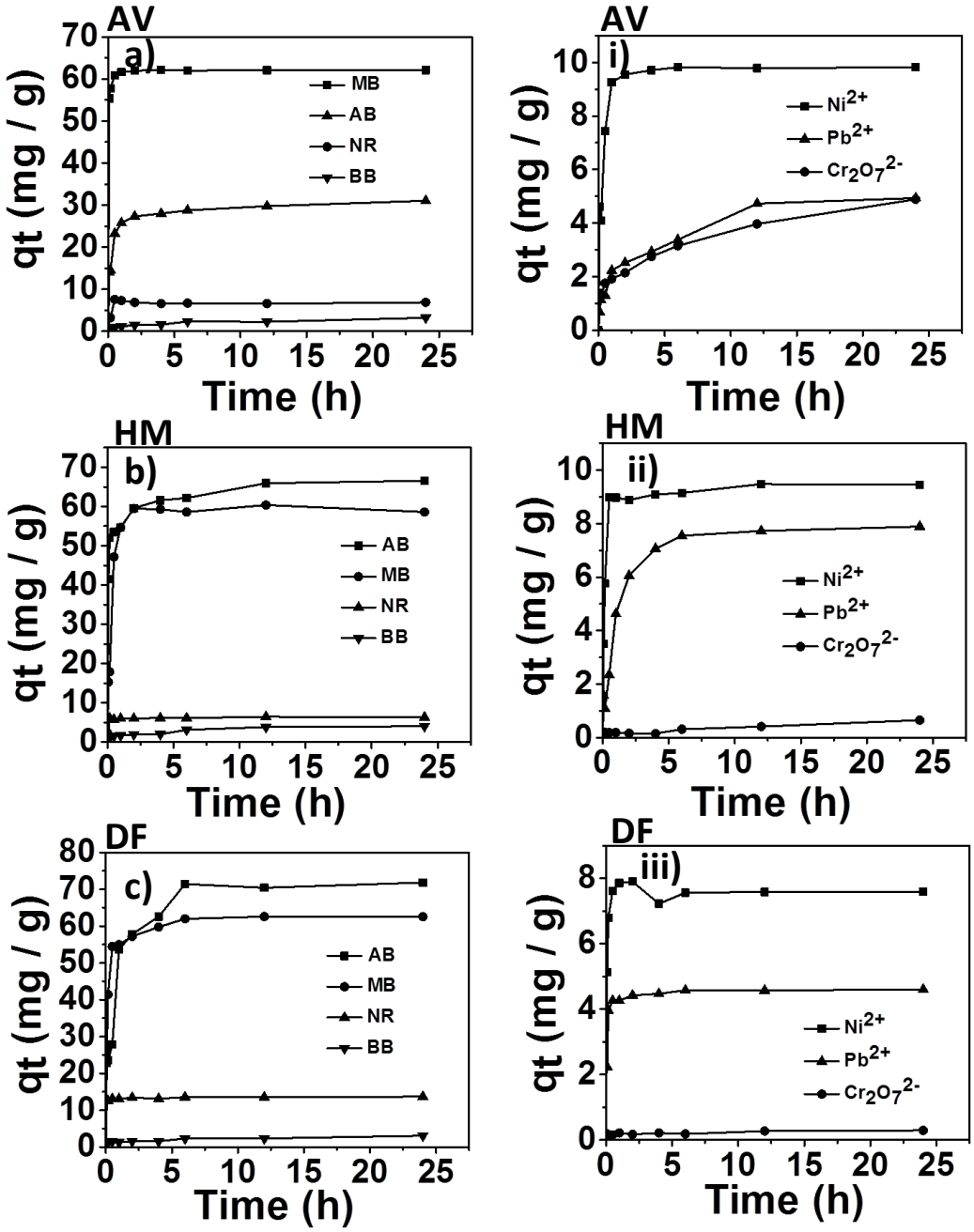
AV
a)
MB
AB
NR
BB
qt (mg / g)
Time (h)
AV
i)
Ni^{2+}
Pb^{2+}
$Cr_2O_7^{2-}$
qt (mg / g)
Time (h)
HM
b)
AB
MB
NR
BB
qt (mg / g)
Time (h)
HM
ii)
Ni^{2+}
Pb^{2+}
$Cr_2O_7^{2-}$
qt (mg / g)
Time (h)
DF
c)
AB
MB
NR
BB
qt (mg / g)
Time (h)
DF
iii)
Ni^{2+}
Pb^{2+}
$Cr_2O_7^{2-}$
qt (mg / g)
Time (h)

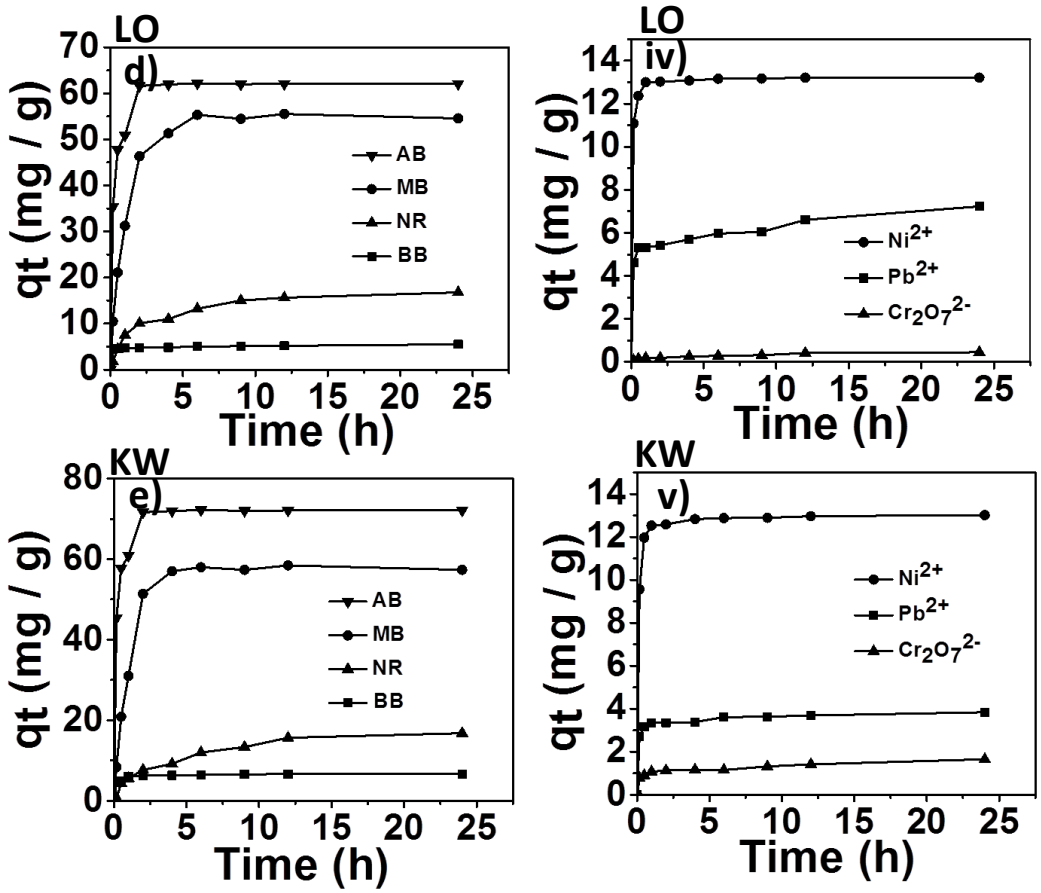

Figure 3.5. Variation of adsorption capacity of dyes (a, b, c, d and e) and heavy metal ions (i, ii, iii, iv and v) for avocado (a, i), hamimelon (b, ii), dragon fruit (c, iii), longan (d, iv) and kiwi (e, v) peels.

3.2.3. Effect of pH on the adsorption of different pollutants

The plots of the percentage removal of the different pollutants for the different peels against pH at room temperature are shown in Figure 3.6. For cationic pollutants (Pb^{2+}, Ni^{2+}, Alcian blue and Methylene blue) and Neutral red, it was observed that the percentage removal of pollutants increased with increasing pH. This might be due to the presence of electrostatic attraction of oppositely charged ions involved in the adsorption process. At low pH values (acidic medium), there was an excess of mobile H^+ ions present and there might be competition faced between H^+ and the cationic pollutants for the adsorption sites which led to the decrease in adsorption. The adsorbent surface could also become positively charged due to the presence of the high concentration of H^+ ions.[28] However as the pH values increased, adsorption also increased due to the decrease in H^+ ions and presence of more negatively charged adsorption sites leading to increased ionic interactions.[30,31] For anionic pollutants

(Brilliant blue and $Cr_2O_7^{2-}$) high percentage removal was attained at low pH values. This could indicate that at lower pH where the concentration of H^+ was high, the positively charged adsorbent surface might attract the negatively charged pollutants due to electrostatic forces of attraction. It should be noted that chromate ions exist in two forms, $HCrO_4^-$ and CrO_4^{2-} ions in aqueous solution. The $HCrO_4^-$ ions are stable and dominant at pH values lower than 5.[32]Thus adsorption happens due to electrostatic attraction between the adsorbent and anions. The adsorption behavior of all peels towards different pollutants at different pH was almost same.

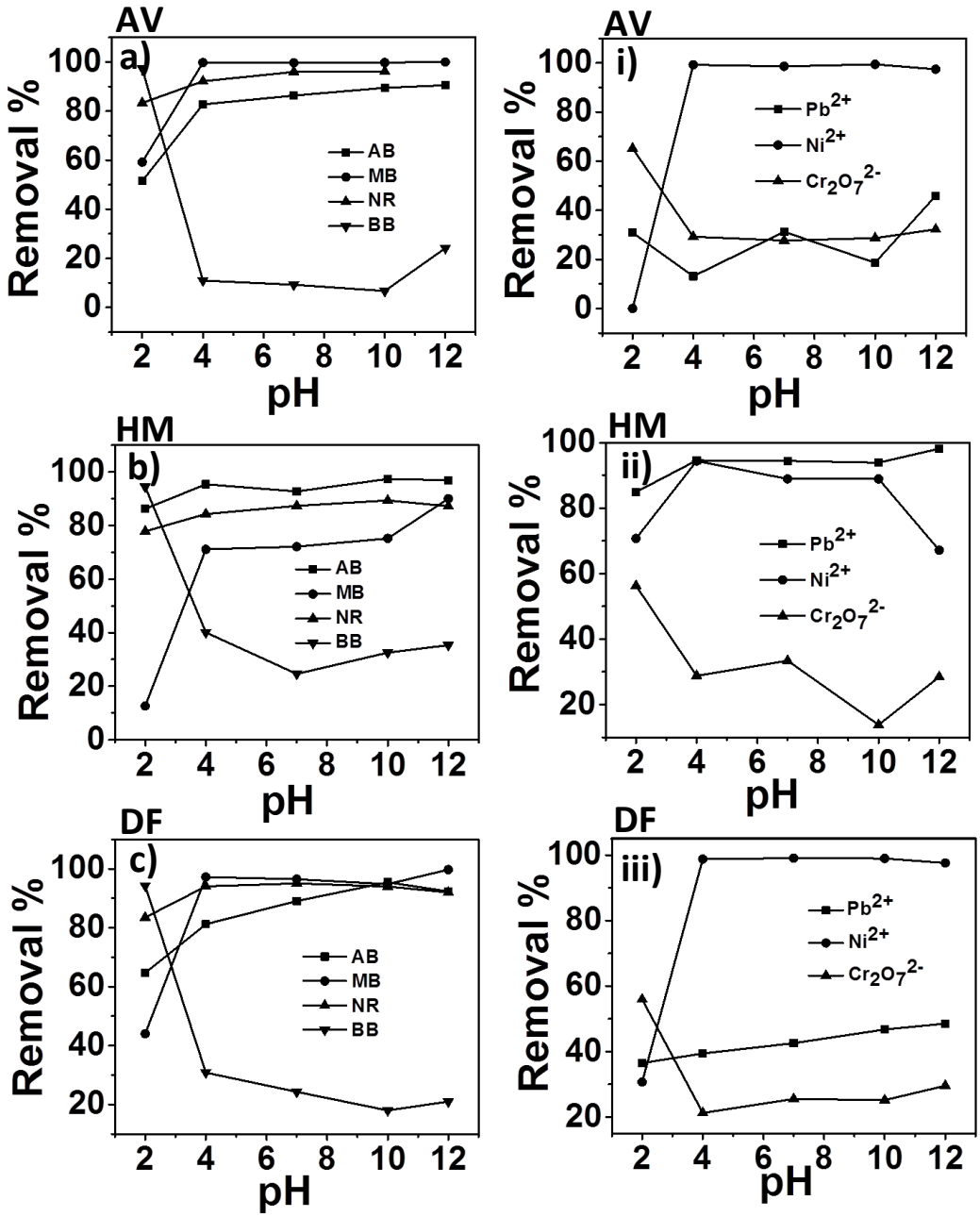

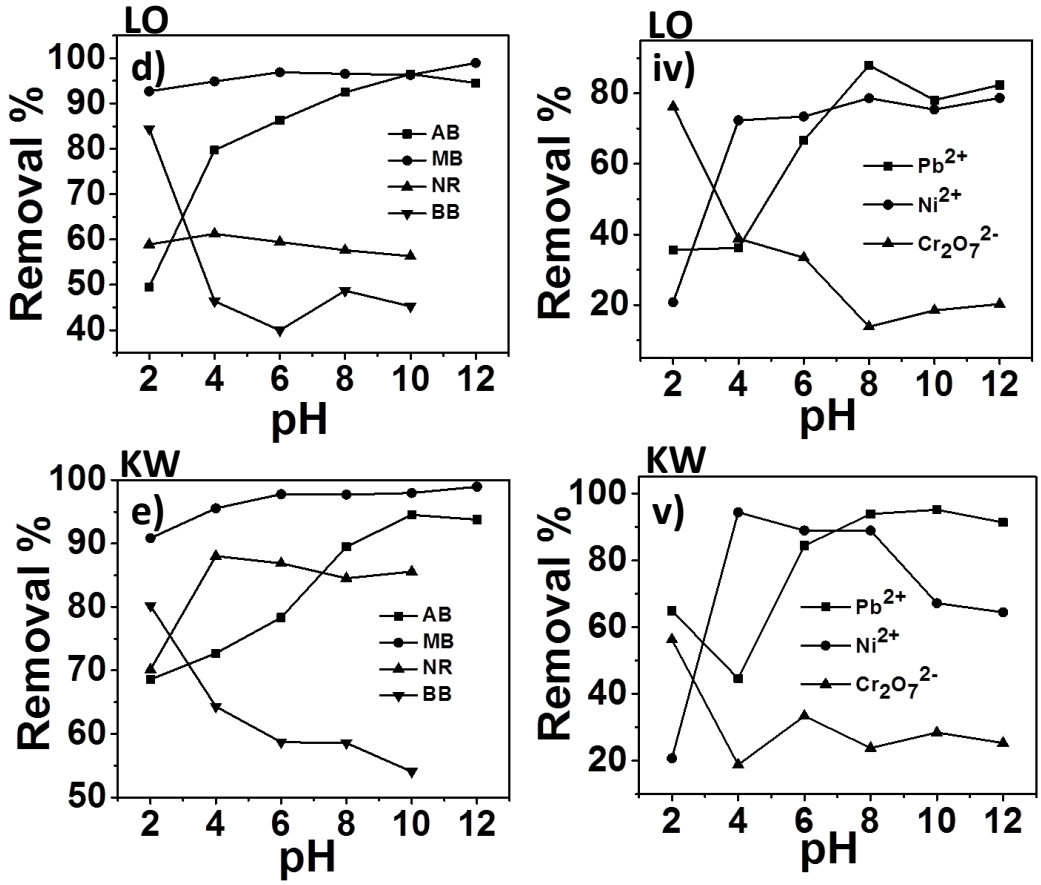

Figure 3.6. Effect of pH on adsorption capacity of dyes (a, b, c, d and e) and heavy metal ions (i, ii, iii, iv and v) for avocado (a, i), hamimelon (b, ii), dragon fruit (c, iii), longan (d, iv) and kiwi (e, v) peels.

3.3. Conclusion

We reported, five novel biopeels:- namely avocado peel, hami melon peel, longan, kiwi and dragon fruit peel which had been studied for their effectiveness in the removal of pollutants in water. The adsorption of various pollutants was evaluated and adsorption studies were conducted to aid in the proposal of the adsorption mechanism. The extraction efficiency was optimised by varying factors such as pH of solution and contact time. The maximum adsorption capacities of different biopeels towards various pollutants were shown in Table 3.2. The results clearly indicate that all biopeels adsorb cationic pollutants (AB, MB, Ni^{2+}) more efficiently than anionic pollutants (BB, $Cr_2O_7^{2-}$).

Table 3.2. Maximum adsorption capacities (mg/g) of different pollutants using biopeels

Bio peel	Adsorption capacities (mg /g)						
	AB	**MB**	**NR**	**BB**	**Pb^{2+}**	**Ni^{2+}**	**$Cr_2O_7^{2-}$**
Avocado	31.04	62.11	6.88	3.23	4.93	9.82	4.89
Hami melon	66.55	58.60	6.31	4.03	7.89	9.45	0.65
Dragon fruit	71.85	62.58	13.68	3.06	4.60	7.59	0.29
Longan	72.11	57.34	16.77	6.64	3.84	13.02	1.65
Kiwi	62.11	54.58	16.77	5.50	7.23	13.21	0.45

To improve the adsorption of anionic pollutants, the functional groups on the three peels can be modified for example, by embedding Zr onto the peel.[43] All five peels showed good potential to be used as efficient and effective adsorbents for the treatment of water and they may have future applications in the purification of water in many parts of the world.

3.4. References

(1) The Millennium Development Goals Report, United Nations, New York 2008

(2) Mohanty, K.; Das, D.; Biswas, M. N. *Chemical Engineering Journal* **2005**, *115*, 121.

(3) Hossain, M. A.; Kumita, M.; Michigami, Y.; Mori, S. *Adsorption* **2005**, *11*, 561.

(4) Veglio, F.; Beolchini, F. *Hydrometallurgy* **1997**, *44*, 301.

(5) Crini, G. *Bioresource Technology* **2006**, *97*, 1061.

(6) Gulnaz, O.; Kaya, A.; Matyar, F.; Arikan, B. *Journal of Hazardous Materials* **2004**, *108*, 183.

(7) O'Neill, C.; Hawkes, F. R.; Hawkes, D. L.; Lourenço, N. D.; Pinheiro, H. M.; Delée, W. *Journal of Chemical Technology and Biotechnology* **1999**, *74*, 1009.

(8) Vandevivere, P. C.; Bianchi, R.; Verstraete, W. *Journal of Chemical Technology and Biotechnology* **1998**, *72*, 289.

(9) Barragán, B. E.; Costa, C.; Carmen Márquez, M. *Dyes and Pigments* **2007**, *75*, 73.

(10) Kumar, U.; Bandyopadhyay, M. *Bioresource Technology* **2006**, *97*, 104.

(11) Nawar, S. S.; Doma, H. S. *Science of The Total Environment* **1989**, *79*, 271.

(12) Biswas, B. K.; Inoue, K.; Ghimire, K. N.; Ohta, S.; Harada, H.; Ohto, K.; Kawakita, H. *Journal of Colloid and Interface Science* **2007**, *312*, 214.

(14) Adak, A.; Pal, A.; Bandyopadhyay, M. *Colloids and Surfaces A: Physicochemical and Engineering Aspects* **2006**, *277*, 63.

(15) Malkoc, E.; Nuhoglu, Y. *Journal of Hazardous Materials* **2005**, *127*, 120.

(16) Malkoc, E.; Nuhoglu, Y. *Chemical Engineering Science* **2006**, *61*, 4363.

(17) Garg, U. K.; Kaur, M. P.; Garg, V. K.; Sud, D. *Journal of Hazardous Materials* **2007**, *140*, 60.

(18) Al-Asheh, S.; Banat, F.; Al-Omari, R.; Duvnjak, Z. *Chemosphere* **2000**, *41*, 659.

(19) Ray, P. K. *Breeding Tropical and Subtropical fruits*, Narosa Publishing House, New Delhi, India, **2002**, *XVI*, 338.

(20) http://www.answers.com/topic/chemical-composition-of-avocado-1

(21) Devi, R.; Singh, V.; Kumar, A. *Bioresource Technology* **2008**, *99*, 1853.

(22) http://aciar.gov.au/files/node/2249/p105chapter1.pdf#page=38

(23) http://www.chinaculture.org/gb/en_aboutchina/2003-09/24/content_22024.htm

(24) http://www.naturalfoodbenefits.com/display.asp?CAT=1&ID=41

(25) Tang, P.Y.; Wong, C. J.; Woo, K. K. *Asian Journal of Biological Sciences* **2011**, *4*, 189.

(26) Dhakal, R. P.; Ghimire, K. N.; Inoue, K. *Hydrometallurgy* **2005**, *79*, 182.

(27) Haris, M.R.H.M.; Sathasivam, K. *American Journal of Applied Science* **2009**, *6*, 1690.

(28) Salleh, M. A. M.; Mahmoud, D. L.; Awang Abu, N. A. B.; Abdul Karim, W. A. W.; Idris, A. B. *Journal of Purity, Utility Reaction and Environment*, **2012**, *1*, 472.

(29) Chand, R.; Narimura, K.; Kawakita, H.; Ohto, K.; Watari, T.; Inoue, K. *Journal of Hazardous Materials* **2009**, *163*, 245.

(30) Mallampati, R.; Valiyaveettil, S. *RSC Advances* **2012**, *2*, 9914.

(31) Homagai, P. L.; Ghimire, K. N.; Inoue, K. *Bioresource Technology* **2010**, *101*, 2067.

(32) Nakajima, A.; Baba, Y. *Water Research* **2004**, *38*, 2859.

(33) Langmuir, I. *The Journal of the American Chemical Society* **1916**, *38*, 2221.

(34) Langmuir, I. *The Journal of the American Chemical Society* **1918**, *40*, 1361.

(35) Gadd, G. M. *Journal of Chemical Technology & Biotechnology* **2009**, *84*, 13.(36) Hall, K.R.; Eagleton, L.C.; Acrivos, A.; Vermeulen, T. *Industrial and Engineering Chemistry Fundamentals* **1966**, *5*, 212.

(36) Hall, K. R.; Eagleton, L. C.; Acrivos, A.; Vermeulen, T. *Industrial & Engineering Chemistry Fundamentals* **1966**, ***5***, 212.

(37) Freundlich, H.M.F. *Journal of physical chemistry* **1906**, *57*, 385.

(38) Redlich, O.; Peterson, D. L. *The Journal of Physical Chemistry* **1959**, *63*, 1024.

(39) Verma, V. K; Mishra, A. K. *Global NEST Journal* **2010**, *12*, 190.

(40) Duran, C.; Ozdes, D.; Gundogdu, A.; Senturk, H. B. *Journal of Chemical & Engineering Data* **2011**, *56*, 2136.

(41) Lagergren, S. *Band* **1898**, *24*, 1.

(42) Ho, Y. S.; McKay, G. *Chemical Engineering Journal* **1998**, *70*, 115.

(43) Biswas, B. K.; Inoue, J.-i.; Inoue, K.; Ghimire, K. N.; Harada, H.; Ohto, K.; Kawakita, H. *Journal of Hazardous Materials* **2008**, *154*, 1066.

CHAPTER 4

EXTRACTION OF VARIOUS POLLUTANTS FROM WATER USING TOMATO AND APPLE PEEL

Publications from the chapter:

R. Mallampati and S. Valiyaveettil, Application of Tomato peel as an efficient adsorbent for water purification – Alternative Biotechnology*? RSC Advances*, 2012, 2, 9914–9920.

4.1. Introduction

Scarcity of clean water is a common problem throughout the world. Dissolved heavy metal salts, organic pollutants and nanomaterials show more chronic toxicity on human health.[1-3] Many water purification methods have been developed such as chemical coagulation, flocculation, membrane separation, activated sludge formation, trickling filter, photodegradation and ion exchange to remove such pollutants[4-7] but there is no ideal material or method which can eliminate all pollutants from potable water. Among water purification techniques, active adsorption has been a promising method to treat effluents, offering advantages over conventional processes. Desirable qualities such as low cost, simplicity of design, availability in large amounts and ability to treat pollutants in more concentrated form made the design and synthesis of new adsorption materials are of particular interest. Activated carbon was considered as a suitable adsorbent for most of the pollutants[8-13] but it suffers from limitations such as poor regeneration, low surface area and disposal of used contaminated carbon. Many natural polymers, such as pectin, cellulose, hemicelluloses, protein, chitosan and chitin have functional groups to bind different pollutants. In addition, natural polymers are biodegradable, non-toxic and readily available. Several studies have been reported during recent years to investigate pollutant binding efficiency of several biosorbents (e.g. fungus, chitosan and silk worm).[14-16] Utilization of biowaste (e.g. almond shell, wheat shell, coconut husk and coir pith)[17-18] and biomembranes (e.g. orange peel, banana peel, rice husk, lemon peel)[19-23] for the extraction of heavy metal ions, pesticides and organic dyes offers an alternative low cost option for economically poor countries for water purification. Often, people living in poor countries depend on the contaminated ground water or local rivers for daily water needs. Here we show a low cost and highly efficient method to use materials easily accessible in rural areas for water purification.

Tomato (*Lycopersicon esculentum*) is the second most consumed (37 million tonnes / year) vegetable in the world and approximately 30% is consumed as processed products.[24] Similarly, apples (Malus domestica Borkh) are a very

significant part of the diet in humans. Disposal of the skin and other fibrous materials (90% skin) is an economic waste for many food processing industries. Developing a route to use tomato and apple peels for water treatment solve the problem of waste disposal and serves as an alternative biotechnology for water purification. Tomato peel contains pectin, carotene and phenolic compounds with functional groups such as -NH_2, -OH and –COOH.[25-27] Apples contain a large concentration of flavonoids, as well as a variety of other phytochemicals. Some of the most well studied antioxidant compounds in apples include quercetin-3-galactoside, quercetin-3-rhamnoside, catechin, epicatechin, procyanidin, quercetin-3-glucoside, cyanidin-3-galactoside, coumaric acid, chlorogenic acid, gallic acid, and phloridzin.[22] These functional groups act as potential adsorption sites for various pollutants especially for cationic pollutants.

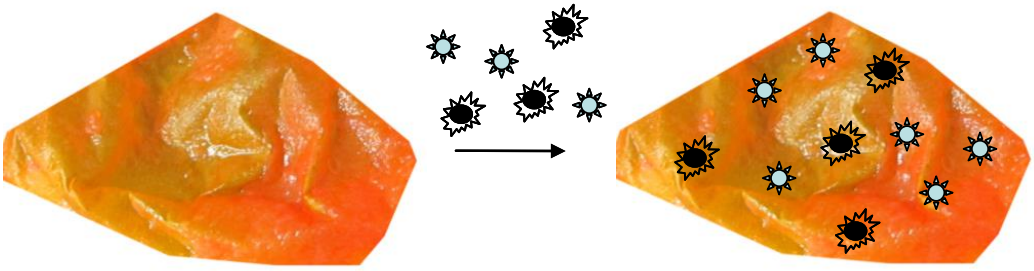

Figure 4.1. Schematic representation of the pollutant extraction by Tomato peel. Different dots indicates different classes of pollutants in water

This chapter includes complete characterization of a readily available and low cost tomato and apple peels as strong adsorbents, which can be used for extraction of different types of pollutants from water. In order to understand the adsorption mechanism, efficient extraction of heavy metal ions (Pb^{2+}, Ni^{2+}, AsO_2^- and $Cr_2O_7^{2-}$), dyes (alcian blue (AB), brilliant blue (BB), methylene blue (MB) and neutral red (NR)) and pesticides (phenol, *p*-chlorophenol (PCP), 2,4,6-tricholorophenol (TCP) and *p*-nitrophenol (PNP)) from water were investigated and analysed.

4.2. Characterisation of the tomato and apple peel

The chemical constituents of tomato peels were well studied.[27] The FT-IR spectra of tomato peel in the range of 4000 - 400 cm^{-1} is shown in Figure 4.2a. Similar spectrum was obtained for apple peel (Figure 4.2b) also. The broad band in the range of 3226 - 3670 cm^{-1} corresponds to the O-H bond stretch of phenols (usually between 3700 and 3200 cm^{-1}), and O-H bond vibration of carboxylic acids (3400 and 2400 cm^{-1}). The sharp peak at 2920 cm^{-1} belongs to the sp^3 C-H stretch. The sharp peak at 1760 cm^{-1} corresponds to the >C=O stretch in the carbonyl group of -COOH. The absorption in the range of 1600 - 1585 cm^{-1} and 1500 - 1400 cm^{-1} are accountable to stretching of C=C bond in the aromatic rings. The peaks due to the angular deformation in the plane of C-H bonds of the aromatic rings (1300 - 1000 cm^{-1}), axial bending of C-O bond in phenols (1260 - 1000 cm^{-1}), and axial bending of C-O bond in -COOH (1320 - 1210 cm^{-1}) were visible in the spectrum. IR analysis of functional groups present in tomato peel matches with reported literature values.[25-26]

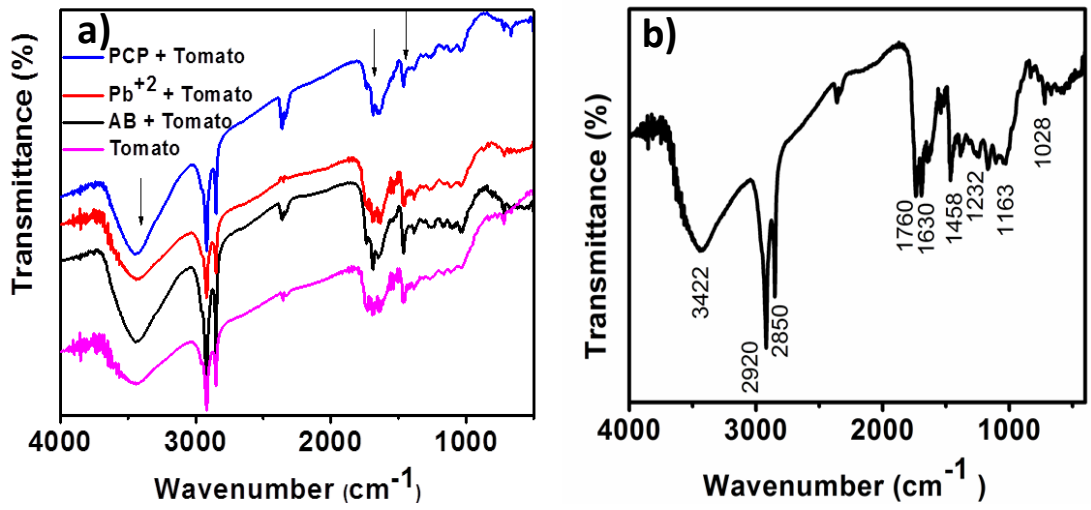

Figure 4.2. FT-IR spectrum of tomato peel before and after adsorption of pollutants (a) and apple peel (b).

Upon comparing FT-IR spectra before and after adsorption of pollutants, significant differences were observed in the position of peaks in the spectrum. Noticeable shift in the asymmetrical stretching of –O-H vibration from 3425 cm^{-1} to 3445 cm^{-1}, asymmetric and symmetric stretching of C-O bond from and from

1464 cm^{-1} to 1458 cm^{-1}, respectively, were observed. These shifts might be due to the binding of pollutants on the adsorbent.

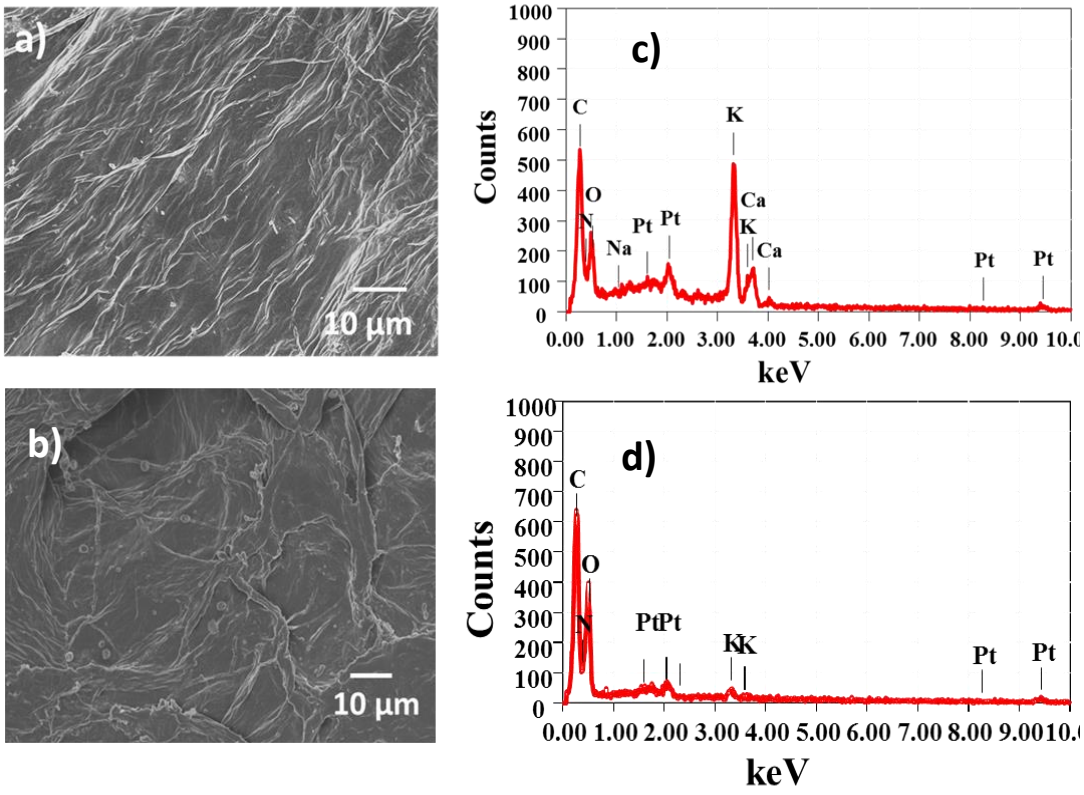

Figure 4.3. FESEM (a, b) and EDS (c, d) of tomato peel (a, c) and apple peel (b, d) surface.

SEM image of tomato (Figure 4.3a) and apple peels (Figure 4.3b) are shown in Figure 3, which shows fibrous structure with a fiber thickness in the range of 9 - 25 µm. EDS analysis (Figure 4.3c & 4.3d) shows that the major chemical constituents present in on the fiber surface are carbon, oxygen and nitrogen atoms, which is useful for extracting pollutants from water.

4.3. Batch adsorption experiments

4.3.1. Effect of pH

Peels (0.1 g) were added to the pollutant solutions (100 ppm, 10 mL) and left on orbital shaker (200 rpm) for 24 h at room temperature (30 °C). The removal percentages of different pollutants with varying pH were presented in Figure 4.4 (tomato peel: a, b & c; apple peel: d, e & f). The pK_a values of PNP, PCP, TCP

and phenol are 7.15, 9.41, 6.15 and 9.89 respectively,[32] making them strongly pH dependent. At a pH above the pK_a, the phenol groups were converted to phenolate ions. This generated repulsion between negatively charged ions and peel surface, reducing adsorption. Similar trends were reported in the adsorption of PCP, PNP and phenol on chitosan membrane.[31] However, the removal of cationic pollutants (Ni^{2+}, Pb^{2+}, AB, NR, and MB) was found to increase as pH increases.

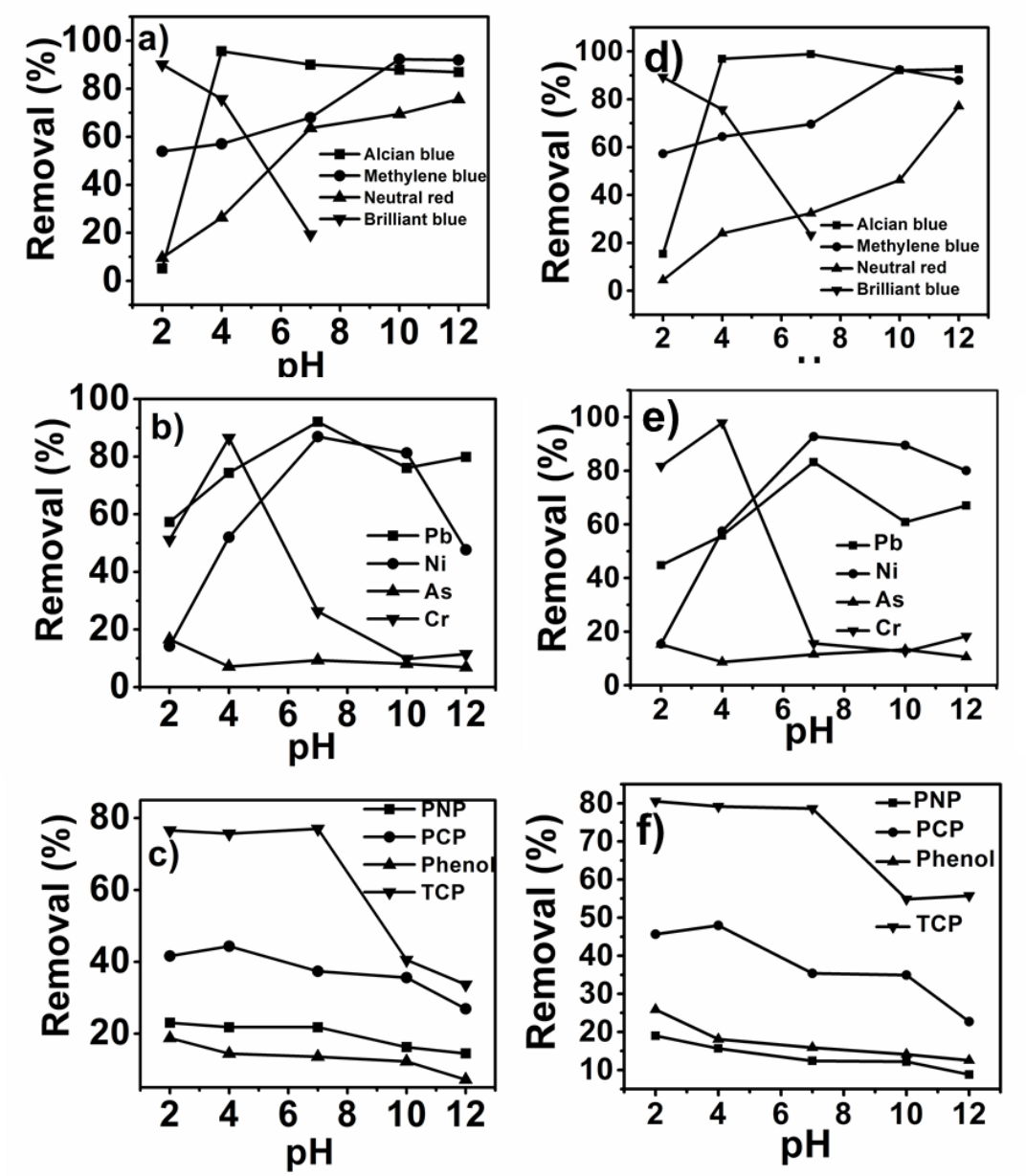

Figure 4.4. Effect of pH on the adsorption of dyes (a, d), metal ions (b, e) and pesticides (c, f).

It is noted that ionic interactions are involved in the adsorption process. For cationic pollutants, lower adsorption at acidic pH was due to the presence of excess H^+ ions competing with the pollutant cations for adsorption sites. At higher pH, the acidic functional groups on the surface of the peels get ionised, which enhances the adsorption of positively charged cations through electrostatic attraction.[20] In the case of anionic pollutants (BB, AsO_2^-, $Cr_2O_7^{2-}$), the lower pH resulted in higher adsorption as the positively charged surface of the peels could absorb negatively charged pollutants. Further, the adsorption of arsenic (III) is not a strong function of pH because it exists mostly as neutral H_3AsO_3, preventing adsorption. Adsorption of chromate and arsenite was higher at acidic pH owing to the affinity between the positively charged peels and the anions.

4.3.2. Effects of initial pollutant concentration and contact time

Peels (0.1 g) were added to the pollutant solutions (100 ppm, 10 mL) and left on orbital shaker (200 rpm) for 24 h at room temperature (30 °C). Optimum pH for each pollutant was maintained according to the conclusions from pH studies. The adsorption efficiency versus the adsorption time for different pollutants are shown in Figure 4.5 (tomato peel: a, b & c; apple peel: d, e & f). The amount of pollutant adsorbed (mg/g) increased with increase in time and then reached equilibrium. The adsorption of organic pesticides (Figure 4.5c & 4.5f) is less than that of heavy metal ions (Figure 4.5b & 4.5e) and dyes (Figure 4.5a & 4.5d) which may be due to weak interactions (π - π and hydrogen bonding) with the adsorbent,[28] but the adsorption efficiencies are comparable with the reported natural peels.[29-31] Metal cations and cationic dyes showed higher adsorption values whereas arsenate, chromate anions and anionic dyes showed lower values. These results indicate that these peels tend to bind cationic pollutants more favourably than anionic pollutants. This may be due to the presence of higher percentage of acid and alcoholic functional groups on the surface of tomato and apple peels.

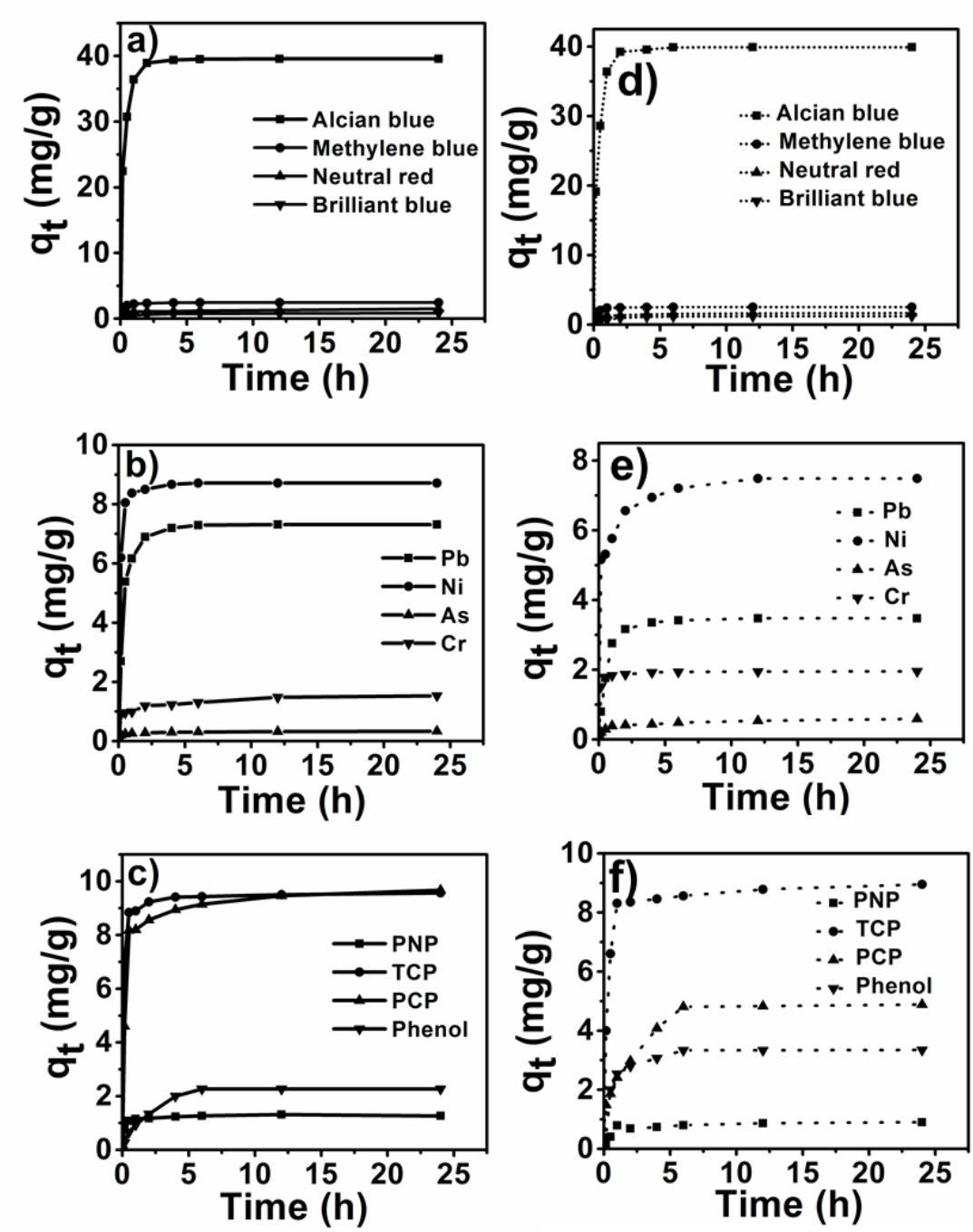

Figure 4.5. The variation of adsorption capacity of dyes (a, d), heavy metal ions (b, e) and pesticides (c, f) with time.

4.3.3. Isotherm studies

4.3.3.1. Langmuir Isotherm

The Langmuir isotherm which has been commonly used for sorption processes can be applied to explain the adsorption of pollutants on tomato and apple peels. Basic assumption of the Langmuir theory is that adsorption takes place at specific sites within the adsorbent.[33-35] The data obtained from the adsorption experiment for different pollutants were analysed using isotherm equation. The saturation monolayer can be expressed by the equation

$$\frac{1}{q_e} = \frac{1}{q_m} + \frac{1}{Kq_m C_e} \qquad (4.1)$$

$$q_e = \frac{Kq_m C_e}{1 + q_m C_e} \qquad (4.2)$$

A plot of $1/q_e$ versus $1/ C_e$ results in a linear graphical relation indicating the applicability of the Langmuir model for different pollutants as shown in Figure 4.6a & 4.6b (tomato) and Figure 4.6c &4.6d (apple). The Langmuir constants are elucidated from the slope and intercept of straight lines for different pollutants. The observed linear relationship is statistically significant as evidenced by the R^2 values (close to unity), implying the applicability of isotherm for our extraction studies. The Langmuir isotherm constants along with correction coefficients are reported in Table 4.1.

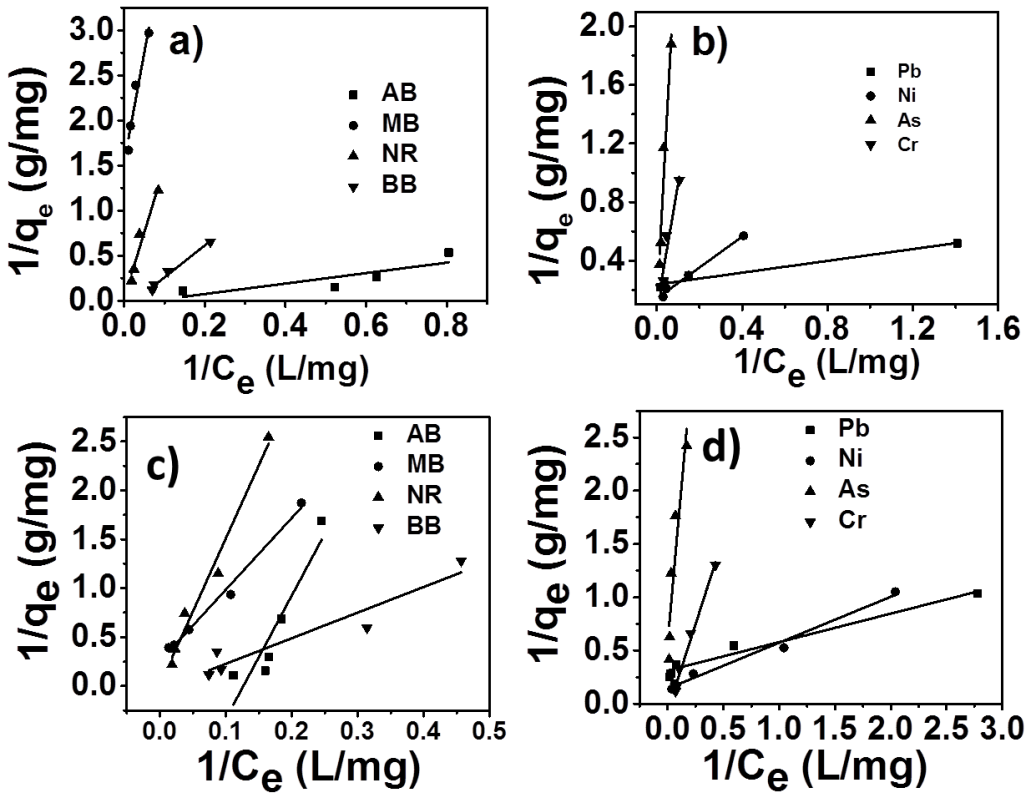

Figure 4.6. Langmuir isotherms for dyes (a, c) and metal ions (b, d)

Table 4.1. Langmuir and Freundlich isotherm model constants and correlation coefficients for adsorption of different pollutants on tomato peel

Pollutant	Langmuir constants			Freundlich constants		
	K (L/g)	R_L	R^2	K_F (mg/g)(L/g)^n	1/n	R^2
AB	0.0726	0.2159	0.8404	2.4920	0.7574	0.8194
BB	0.0270	0.4252	0.9922	0.1598	1.4146	0.9701
MB	0.0634	0.2397	0.9740	0.1328	0.3276	0.9967
NR	0.0020	0.9091	0.9725	0.0462	1.1117	0.9692
Pb^{2+}	1.1791	0.0167	0.9861	2.1359	0.2005	0.9919

Ni^{2+}	0.1342	0.1297	0.9962	1.2181	0.4679	0.9876
AsO_2^-	0.0026	0.8853	0.9761	0.0297	1.0383	0.9795
$Cr_2O_7^{2-}$	0.0087	0.6964	0.9690	0.1318	0.9052	0.9603

Table 4.2. Langmuir and Freundlich isotherm model constants and correlation coefficients for adsorption of different pollutants on apple peel

Pollutant	Langmuir			Freundlich		
	K (L/g)	R_L	R^2	K_F $(mg/g)(L/g)^n$	1/n	R^2
AB	0.1265	0.1365	0.9292	0.0388	2.4346	0.9267
BB	0.0132	0.6025	0.9542	0.2299	1.2884	0.9273
MB	0.0343	0.3682	0.9951	0.2397	0.5890	0.9858
NR	0.0009	0.9548	0.9896	0.0868	0.9209	0.9829
Pb^{2+}	1.1672	0.0168	0.9846	1.1812	0.3184	0.9743
Ni^{2+}	0.3288	0.0573	0.9934	1.1426	0.5775	0.8854
AsO_2^-	0.0492	0.2890	0.9302	0.0935	0.7074	0.9784
$Cr_2O_7^{2-}$	0.0208	0.4904	0.9944	0.2802	1.1924	0.9839

The essential characteristic of the Langmuir isotherm can be expressed in terms of a dimensionless equilibrium parameter, such as the separation factor (R_L) used in the following equation

$$R_L = \frac{1}{1 + KC_e} \qquad (4.3)$$

where K is the Langmuir constant and C_e is the equilibrium concentration of the adsorbate in solution. This parameter indicates that isotherm will be shaped according to the following adsorption characteristics: $R_L > 1$ unfavourable; $R_L = 1$ corresponds to linear; $0 < R_L < 1$ is favourable and $R_L = 0$ is irreversible. It can be seen that the adsorption of pollutants on to tomato (Table 4.1) and apple peels (Table 4.2) are favourable.

4.3.3.2. Freundlich isotherm

Freundlich model is an empirical equation based on adsorption on heterogeneous surfaces. It is assumed that the stronger binding sites are occupied first and the binding affinity decreases with an increasing degree of site occupation.[36, 37] The isotherm is expressed as:

$$\log q_e = \log K + \beta \log C \qquad (4.4)$$

where K_f and n are Freundlich constants related to sorption capacity and sorption intensity of the adsorbent, respectively. K_f can be defined as the adsorption coefficient and represents the quantity of pollutant adsorbed onto biopeel for a unit equilibrium concentration. A value for 1/ n below one indicates a normal Langmuir isotherm while 1/n above one is indicative of cooperative adsorption.

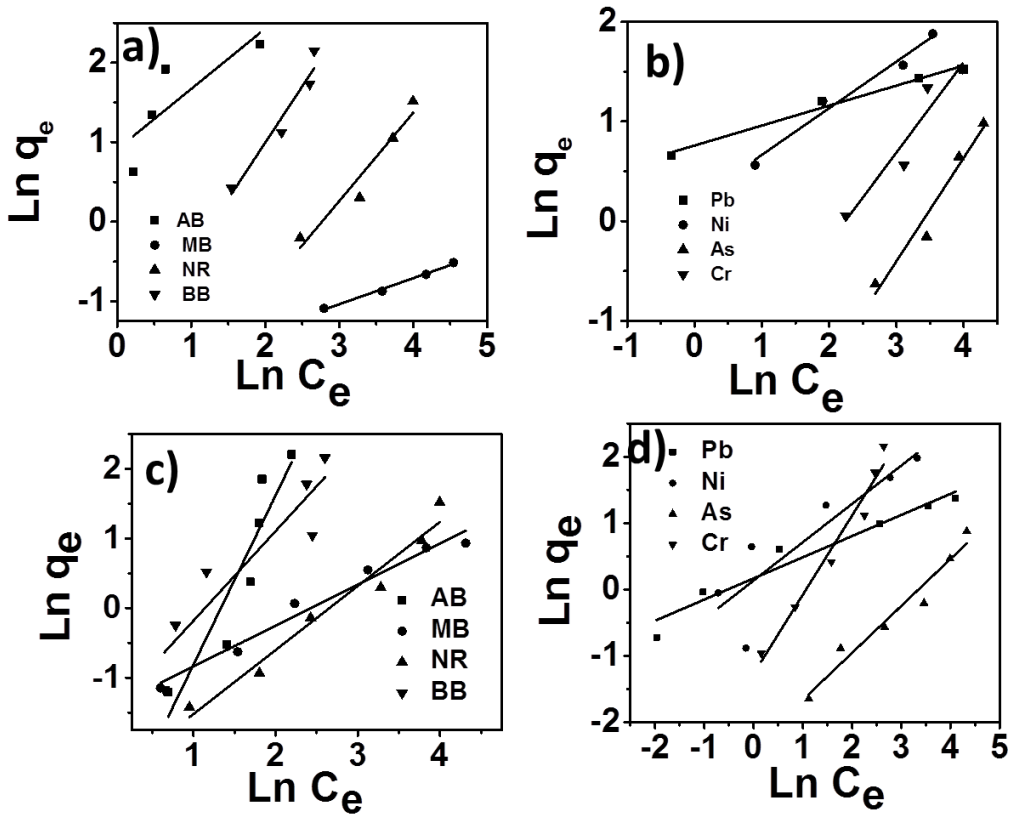

Figure 4.7. Freundlich isotherms for the adsorption of dyes (a, c) and metal ions (b, d) on tomato (a, b) and apple (c, d) peel

The Freundlich isotherm model (Figure 4.7, Table 4.1 & 4.2) yielded the best fit with the highest R^2 value (.99) for pollutants as compared to Langmuir model. It can be seen from table that Freundlich model was found to fit the data significantly better indicating heterogeneous nature of bio peels.

4.3.4. Adsorption kinetics

Kinetic models elucidating the mechanism by which pollutants are adsorbed on adsorbent surfaces have been proposed.[38-40] Both pseudo-first-order and pseudo-second-order kinetic models were used to investigate the adsorption mechanism. A pseudo-first-order equation is represented as

$$\log (q_e - q_t) = \log q_e - \left(\frac{k_1}{2.303}\right) t \qquad (4.5)$$

where q_e and q_t indicate the amount of pollutant adsorbed (mg / g) at equilibrium and at any time t, respectively. $k_1(min^{-1})$ is the first order rate constant applied in the present studies of pollutant adsorption. The plot of log ($q_e - q_t$) versus t for different pollutants (Figure 4.8) gave first order rate constants k_1 (slope) and equilibrium concentration q_e (intercept). The values of k_1 and q_e for different pollutants were calculated from the plots and shown in Table 4.3.

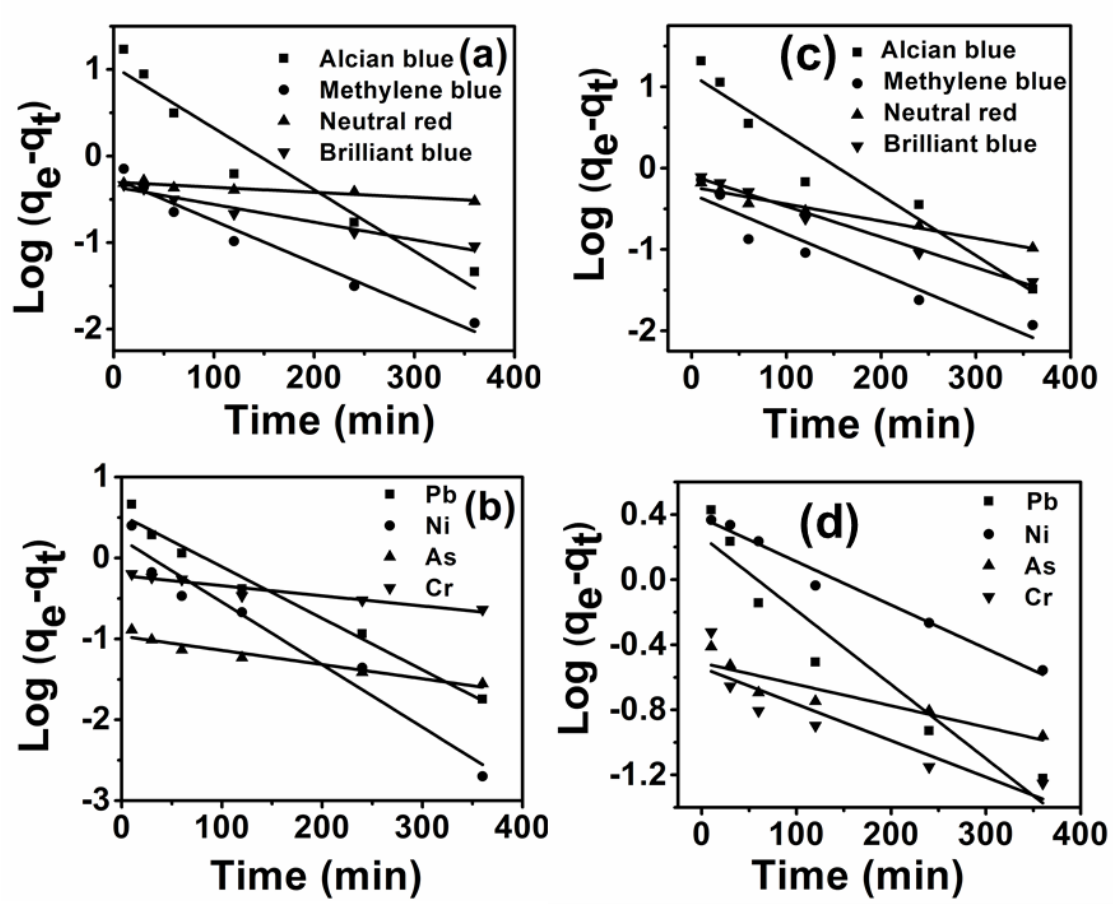

Figure 4.8. Pseudo first order kinetics for adsorption of dyes (a, c) and heavy metal ions (b, d) on to tomato (a, b) and apple (c, d) peel

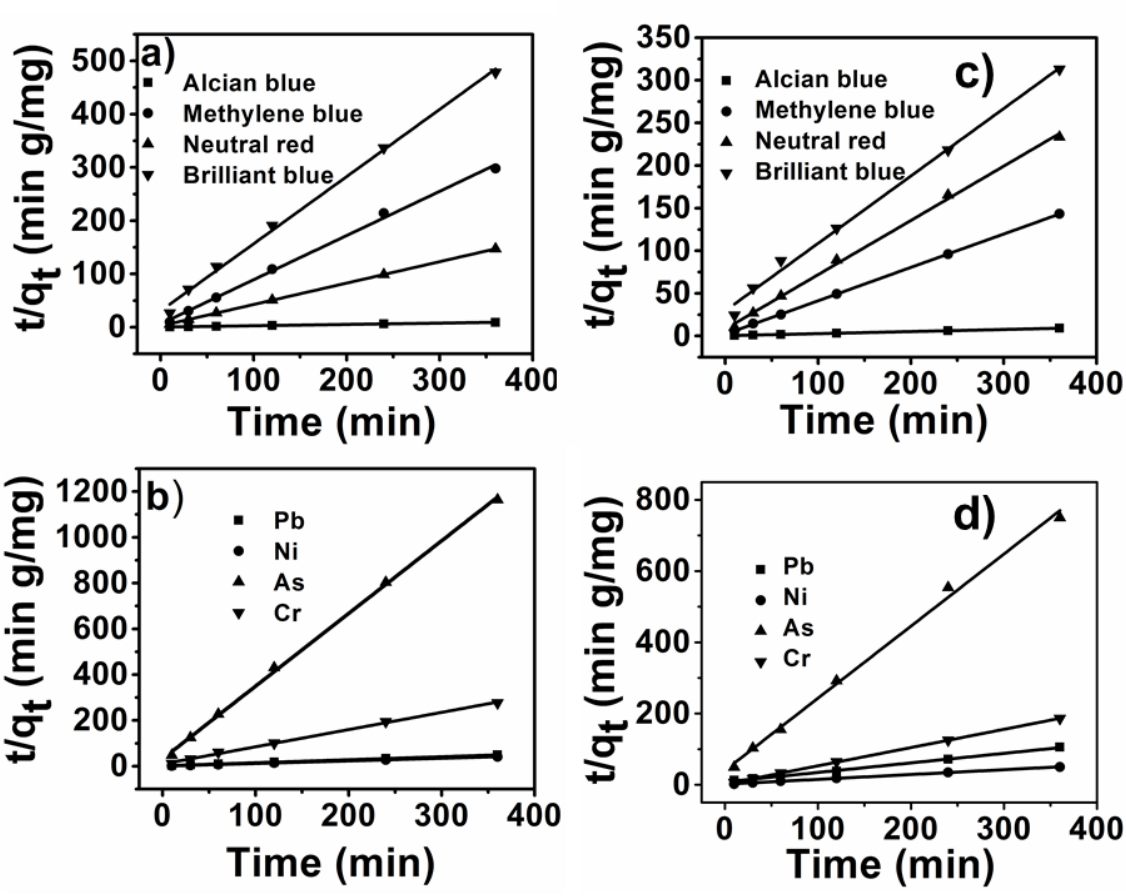

Figure 4.9. Pseudo second order kinetics for adsorption dyes (a, c) and heavy metal ions (b, d) on to tomato (a, b) and apple (c, d) peel

The adsorption kinetics of some systems can also be explained by a pseudo-second-order reaction. The pseudo-second-order equation based on adsorption equilibrium capacity may be expressed in the form

$$\frac{t}{q_t} = \frac{1}{k_2 {q_e}^2} + \left(\frac{1}{q_e}\right) t \qquad (4.6)$$

Where k_2 is the rate constant of pseudo-second-order adsorption and q_e is the equilibrium adsorption capacity (mg / g). The k_2 and q_e values of different pollutants can be calculated experimentally from the slope and the intercept of t / q_t versus t plots. From Table 4.3 (tomato) & Table 4.4 (apple), the correlation coefficient R^2 shows that the pseudo-second-order model fits the experimental data better than the pseudo-first-order model. The calculated correlations are

closer to unity for the second-order kinetics model and calculated equilibrium adsorption capacities of all pollutants matched with experimental values. The calculated k_2 (g / mg min) and q_e are listed in Table 4.3 & 4.4.

Table 4.3. Pseudo first order and pseudo second order constants and correlation coefficients for adsorption of different pollutants on tomato peel

Pollutant	Qe (exp)	Pseudo first order kinetic model			Pseudo second order kinetic model		
		Qe (mg/g)	K1 (min^{-1})	R^2	Qe (mg/g)	K2 (g/mg min)	R^2
AB	39.5632	10.8019	0.0164	0.941	39.6825	0.0052	0.999
BB	0.8435	0.4432	0.0046	0.969	0.8095	0.0457	0.999
MB	2.4405	0.5566	0.0113	0.971	2.4770	0.0730	0.999
NR	1.5074	0.4986	0.0138	0.971	1.3192	0.0408	0.996
Pb^{2+}	7.3120	3.3705	0.0147	0.980	7.6104	0.0091	0.999
Ni^{2+}	8.7160	1.6904	0.0177	0.958	8.7951	0.0329	0.999
AsO_2^-	0.3373	0.0939	0.0028	0.904	0.3252	0.2172	0.990
$Cr_2O_7^{2-}$	1.5333	0.6106	0.0032	0.975	1.4940	0.0242	0.994

Table 4.4. Pseudo first order and pseudo second order constants and correlation coefficients for adsorption of different pollutants on apple peel

Polutant	Qe(exp) (mg/g)	Pseudo first order kinetic model			Pseudo second order kinetic model		
		Qe (mg/g)	K1 (min^{-1})	R^2	Qe (mg/g)	K2 (g/mg min)	R^2
AB	39.9086	14.0378	0.0170	0.941	40.1606	0.0038	0.999
BB	0.9741	0.4432	0.0046	0.969	1.2223	0.0264	0.989
MB	2.5247	0.3731	0.0089	0.949	2.5981	0.0274	0.999
NR	1.6471	0.5440	0.0041	0.979	1.6661	0.0280	0.999
Pb^{2+}	3.4740	1.8382	0.0105	0.925	3.7327	0.0092	0.997
Ni^{2+}	7.4840	2.3900	0.0062	0.983	7.36377	0.0116	0.998
AsO_2^-	0.5893	0.2886	0.0025	0.916	0.5468	0.0539	0.995
$Cr_2O_7^{2-}$	1.9506	0.2880	0.0050	0.825	1.9924	0.0680	0.999

4.3.5. Effect of temperature on adsorption

Adsorption capacities of tomato peel with different pollutants at various temperatures were determined. Tomato peels (0.05 g) were added to aqueous solutions (10 mL) of three different pollutants (AB, Pb^{2+}, PCP) in separate tubes with an initial concentration of 100 mg/L each. The solutions were placed on an orbital shaker incubator for 2 h at 250 rpm. The data presented in Table 4.5 showed that the adsorption of pollutants by the tomato peel increased with increase in temperature.[41] However, the magnitude of such increase in adsorption decreased with an increase in temperature from 30 to 60 °C. Such decrease may

be due to increase in desorption of pollutants (PCP) from the membrane surface and increase in solubility of the pollutants in water.

Table 4.5. Adsorption capacities of tomato peels towards different pollutants at different temperatures.[41]

Temperature (°C)	Adsorption capacity (mg/g)		
	Alcian blue	Pb^{2+}	*P*-chlorophenol
30	25.64	6.43	10.00
40	27.18	7.36	15.52
50	30.77	7.75	7.59
60	31.80	8.39	4.83

4.3.6. Diffusion rate constant study

In the process of the adsorption of pollutants using tomato peel, there is the possibility of intra-particle diffusion;

$$q_t = K_p\, t^{1/2} + C \qquad (4.7)$$

According to Weber and Morris,[42, 43] If the adsorption mechanism involves an intra-particle diffusion processes, a plot of q_t versus $t^{½}$ should be a straight line with a slope K_p and intercept C. K_p was calculated from the slope of the linear portions of these plots, as shown in Table 4.6 (tomato) and 4.7 (apple). It is conceivable that the initial curved portion show the boundary layer diffusion effects (Figure 4.10) and the linear portion arises from the intra-particle diffusion effects. The linear plots are explained using fast diffusion to the accessible site for adsorption via available adsorbing sites on the adsorbent surface. The adsorption process for solids can be separated into three stages: (a) mass transfer (boundary-layer diffusion); (b) sorption of ions onto sites and (c) intra-particle diffusion. The

correlation coefficient R^2 values are close to unity (Table 4. 4), which support the appropriateness of the application of this model. The divergence in the value of the slope from 0.5 indicates that the contribution of intra-particle diffusion is one of the rate-limiting steps. In addition, there are many other processes controlling the rate of adsorption, all of which are most likely operating simultaneously.

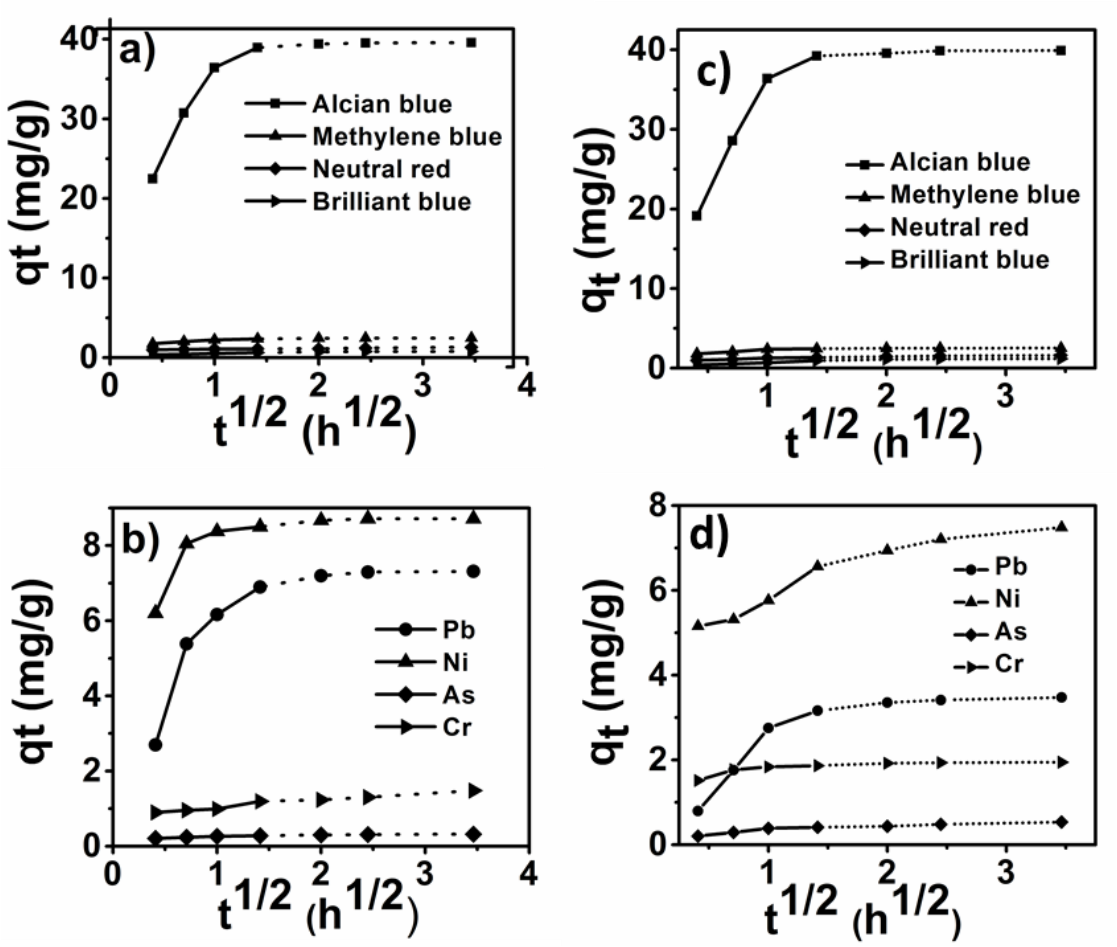

Figure 4.10. Weber and Morris intraparticle diffusion plots for removal of dyes (a, c) and heavy metal ions (b, d) by tomato (a, b) and apple (c, d) peel.

Table 4.6. Intraparticle diffusion model constants and correlation coefficients for adsorption of different pollutants on tomato peel

pollutant	Intraparticle diffusion model					
	K_{p1}	C_1	R^2	K_{p2}	C_2	R^2
AB	23.6110	13.2210	0.990	0.1407	38.994	0.531
BB	0.2516	0.2647	0.944	0.0556	0.5857	0.893
MB	0.8261	1.4187	0.994	0.1208	2.3629	0.568
NR	0.1549	0.9179	0.987	0.0236	0.9059	0.985
Pb^{2+}	5.8783	0.6033	0.911	0.1860	6.7407	0.699
Ni^{2+}	3.6860	4.9438	0.862	0.0938	8.4324	0.640
AsO_2^-	0.0947	0.1706	0.994	0.0157	0.2645	0.931
$Cr_2O_7^{2-}$	0.1061	1.0464	0.934	0.1545	0.8393	0.972

Table 4.7. Intraparticle diffusion model constants and correlation coefficients for adsorption of different pollutants on apple peel

polutant	Intraparticle diffusion model					
	K_{p1}	C_1	R^2	K_{p2}	C_2	R^2
AB	29.168	7.468	0.9976	0.1705	39.21	0.6098
BB	0.4532	0.2223	0.9967	0.0581	0.9511	0.6306
MB	0.9894	1.3858	0.9916	0.0021	2.4405	0.5531
NR	0.4966	0.778	0.9955	0.0817	1.2887	0.8384
Pb^{2+}	3.3121	0.5666	0.9998	0.1417	3.0212	0.8226

Ni^{2+}	1.0225	4.6911	0.9242	0.4411	6.0204	0.9497
AsO_2^-	0.312	0.0738	0.9992	0.0528	0.3394	0.9765
$Cr_2O_7^{2-}$	0.5441	1.3221	0.8985	0.0313	1.842	0.8764

4.3.7. Regeneration of adsorbent

Mechanism of adsorption can be further investigated by using desorption and regeneration process. The nature of the adsorption of pollutant onto the surface of the material involves electrostatic attractions between -OH and -COOH on the surface of peels and positive centres of the pollutants. Adsorption experiments showed that both tomato and apple peels can adsorb cationic pollutants (cationic dyes, Pb^{+2} and Ni^{+2}) more efficiently than other pollutants. Desorption of these cationic pollutants were studied at different pH (4, 7 and 10) at a constant temperature of 30 °C. 2% desorption was observed at pH 10 but 96% of pollutants were desorbed at pH 4 within 10 min. Under acidic condition, H^+ ions will replace cationic pollutants from peel surface. Low extraction capacity of anionic pollutants (anionic dyes, Arsenate and Chromate ions) further supports such an adsorption mechanism. In order to show the reusability of the adsorbent, the adsorption-desorption cycle of pollutants were repeated five times using the same experimental conditions. These results showed that recycling of tomato and apple peels is efficient and can be used in consecutive pollutant adsorption studies without detectable losses in their adsorption capacities.

4.4. Conclusions

Adsorption of different pollutants was evaluated using tomato and apple peels as adsorbents. Adsorption and desorption studies were conducted to understand the adsorption mechanism. Langmuir and Freundlich isotherm models were used to validate the adsorption process. Kinetic studies were done to further understand the adsorption process. Adsorptions on bio peels follow pseudo-second-order

kinetics. Both peels showed efficient adsorption towards different cationic pollutants such as alcian blue (39.6 mg/g) dye and metal cations such as Ni^{2+}(8.7 mg/g). Experimental factors such as pH and temperature of the medium also influence the extraction efficiency. The functional groups on both peels can be further modified for the extraction of different contaminants in water. It is conceivable that the use of such biowaste is simple, cost effective and efficient method for water treatment and can be used in large scale applications.

4.5. References

(1) Jezierska, B.; Ługowska, K.; Witeska, M. *Fish Physiology and Biochemistry* **2009**, *35*, 625.

(2) Jomova, K.; Jenisova, Z.; Feszterova, M.; Baros, S.; Liska, J.; Hudecova, D.; Rhodes, C. J.; Valko, M. *Journal of Applied Toxicology* **2011**, *31*, 95.

(3) Mansour, S. A. *Advances in Food Protection* **2011**, 73.

(4) Mahanta, N.; Leong, W. Y.; Valiyaveettil, S. *Journal of Materials Chemistry* **2012**, *22*, 1985.

(5) Mallampati, R.; Valiyaveettil, S. *Journal of Nanoscience and Nanotechnology* **2012**, *12*, 618.

(6) Fernandes, A.; Morao, A.; Magrinho, M.; Lopes, A.; Gonçalves, I. *Dyes and Pigments* **2004**, *61*, 287.

(7) Mahmoodi, N. M.; Arami, M.; Limaee, N. Y.; Tabrizi, N. S. *Journal of Colloid and Interface Science* **2006**, *295*, 159.

(8) Gupta, V. K.; Mittal, A.; Jain, R.; Mathur, M.; Sikarwar, S. *Journal of Colloid and Interface Science* **2006**, *303*, 80.

(9) Mohanty, K.; Naidu, J. T.; Meikap, B. C.; Biswas, M. N. *Industrial and Engineering Chemistry Research* **2006**, *45*, 5165.

(10) Hamdaoui, O.; Naffrechoux, E. *Journal of Hazardous Materials* **2007**, *147*, 401.

(11) Wang, S. L.; Tzou, Y. M.; Lu, Y. H.; Sheng, G. *Journal of Hazardous Materials* **2007**, *147*, 313.

(12) Orozco, A. M. F.; Contreras, E. M.; Zaritzky, N. E. *Journal of Hazardous Materials* **2008**, *150*, 46.

(13) Prahas, D.; Kartika, Y.; Indraswati, N.; Ismadji, S. *Chemical Engineering Journal* **2008**, *140*, 32.

(14) Günay, A.; Arslankaya, E.; Tosun, I. *Journal of Hazardous Materials* **2007**, *146*, 362.

(15) Han, R.; Zou, W.; Yu, W.; Cheng, S.; Wang, Y.; Shi, J. *Journal of Hazardous Materials* **2007**, *141*, 156.

(16) Hameed, B. H.; Mahmoud, D. K.; Ahmad, A. L. *Journal of Hazardous Materials* **2008**, *158*, 499.

(17) Krishnani, K. K.; Meng, X.; Christodoulatos, C.; Boddu, V. M. *Journal of Hazardous Materials* **2008**, *153*, 1222.

(18) Febrianto, J.; Kosasih, A. N.; Sunarso, J.; Ju, Y. H.; Indraswati, N.; Ismadji, S. *Journal of Hazardous Materials* **2009**, *162*, 616.

(19) Mittal, A.; Malviya, A.; Kaur, D.; Mittal, J.; Kurup, L. *Journal of Hazardous Materials* **2007**, *148*, 229.

(20) Wan Ngah, W. S.; Hanafiah, M. A. K. M. *Bioresource Technology* **2008**, *99*, 3935.

(21) Crini, G. *Bioresource Technology* **2006**, *97*, 1061.

(22) Sun, J.; Chu, Y. F.; Wu, X.; Liu, R. H. *J Agric Food Chem* **2002**, *50*, 7449.

(23) Bhatnagar, A.; Minocha, A. K.; Sillanpää, M. *Biochemical Engineering Journal* **2010**, *48*, 181.

(24) a. http://www.foodproductiondaily.com/Packaging/Using-tomato-waste-in-food-production, b. http://www.tomatonews.com/resources.html

(25) Navarro-González, I.; García-Valverde, V.; García-Alonso, J.; Periago, M. J. *Food Research International* **2011**, *44*, 1528.

(26) Hetzroni, A.; Vana, A.; Mizrach, A. *Postharvest Biology and Technology* **2011**, *59*, 80.

(27) Gahler, S.; Otto, K.; Böhm, V. *Journal of Agricultural and Food Chemistry* **2003**, *51*, 7962.

(28) Denizli, A.; Cihangir, N.; Tüzmen, N.; Alsancak, G. *Bioresource Technology* **2005**, *96*, 59.

(29) Jung, M. W.; Ahn, K. H.; Lee, Y.; Kim, K. P.; Rhee, J. S.; Park, J. T.; Paeng, K. J. *Microchemical Journal* **2001**, *70*, 123.

(30) Kennedy, L. J.; Vijaya, J. J.; Kayalvizhi, K.; Sekaran, G. *Chemical Engineering Journal* **2007**, *132*, 279.

(31) Radhika, M.; Palanivelu, K. *Journal of Hazardous Materials* **2006**, *138*, 116.

(32) Li, J. M.; Meng, X. G.; Hu, C. W.; Du, J. *Bioresource Technology* **2009**, *100*, 1168.

(33) Langmuir, I. *The Journal of the American Chemical Society* **1916**, *38*, 2221.

(34) Langmuir, I. *J. Am. Chem. Soc.* **1916**, *40*, 1361.

(35) Langmuir, I. *The Journal of the American Chemical Society* **1918**, *40*, 1361.

(36) Freundlich, H. *Z. Phys. Chem.* **1906**, *57*, 385.

(37) Redlich, O.; Peterson, D. L. *Journal of Physical Chemistry* **1959**, *63*, 1024.

(38) Verma, V. K.; Mishra, A. K. *Global Nest Journal* **2010**, *12*, 190.

(39) Duran, C.; Ozdes, D.; Gundogdu, A.; Senturk, H. B. *Journal of Chemical and Engineering Data* **2011**, *56*, 2136.

(40) Bhattacharyya, K. G.; Gupta, S. S. *Desalination* **2011**, *272*, 66.

(41) Manju, G. N.; Raji, C.; Anirudhan, T. S. *Water Res.* **1998**, *32*, 30662.

(42) Weber, W. J.; Morris, J. C. *J. Sanit. Eng. Div. Am. Soc. Civ. Eng.* **1963**, *89*, 31.

(43) Weber Jr, W. J.; Rummer, R. R. *Water Resour. Res.* **1965**, *1*, 361.

CHAPTER 5

REMOVAL OF ANIONS AND NANOPARTICLES BY USING Zr IMMOBILIZED APPLE PEEL

Publication from chapter

R. Mallampati and S. Valiyaveettil, Apple peels – a versatile biomass for water purification?, *ACS applied materials & Interfaces*, 2013, 5, 4443−4449.

5.1. Introduction

Ground water contaminated with anions such as chromate ($Cr_2O_7^{2-}$), arsenite (AsO_2^-), arsenate (AsO_4^{3-}) and other anions has become one of the most serious problems throughout the world.[1] These Oxoanions are known to be highly toxic even at low concentrations and can accumulate in human body causing various diseases and disorders.[2] These anions are considered as toxic contaminants found in water and can exist as various forms in the environment. Arsenic is present as arsenite (AsO_3^{3-}) and arsenate (AsO_4^{3-}) salts are common in natural waters. Chromium can exist in oxidation states from +2 to +6, but only Cr(III) and Cr(VI) are of environmental significance.[3] Long term consumption of arsenic and chromium contaminated drinking water led to many health problems including cardiovascular effects, bladder, skin cancer and anemia among the population in different parts of the world.[4-8] High levels of phosphate in waste water disturb the nutrient equilibrium, leading to enhanced growth of aquatic plants and subsequent eutrophication of lakes and rivers.[9-11] Therefore, it is important to develop effective methods to remove such toxic anions from water. The production of nanoparticles and its current usage is rapidly increasing due to the recent development of nanotechnology, engineered nanoparticles (NPs) are widely used in consumer products such as clothing, toys, house-hold products, medicine and personal care products.[7] This huge increase in the production and usage of nanomaterials may increase human and environmental exposure to nanoparticles. For instance, many *invitro* and *invivo* studies have demonstrated the toxicity of silver and gold nanoparticles to cells from mammalian organs such as lungs, liver, kidneys, brain and reproductive systems.[12] The removal of nanoparticles from water is a growing challenge for the future. Owing to the surface negative charge of these nanoparticles, we consider them as anionic contaminants.

Many water treatment technologies include filtration, precipitation, oxidation, coagulation and anion exchange.[13-17] Most of these chemical methods are efficient in removing pollutants, including anions from aqueous media. Such technologies also produce large amounts of secondary wastes that require further

decontamination before proper disposal. Adsorption of anions onto an active surface has been considered as an efficient alternative method for purifying contaminated water.[18,19] Different adsorbents including activated alumina,[20] sand,[21] iron and manganese oxide or hydroxide,[22-24] hydroxyapatite,[25,26] activated carbon,[18,27] and biomaterials[19,28-31] were applied for the removal of anions. These adsorbents have different adsorption capacities that depend on the sorbent mass, pH, contact time, functional groups and initial concentration of the adsorbate in the solution. Adsorption of anions using biomass has emerged as a viable option for developing economic and eco-friendly wastewater treatment processes. Natural materials have been tested for removal of pollutants from water. A number of studies have shown the use of bioadsorbents including biochar,[32] fungal biomass,[33] chicken feathers,[34] methylated yeast biomass[35] and alginate[36] to remove anions from aqueous solution. Many biopeels such as banana peel, orange peel, papaya peel, potato peel, water melon shell, mango peel, to name a few were exploited for the extraction of different pollutants.[29,30] In most cases, pollutants such as dyes, pesticides and cations were extracted from water. Extraction of anions is much tougher than the other pollutants. A cationic adsorbent is needed to extract anions and functionalization via chemical treatment methods are used to transform biopeels as efficient adsorbents for anion removal. Some of the surface modifcations involve immobilization of chitosan, PEI, and metal ion. Only a few reports exist on the use of fruit peels for anion extraction from water. Metal cations such as La (III), Ce (IV), Fe (III) and Zr (IV) loaded orange waste were used for the extraction of arsenic and phosphate anions. Modified banana peel[29] was reported for the extraction of chromate anion and lemon peel[30]was used for the removal of anionic dyes. However these modified biopeels were used for the extraction of single anion. We used Zr immobilized apple peel to extract different anions efficiently.

Advantages of biomembranes include low cost, nontoxic, easy processing and presence of abundant functional groups. However, these biomembranes with surface functional groups such as -COOH, -OH can remove cationic pollutants

more effectively than anions.[37] Therefore adsorption based on ligand substitution with metal loaded adsorbents gaining more attention. It is shown that loaded metal cations with high positive charges can bind oxoanionic species such as arsenate, arsenite[9, 38] and phosphate ions.[10,11] Removal of arsenic and chromium anions were reported by using zirconium salt treated adsorbents,[39] because zirconium in its hydrated form can generate tetranuclear ions as well as octanuclear species which have hydroxyl ions and water molecules to take part in ligand exchange with phosphate and arsenic species. Moreover, hydrated zirconium cations are resistant to attack by acids alkali, oxidants, and reductants.[40] Apple peels are available worldwide as biowaste from food processing industries and offer abundant functional groups which can be exploited for water treatment. Apples contain a large concentration of flavonoids of the procyanidins, catechin, epicatechin, chlorogenic acid, phloridzin and the quercetin conjugates.[41, 42] These functional groups from these compound are expected to bind Zr(IV) strongly on the membrane surface. Here we demonstrated an efficient adsorbent using low cost and easily available apple peel immobilized with Zr(IV) ions on the surface to develop an efficient adsorbent to extract different anions from aqueous media.

5.2. Characterization of adsorbent

The chemical constituents of apple peels were well studied.[41] The FT-IR spectra of apple peel in the range of 4000 - 400 cm^{-1} is shown in Figure 5.1. The broad band in the range of 3226 - 3670 cm^{-1} corresponds to the O-H bond stretch of phenols (usually between 3700 and 3200 cm^{-1}), and O-H bond vibration of carboxylic acids (3400 and 2400 cm^{-1}). The sharp peak at 2920 cm^{-1} belongs to the sp^3 C-H stretch. The sharp peak at 1760 cm^{-1} corresponds to the >C=O stretch in the carbonyl group of -COOH. The absorption in the range of 1600 - 1585 cm^{-1} and 1500 - 1400 cm^{-1} are accountable to stretching of C=C bond in the aromatic rings. The peaks due to the angular deformation in the plane of C-H bonds of the aromatic rings (1300 - 1000 cm^{-1}), axial bending of C-O bond in phenols (1260 - 1000 cm^{-1}), and axial bending of C-O bond in -COOH (1320 - 1210 cm^{-1}) were

visible in the spectrum. IR analysis of functional groups present in apple peel matches with reported literature values.[41]

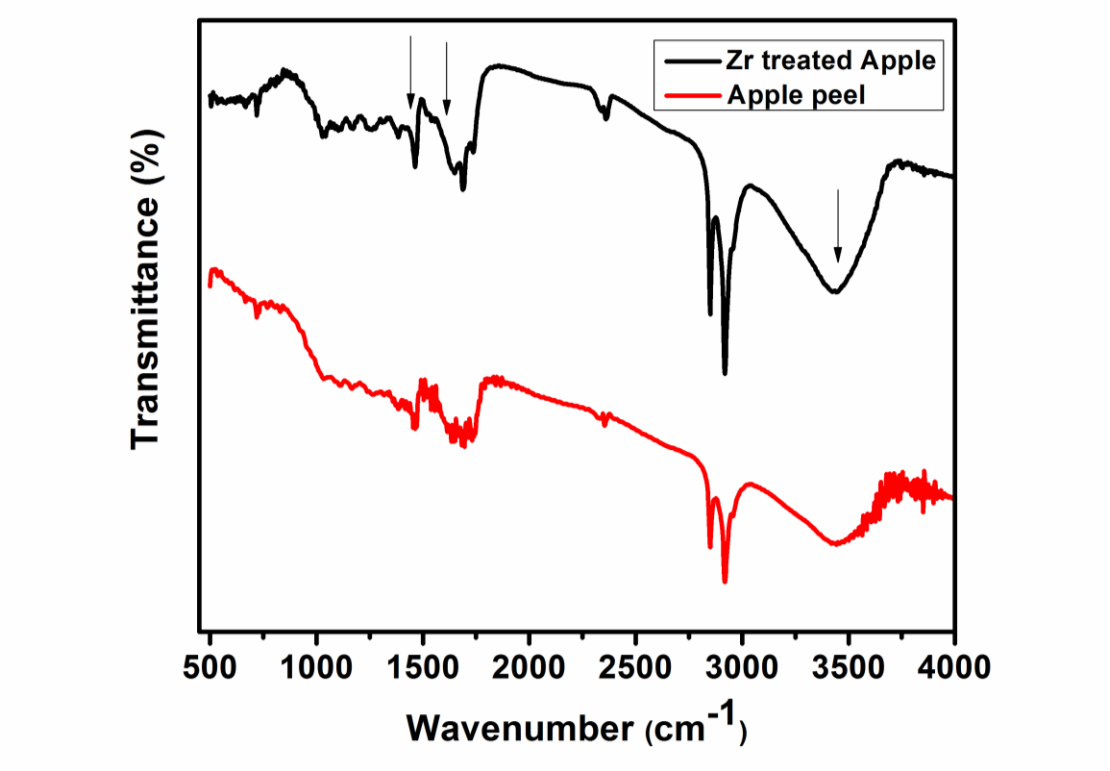

Figure 5.1. FT-IR spectrum of raw apple peel and Zr treated apple peel.

The FT-IR spectra of the peels before and after treatment with Zr(IV) show significant differences in the position of peaks in the spectrum. Noticeable shifts in the asymmetrical stretching of –O-H vibration from 3425 cm^{-1} to 3445 $cm^{-1}$and asymmetric and symmetric stretching of C-O bond from 1464 cm^{-1} to 1458 cm^{-1} were observed. IR spectra of adsorbent were recorded before and after adsorption of different anions and significant differences were not observed. Morphological changes due to immobilization of Zr were investigated by SEM. SEM image of apple peel before and after chemical treatment are shown in Figure 5.2. Apple peel has fibrous structure with a fiber diameter in the range of 9 - 25 µm with Zr nanoparticles bonded on the surface. EDS analysis (Figure 5.2) indicated carbon, oxygen and sulphur atoms on the untreated peel surface and significant amounts of Zr on the treated surface.

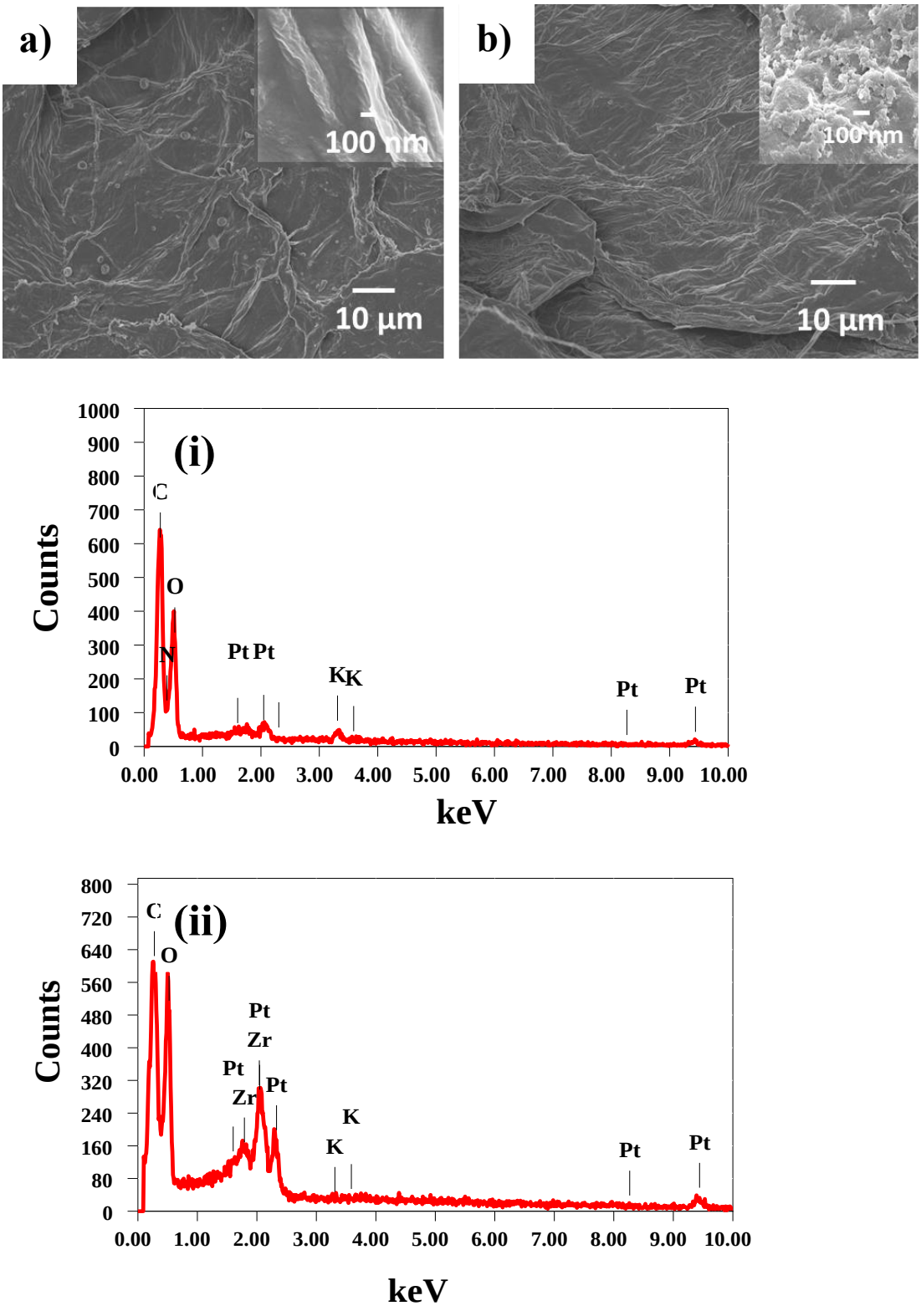

Figure 5.2. FESEM micrographs (a, b) and EDS (i, ii) analysis of apple peel surface before (a, i) and after (b, ii) Zr treatment. Inset in (a) and (b) shows the magnified surface image

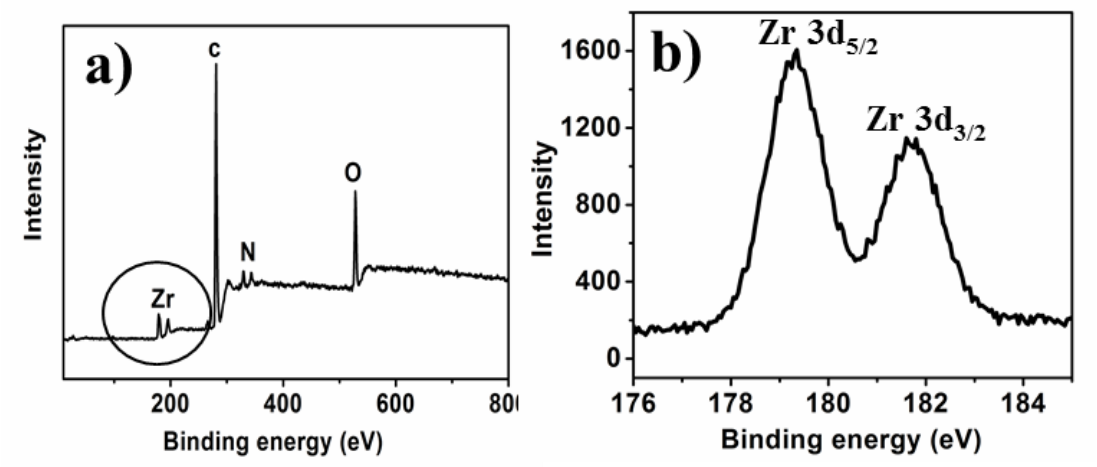

Figure 5.3. XPS profile (a) and expanded region for Zr peaks (b) of treated apple peel surface.

Figure 5.3a shows XPS profile of Zr treated apple peel. The spectrum indicates the presence of carbon (281 eV, 1s), nitrogen (396 eV, 1s), oxygen (528 eV, 1s), and Zr (179 eV, 3d) on the surface of apple peel. The peaks corresponding to the binding energies at 179 eV and 182 eV in Figure 5.3b clearly indicates that Zr is bonded to apple peel surface and exists in (+) 4 oxidation state. This high positive charge of the Zr immobilized surface is responsible for the binding of anions.[43]

5.3. Characterization of NPs

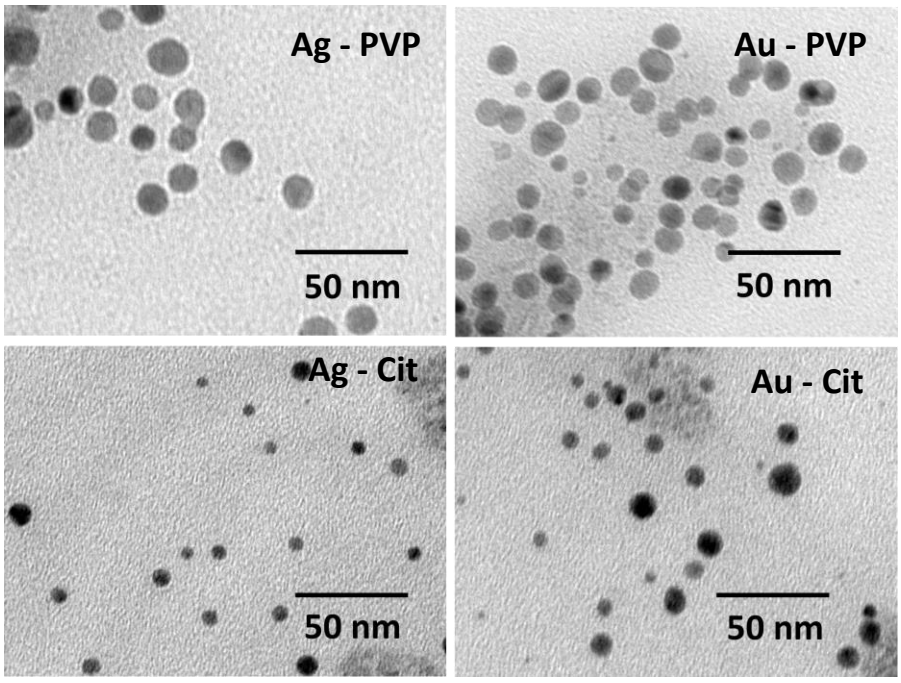

Figure 5.4. TEM images of Ag and Au NPs with different capping agents.

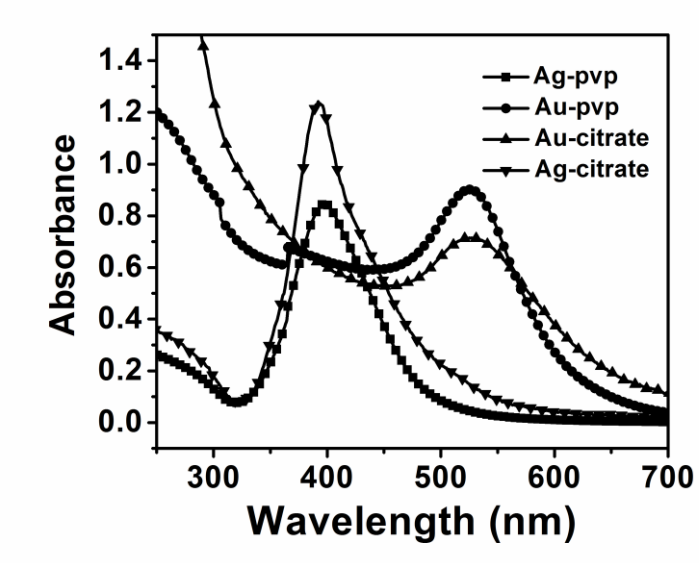

Figure 5.5. UV-Vis spectra of different NPs

The size of the NPs was determined using TEM (Figure 5.4). It clearly shows that all NPs prepared are in the size range of 15-20 nm. The Au and Ag show UV-Vis adsorption due to surface plasmon resonance. The λ_{max} of the NPs change with the

size. The UV-Vis spectra of all NPs were recorded (Figure 5.5). PVP or citrate capped Au-nanoparticles showed absorption maxima at 520 nm and 519 nm respectively, which were similar to the reported values in the literature.[28] Similarly, Ag-nanoparticles showed the absorption maxima at 397 nm and 389 nm. The value obtained was consistent with the value reported in the literature[25] and supports the TEM observations. NPs were further characterized using zetasizer to understand the size and properties in solution. The size and surface zeta potentials of all prepared NPs are measured (Table 5.1).

Table 5.1. Dynamic light scattering analysis of NPs

Nanoparticle	Size (nm)	Zeta potential (mv)
Au – Citrate	**16.73**	**- 40.2**
Au – PVP	**89.33**	**- 24.7**
Ag – Citrate	**14.69**	**- 49.3**
Ag – PVP	**29.65**	**- 32.4**

The hydrodynamic diameter of NPs is slightly higher than the TEM measurements. The citrate capped NPs showed higher zeta potential than that of PVP capped NPs. This clearly indicates that citrate capped NPs exhibits higher surface charge than PVP capped NPs. These results prompt us to treat these nanoparticles as anions and design the adsorbent accordingly.

5.4. Batch adsorption studies

5.4.1. Effects of initial pollutant concentration and contact time

The adsorption rate for different pollutants at 303 K is shown in Figure 5.6. The amount of pollutant adsorbed (mg/g) increased with increase in time and reached equilibrium (12h). The adsorption of chromate ($Cr_2O_7^{2-}$) is higher than arsenate (AsO_4^{3-}) and arsenite (AsO_2^{-}) which may be due to strong affinity with the adsorbent.[29-31]The adsorption of citrate capped NPs is higher than the PVP capped NPs, which may be due to the higher negative surface charge of the NPs.

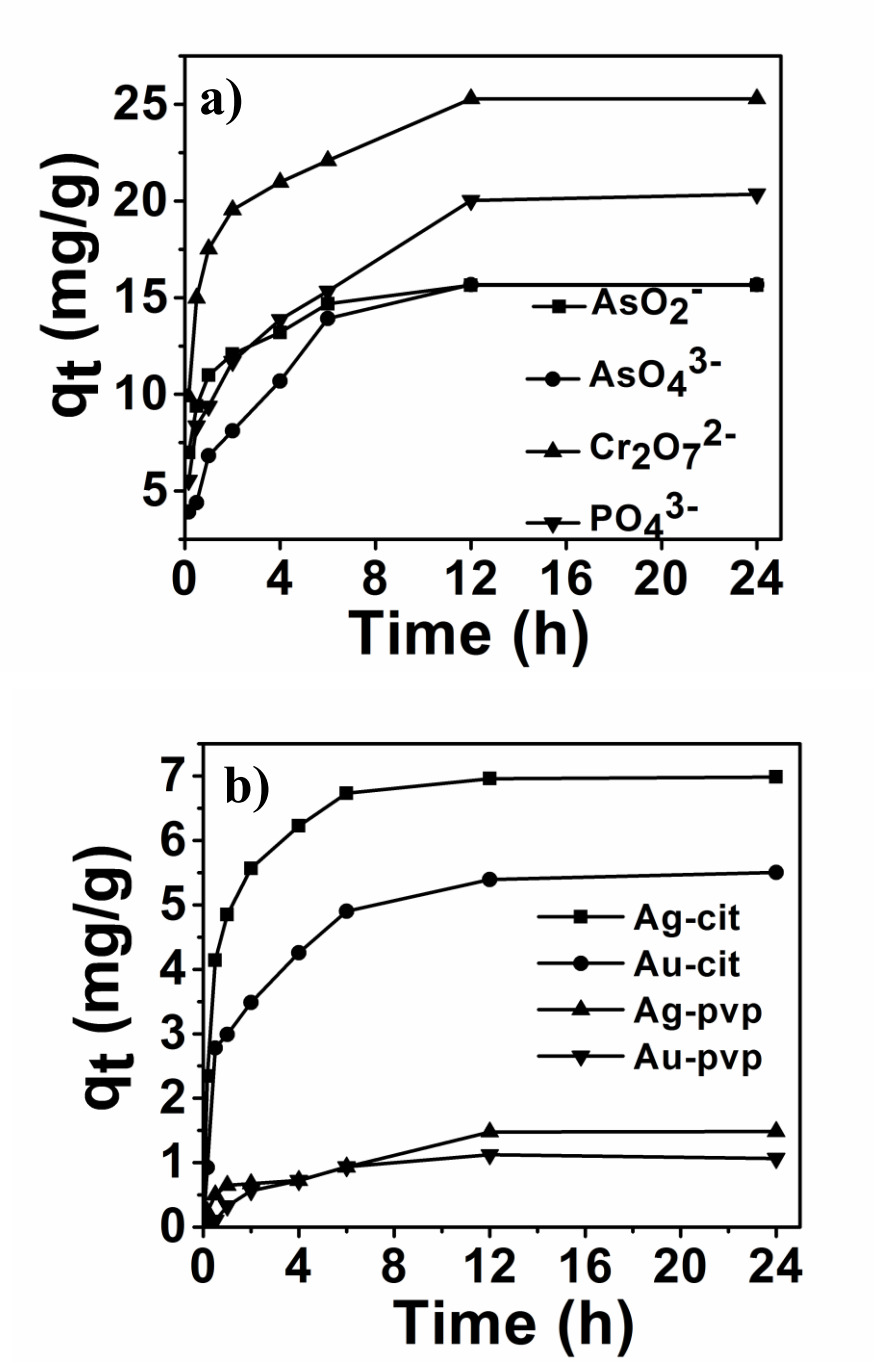

Figure 5.6. The variation of adsorption capacity of Zr treated apple peel towards different anions (a) and nanoparticles (b) with change in time.

The adsorption experiments were carried out for 24 h to evaluate equilibrium adsorption capacity (q_e mg/g) of each anionic pollutant. All anions reach equilibrium within 6 h which indicates faster adsorption. Chromate ions showed highest q_e (25 mg/g) followed by phosphate (18 mg/g), arsenate (14 mg/g) and

arsenite (14 mg/g) ions. Ag-Cit showed highest q_e (6.98 mg/g) followed by Au-Cit (5.50 mg/g), Ag-PVP (1.48 mg/g) and Au-PVP (1.06 mg/g). The results indicate that the Zr treated apple peel bind anionic pollutants efficiently, owing to the high positive charge of Zr cations on the surface.[43]

5.4.2. Effect of pH

The effect of pH on the adsorption of anions onto the Zr loaded apple peel is shown in Figure 5.7, which shows that the adsorption of $Cr_2O_7^{2-}$, AsO_4^{3-} and PO_4^{3-} reaches maximum at acidic pH but AsO_2^- shows higher adsorption at pH 10.

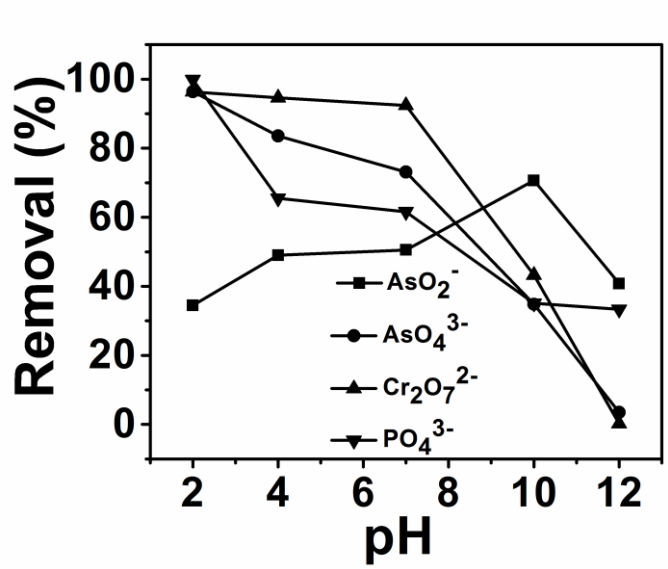

Figure 5.7. The variation of % removal of Zr treated apple peel towards different anions with change in pH.

Arsenic and chromium can exist as different anionic species depending on pH of the solution The dominant species in the acidic pH range are $H_2AsO_4^-$, $HCrO_4^-$, $H_2PO_4^-$ and $HAsO_4^{2-}$ ions which can be adsorbed on the gel by substituting hydroxyl ions from the coordination sphere of the loaded Zr(IV).[43] Maximum adsorption of AsO_2^- was observed at a weakly alkaline environment from pH 9-10 and this was selected for further batch-mode adsorption experiments. This implies that monoanionic ($H_2AsO_3^-$) species are adsorbed by substituting hydroxyl ions or water molecules.[43] At high pH, adsorbates exist as oxoanions and no precipitation was observed. The decrease in arsenic adsorption at higher

pH can be attributed to the competition between the hydroxyl ions and arsenic species for adsorption sites. We selected the Zr cation for chemical modification due to its stability in different pH environments. Release of Zr cations from the peel to the aqueous medium during adsorption studies was tested by analysing Zr content in the adsorbate solution. Elemental analysis showed no detectable concentration of Zr in the solution. We attempted to evaluate the adsorption capacity of the adsorbent towards different NPs at different pHs. We observed that the prepared NPs are not stable at either acidic or basic pH. We conducted all adsorption studies at neutral pH (7).

5.4.3. Isotherm studies

Langmuir Isotherm

The Langmuir isotherm which has been commonly used for describing adsorption processes can be used to explain the adsorption of pollutants on immobilized apple peel. Basic assumption of the Langmuir theory is that adsorption takes place at specific sites within the adsorbent.[33-35] The data obtained from the adsorption experiment for different pollutants were analysed using isotherm equation. The saturation monolayer can be expressed by the equation.[35]

$$\frac{1}{q_e} = \frac{1}{q_m} + \frac{1}{Kq_m C_e} \qquad (5.\ 1)$$

$$q_e = \frac{Kq_m C_e}{1 + q_m C_e} \qquad (5.\ 2)$$

A plot of $1/q_e$ versus $1/ C_e$ results in a linear graphical relation indicating the applicability of the Langmuir model for different anions is shown in Figure 5.8. The Langmuir constants are elucidated from the slope and intercept of straight lines for different anions. The observed linear relationship is statistically significant as evidenced by the R^2 values (close to unity), implying the applicability of isotherm for our extraction studies. Adsorption data for $Cr_2O_7^{2-}$ fits well with Langmuir linear equation with best R^2 value (0.999) than the others. The observed linear relationship is statistically significant as evidenced by the R^2 values; Au-PVP (0.9987), Ag-PVP (0.9919), Au-Cit (0.9961) and Ag-Cit

(0.9978) implying the applicability of isotherm for nanoparticles too. The Langmuir isotherm constants along with correction coefficients are reported in Table 5.2.

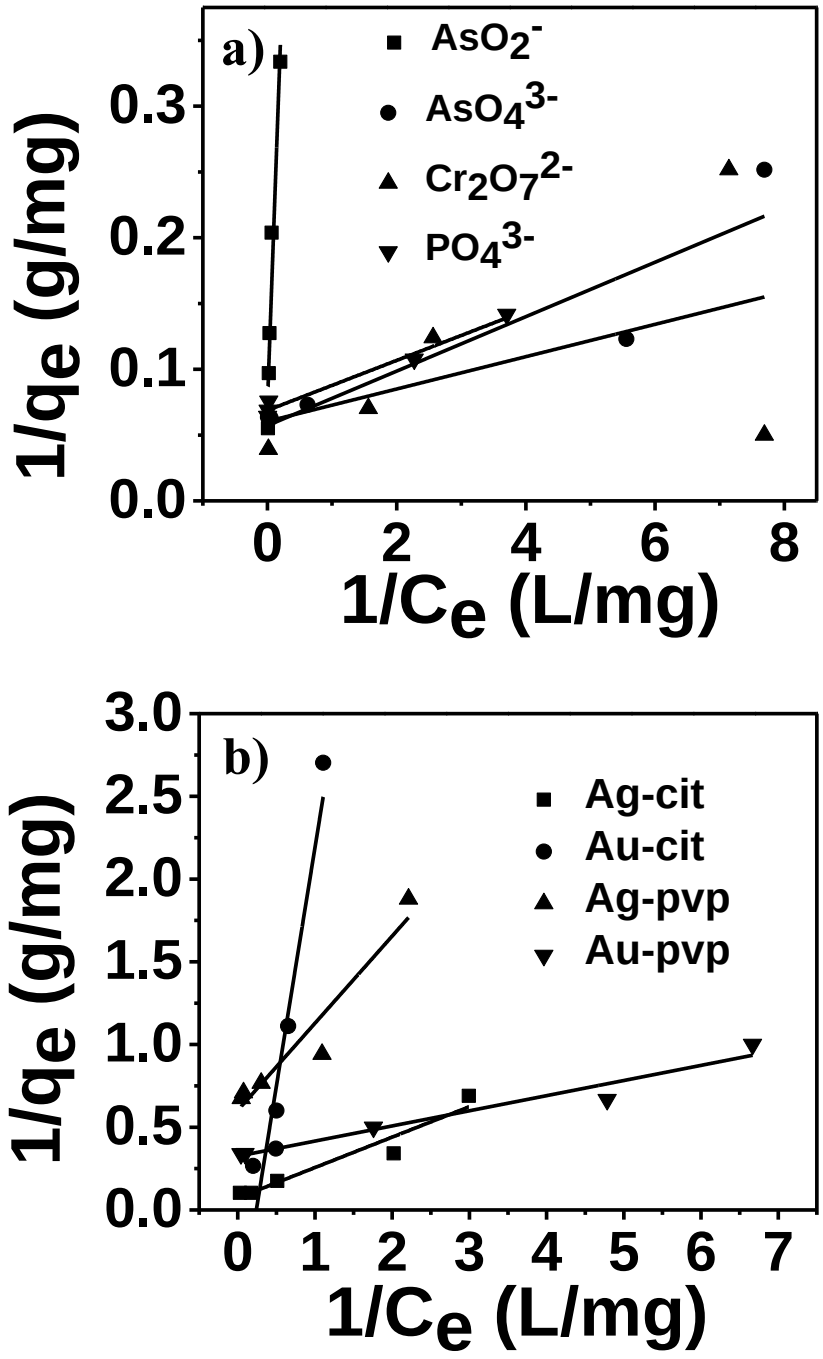

Figure 5.8. Langmuir isotherms for anions (a) and NPs (b) adsorption.

The essential characteristic of the Langmuir isotherm can be expressed in terms of a dimensionless equilibrium parameter, such as the separation factor (R_L) used in the following equation[35]

$$R_L = \frac{1}{1 + KC_e} \qquad (5.\ 3)$$

where K is the Langmuir constant and C_e is the equilibrium concentration of the adsorbate in solution. This parameter indicates that isotherm will be shaped according to the following adsorption characteristics: $R_L > 1$ unfavourable; $R_L = 1$ corresponds to linear; $0 < R_L < 1$ is favourable and $R_L = 0$ is irreversible. The R_L values for AsO_2^- (0.4138), AsO_4^{3-} (0.7578), $Cr_2O_7^{2-}$(0.8294), PO_4^{3-}(0.2468), Au-PVP (0.9105), Ag-PVP (0.4359), Au-Cit (0.6154) and Ag-Cit (0.9001) indicate that the adsorption of anionic pollutants on to treated apple peel is favorable (Table 5.2).

Freundlich isotherm

Freundlich model is an empirical equation based on adsorption on heterogeneous surfaces. It is assumed that the stronger binding sites are occupied first and the binding affinity decreases with an increasing degree of site occupation.[36, 37] The isotherm is expressed as:

$$\text{Ln } q_e = \text{Ln } K_f + \frac{1}{n}\text{Ln } C_e \qquad (5.\ 4)$$

where K_f and n are Freundlich constants related to sorption capacity and sorption intensity of the adsorbent, respectively. K_f can be defined as the adsorption coefficient and represents the quantity of pollutant adsorbed onto treated apple peel for a unit equilibrium concentration. A value for 1/n below 1 refers to a normal Langmuir isotherm while 1/n above 1 represents a cooperative adsorption. The 1/n value for AsO_2^- (0.8124), AsO_4^{3-} (0.8233), $Cr_2O_7^{2-}$(0.9475), PO_4^{3-} (0.5966), Au-PVP (0.8994), Ag-PVP (0.7067), Au-Cit (1.1190) and Ag-Cit (0.9349) indicates that the adsorption follows Freundlich isotherm (Figure 5.9).

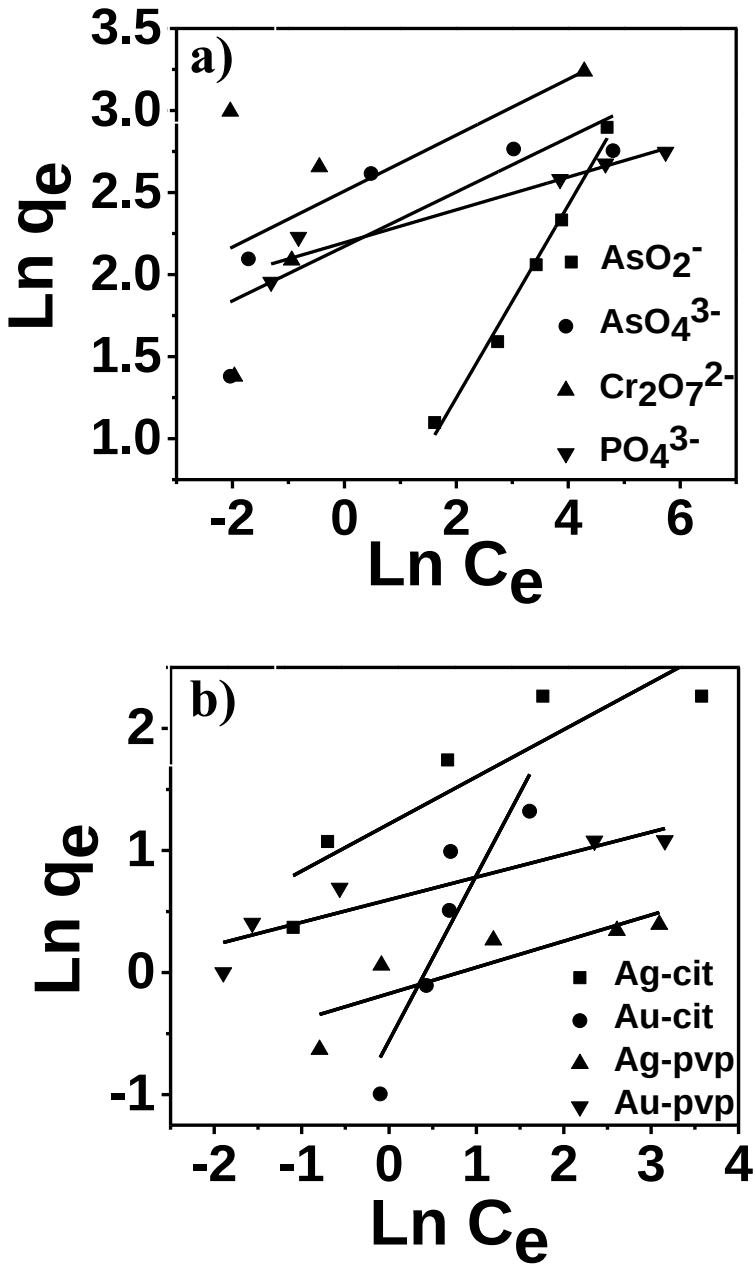

Figure 5.9. Freundlich isotherms for anions (a) and NPs (b) adsorption.

Table 5.2. Langmuir and Freundlich isotherm model constants and correlation coefficients for adsorption of different anions on Zr immobilized apple peel surface.

	Langmuir			Freundlich		
Pollutant	K (L/g)	R_L	R^2	K_F (mg/g)(L/g)^n	1/n	R^2
AsO_2^-	0.0544	0.2687	0.9687	1.0772	0.5873	0.9948
AsO_4^{3-}	2.7666	0.0072	0.9249	8.7716	0.1658	0.8310
$Cr_2O_7^{2-}$	4.9170	0.0041	0.4840	12.2902	0.1707	0.5954
PO_4^{3-}	3.6243	0.0055	0.9895	8.9809	0.0999	0.9706
Ag-Cit	0.3938	0.0483	0.9675	3.3800	0.3862	0.8992
Au-Cit	0.2404	0.0768	0.9555	0.5719	1.3557	0.9126
Ag-PVP	1.1419	0.0172	0.9625	0.8418	0.2149	0.8547
Au-PVP	3.5502	0.0056	0.9771	1.8166	0.1848	0.9256

This isotherm model also yielded good fit with the highest R^2 value for anionic pollutants, which indicates that the adsorption of anions on apple peel surface is a heterogeneous process. Table 5.2 lists the comparison of Langmuir and Freundlich constants for various pollutants on treated apple peel surface. It can be seen from table that Langmuir model was found to fit the data significantly better indicating monolayer adsorption of anions and NPs on apple peel.

5.4.4. Adsorption kinetics

Kinetic models elucidating the mechanism by which pollutants are adsorbed on adsorbent surfaces have been proposed.[38-40] Different adsorption kinetic models were used to investigate the adsorption mechanism. A pseudo-first-order equation (5.5) was used for data analysis.[39]

$$\log (q_e - q_t) = \log q_e - \left(\frac{k_1}{2.303}\right) t \qquad (5.5)$$

where q_e and q_t indicate the amount of pollutant adsorbed (mg / g) at equilibrium and in time t, respectively. $k_1(min^{-1})$ is the first order rate constant applied in the present studies of pollutant adsorption. The plot of log ($q_e - q_t$) versus t for different pollutants (Figure 5.10a & 5.10b) gave first order rate constants k_1 (slope) and equilibrium concentration q_e (intercept). The values of k_1 and q_e for different pollutants were calculated from the plots and shown in Table 5.3. The adsorption kinetics of some systems can also be explained by a pseudo-second-order reaction (Figure 5.10c & 5.10d). The pseudo-second-order equation based on adsorption equilibrium capacity may be expressed in the form,[40]

$$\frac{t}{q_t} = \frac{1}{k_2 {q_e}^2} + \left(\frac{1}{q_e}\right) t \qquad (5.6)$$

where k_2 is the rate constant of pseudo-second-order adsorption and q_e is the equilibrium adsorption capacity (mg / g). The k_2 and q_e values of different pollutants can be calculated experimentally from the slope and the intercept of t / q_t versus t plots. From Table 5.3, the correlation coefficient R^2 for AsO_2^- (0.9937), AsO_4^{3-} (0.9318), $Cr_2O_7^{2-}$(0.9990), PO_4^{3-}(0.9990), Au-PVP (0.9958), Ag-PVP (0.9827), Au-Cit (0.9994) and Ag-Cit (0.9999) indicate that the pseudo-second-order model fits the experimental data better than the pseudo-first-order model. The calculated correlations are closer to unity for the second-order kinetics model and calculated equilibrium adsorption capacities of all pollutants matched with experimental values. The calculated k_2 (g / mg min) and q_e are listed in Table 5.3.

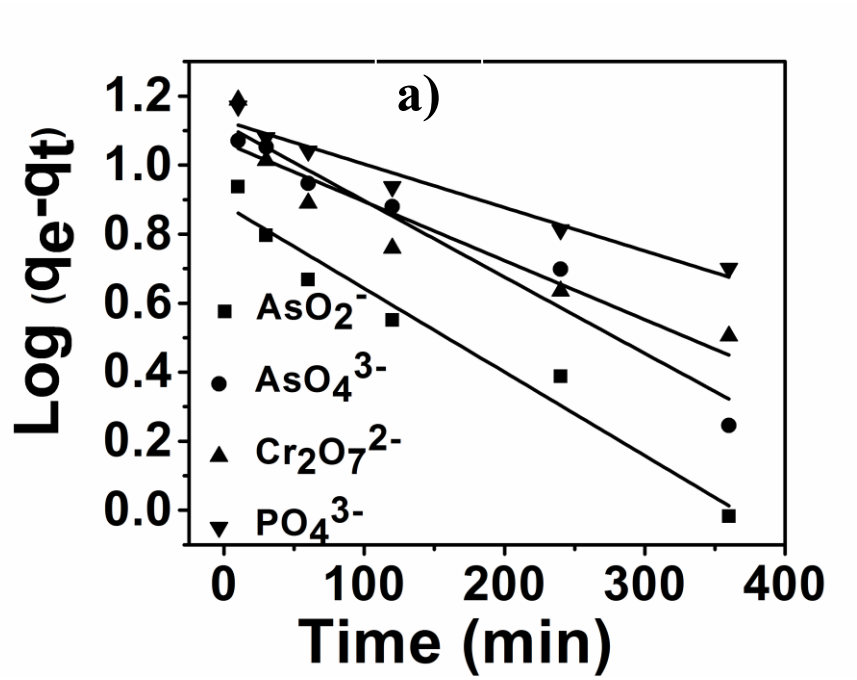
a)
Log (qe-qt)
Time (min)
AsO2-
AsO43-
Cr2O72-
PO43-

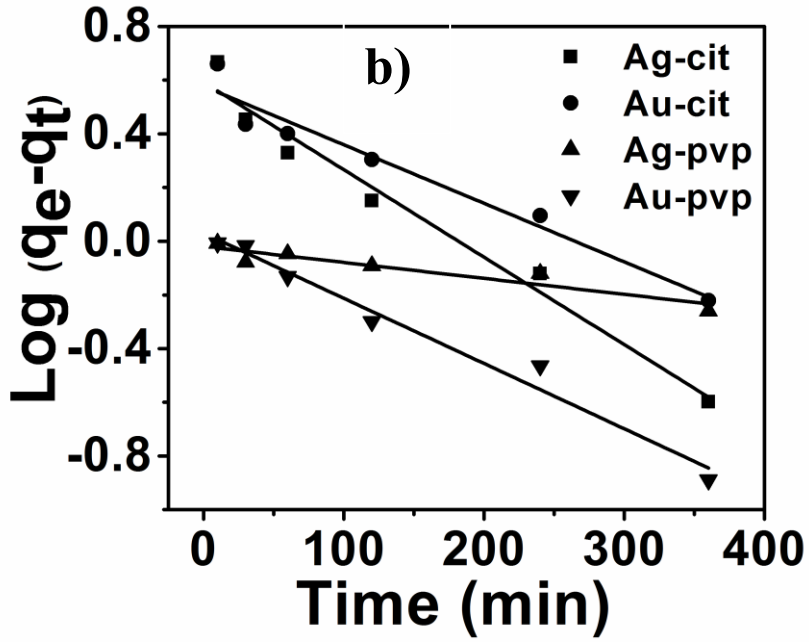
b)
Log (qe-qt)
Time (min)
Ag-cit
Au-cit
Ag-pvp
Au-pvp

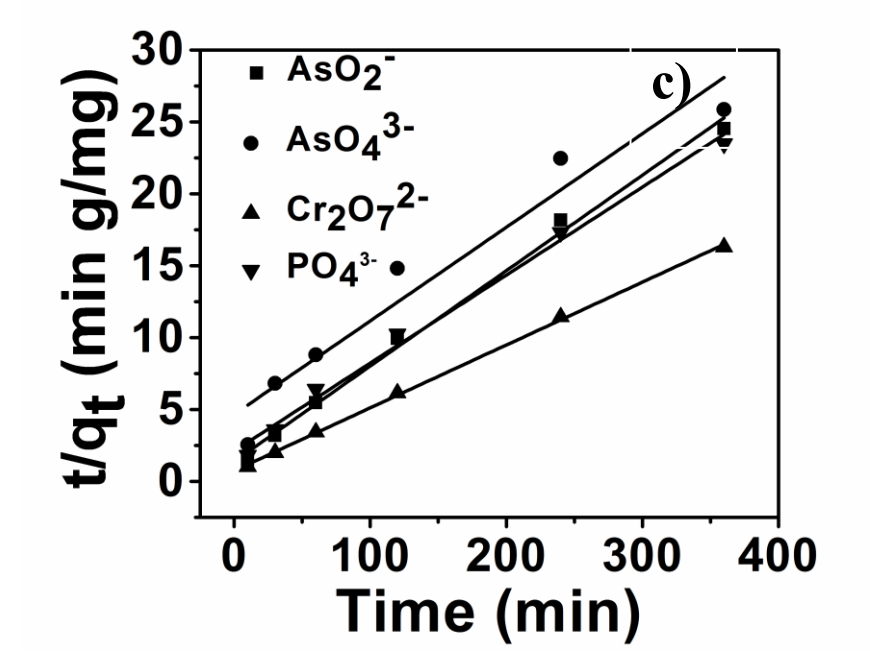

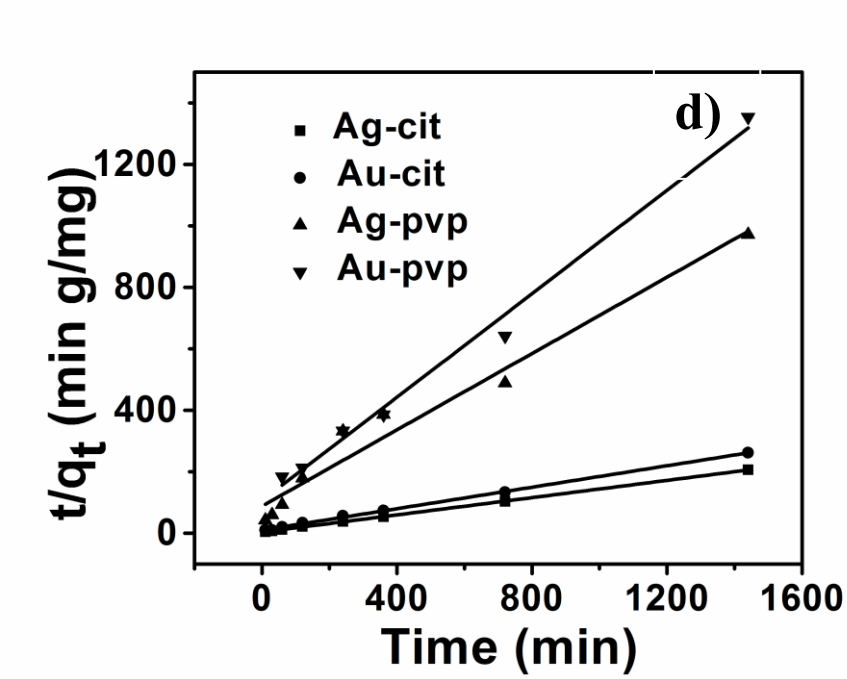

Figure 5.10. Pseudo-first order (a, b) and pseudo-second order (c, d) kinetics for the adsorption of anions (a, c) and NPs (b, d) on to the Zr treated apple peel.

Table 5.3. Pseudo first order and pseudo second order constants and correlation coefficients for adsorption of different anionic contaminants on treated apple peel

Pollutant	Qe(exp) (mg/g)	Pseudo-first order kinetic model			Pseudo-second order kinetic model		
		Qe (mg/g)	K1 (min^{-1})	R^2	Qe (mg/g)	K2 (g/mg min)	R^2
AsO_2^-	15.6400	7.6749	0.0056	0.9542	15.0648	0.0032	0.9937
AsO_4^{3-}	15.6800	13.1039	0.0051	0.9451	15.3681	0.0009	0.9318
$Cr_2O_7^{2-}$	25.2860	11.6322	0.0039	0.8467	22.8676	0.0026	0.9990
PO_4^{3-}	20.3540	13.4444	0.0029	0.9533	16.3425	0.0018	0.9905
Ag-Cit	6.9840	3.9121	0.0075	0.9876	15.0648	7.1250	0.9999
Au-Cit	5.5030	3.7789	0.0050	0.9772	15.3681	5.7277	0.9994
Ag-PVP	1.4810	0.9565	0.0014	0.9378	22.8676	1.6101	0.9827
Au-PVP	1.0640	1.0733	0.0056	0.9890	16.3425	1.1877	0.9958

5.5. Analysis of adsorbent after adsorption

The Zr treated apple peels were analyzed after adsorption of different anions and NPs. SEM (Figure 5.11) clearly shows the NPs adsorbed on the adsorbent surface uniformly. EDS analysis gave characteristic peaks corresponding to Au and Ag. Results indicate that we can successfully remove NPs from water using chemically modified apple peel. The adsorbent was washed with deionised water to remove free anions after adsorption and dried at room temperature. The peels were analyzed using EDS (Figure 5.12) and the peaks corresponding to Cr and As

were seen in the spectra along with Zr, which confirms the binding of anions on the surface of Zr treated apple peel.

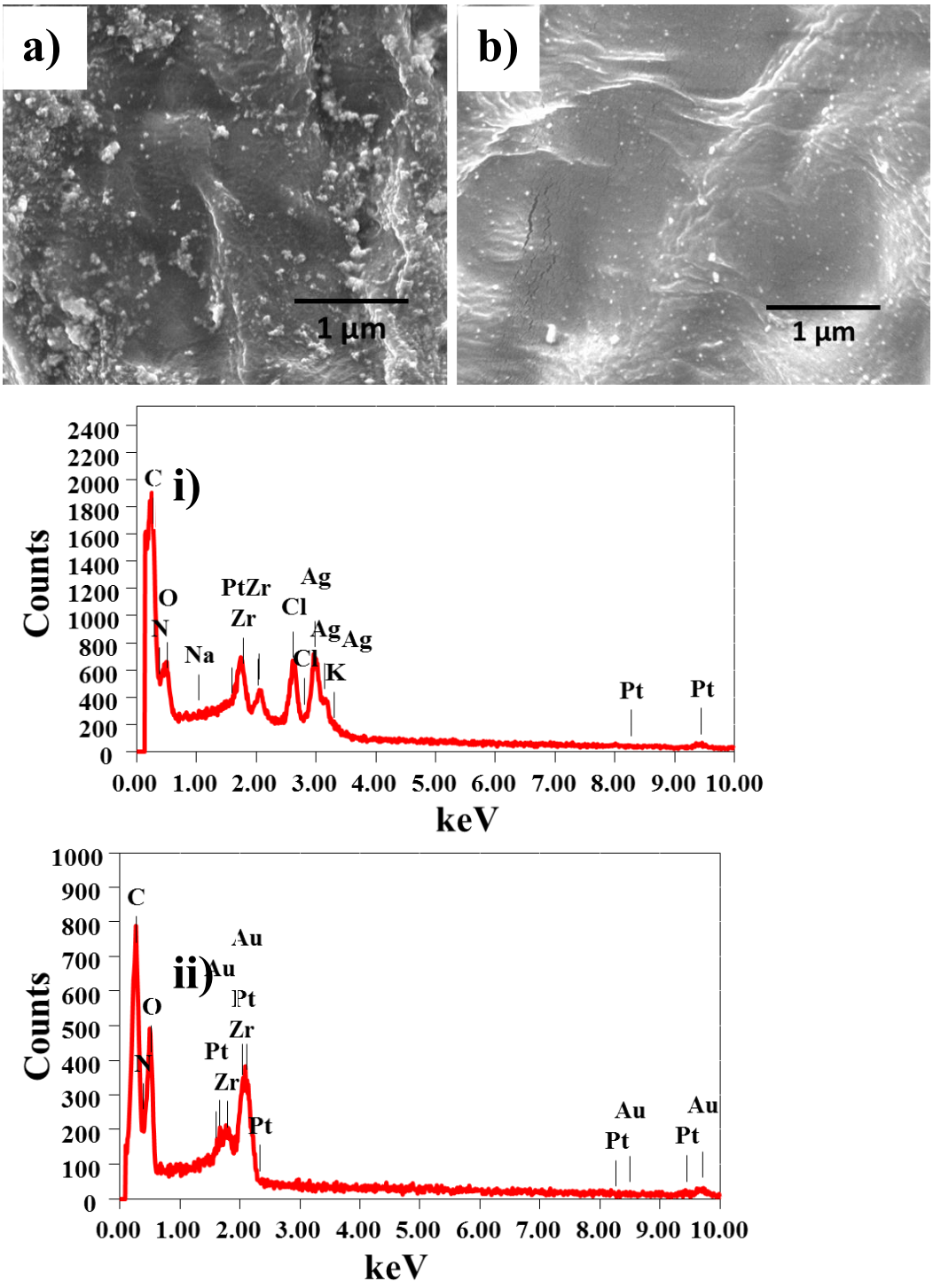

Figure 5.11. SEM (a, b) and EDS (i, ii) analysis of Zr treated apple peel with Ag (a, i) and Au (b, ii) adsorbed on the surface.

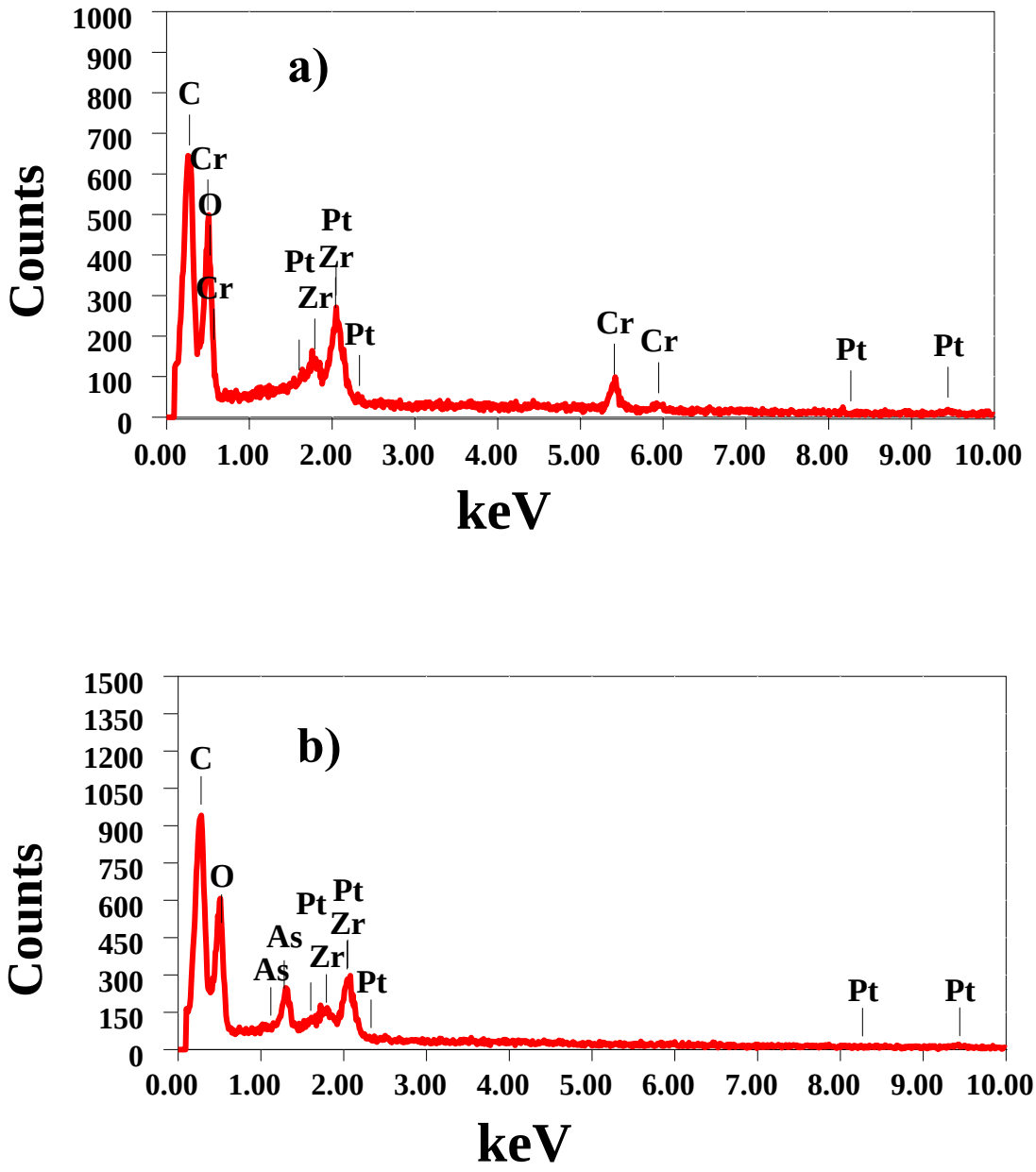

Figure 5.12. EDS analysis of Zr treated apple peel surface after adsorption of chromate (a) and arsenate (b) anions.

5.6. Desorption studies

Binding mechanism can be further investigated by using desorption process. The nature of the adsorption of pollutant onto the surface of the peels involves electrostatic attractions between anions and Zr(IV) present on the surface. Desorption of these pollutants were studied at different pH (2-12) at a constant temperature of 30 °C. Minimum desorption was observed at acidic pH but about 90% of pollutants were desorbed at pH 12 within 10 min (Figure 5.13).

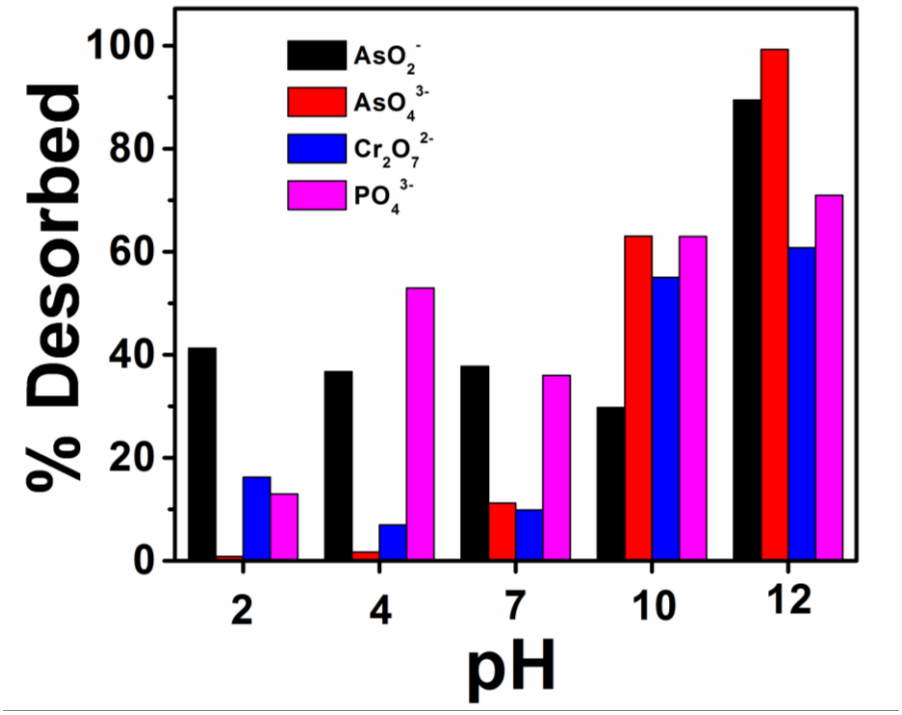

Figure 5.13. Desorption of anions from the Zr immobilized apple peel surface at various pH under ambient conditions.

Under basic condition, OH^- ions will replace anionic pollutants from apple peel surface. In order to show the reusability of the adsorbent, the adsorption-desorption cycle of pollutants were repeated five times using the same experimental conditions. These results showed that recycling of treated apple peel is efficient and can be used in repeated pollutant adsorption studies without detectable losses in their adsorption capacities. We observed the instability of nanoparticles with the change of pH. Regeneration of the NPs adsorbed apple peel is difficult using elution process. Alternative methods should be explored for this purpose.

5.7. Conclusions

We designed chemically modified apple peel as an efficient adsorbent. Extraction of different toxic anions including chromate, phosphate, arsenate and arsenite ions and nanoparticles (Au & Ag) were evaluated using Zr(IV) loaded apple peel as an adsorbent. Adsorption and desorption studies were conducted to understand the adsorption mechanism. Langmuir and Freundlich isotherm models were used to validate the adsorption process. Kinetic studies were done to understand the adsorption process, which follows pseudo-second-order kinetics. Immobilized apple peels showed efficient adsorption towards different anionic pollutants with experimental adsorption capacities (mg/g) of 15.64 (AsO_2^-), 15.68 (AsO_4^{3-}), 25.28 ($Cr_2O_7^{2-}$), 20.35 (PO_4^{3-}), 6.98 (Ag-Cit), 5.50 (Au-Cit) 1.48 (Ag-PVP) and 1.06 (Au-PVP) mg/g. Experimental factors such as pH and contact time of the solution also influence the extraction efficiency. The Zr on apple peel is responsible for the extraction of different contaminants in water. It is conceivable that the use of such biowaste is simple, cost effective and efficient method for water treatment and can be used in large scale applications.

5.8. References

(1) Smedley, P. L.; Kinniburgh, D. G. *Applied Geochemistry* **2002**, *17*, 517.

(2) Gotoh, T.; Matsushima, K.; Kikuchi, K. I. *Chemosphere* **2004**, *55*, 57.

(3) Nriagu, J. O. *Environmental Pollution* **1988**, *50*, 139.

(4) *Guidelines for drinking-water quality,* 2nd ed.; Geneva, Switzerland, Vol. 2, WHO 1996 (ISBN 92 4 154480 5).

(5) Guo, H. R.; Chiang, H. S.; Hu, H.; Lipsitz, S. R.; Monson, R. R. *Epidemiology* **1997**, *8*, 545.

(6) Hopenhayn-Rich, C.; Biggs, M. L.; Smith, A. H. *International Journal of Epidemiology* **1998**, *27*, 561.

(7) Reiss, G.; Hutten, A. *Nature Mateials* **2005**, 4, 725.

(8) Malik, A. H.; Khan, Z. M.; Mahmood, Q.; Nasreen, S.; Bhatti, Z. A. *Journal of Hazardous Materials* **2009**, *168*, 1.

(9) Yuchi, A.; Ogiso, A.; Muranaka, S.; Niwa, T. *Analytica Chimica Acta* **2003**, *494*, 81.

(10) Namasivayam, C.; Sangeetha, D. *Journal of Colloid and Interface Science* **2004**, *280*, 359.

(11) Biswas, B. K.; Inoue, K.; Ghimire, K. N.; Ohta, S.; Harada, H.; Ohto, K.; Kawakita, H. *Journal of Colloid and Interface Science* **2007**, *312*, 214.

(12) Teow, Y.; Asharani, P. V.; Hande, M. P.; Valiyaveettil S. *Chem. Commun.*, **2011**, 47, 7025.

(13) Kundu, S.; Pal, A.; Mandal, M.; Kumar Ghosh, S.; Panigrahi, S.; Pal, T. *Journal of Environmental Science and Health - Part A Toxic/Hazardous Substances and Environmental Engineering* **2004**, *39*, 185.

(14) Deschamps, E.; Ciminelli, V. S. T.; Höll, W. H. *Water Research* **2005**, *39*, 5212.

(15) Gupta, V. K.; Saini, V. K.; Jain, N. *Journal of Colloid and Interface Science* **2005**, *288*, 55.

(16) Deng, S.; Ting, Y. P. *Water Science and Technology* **2007**, *55*, 177.

(17) Zhang, G.; Qu, J.; Liu, H.; Liu, R.; Wu, R. *Water Research* **2007**, *41*, 1921.

(18) Yang, L.; Wu, S.; Chen, J. P. *Industrial and Engineering Chemistry Research* **2007**, *46*, 2133.

(19) Boddu, V. M.; Abburi, K.; Talbott, J. L.; Smith, E. D.; Haasch, R. *Water Research* **2008**, *42*, 633.

(20) Sierra-Alvarez, R.; Field, J. A.; Cortinas, I.; Feijoo, G.; Teresa Moreira, M.; Kopplin, M.; Jay Gandolfi, A. *Water Research* **2005**, *39*, 199.

(21) Chang, Y. Y.; Kim, K. S.; Jung, J. H.; Yang, J. K.; Lee, S. M. *Water Science and Technology* **2007**, *55*, 69.

(22) Masue, Y.; Loeppert, R. H.; Kramer, T. A. *Environmental Science and Technology* **2007**, *41*, 837.

(23) Violante, A.; Del Gaudio, S.; Pigna, M.; Ricciardella, M.; Banerjee, D. *Environmental Science and Technology* **2007**, *41*, 8275.

(24) Zhang, S.; Liu, C.; Luan, Z.; Peng, X.; Ren, H.; Wang, J. *Journal of Hazardous Materials* **2008**, *152*, 486.

(25) Czerniczyniec, M.; Farías, S.; Magallanes, J.; Cicerone, D. *Water, Air, and Soil Pollution* **2007**, *180*, 75.

(26) Ciardelli, M. C.; Xu, H.; Sahai, N. *Water Research* **2008**, *42*, 615.

(27) Chen, W.; Parette, R.; Zou, J.; Cannon, F. S.; Dempsey, B. A. *Water Research* **2007**, *41*, 1851.

(28) Feo, J. C.; Ordoñez, E.; Letek, M.; Castro, M. A.; Muñoz, M. I.; Gil, J. A.; Mateos, L. M.; Aller, A. J. *Water Research* **2007**, *41*, 531.

(29) Ahluwalia, S.S.; Goyal, D. *Bioresource Technology* **2007,** *98*, 2243.

(30) Wan Ngah, W.S.; Hanafiah, M.A.K.M. *Bioresource Technology* **2008**, *99*, 3935.

(31) Oke, I. A.; Olarinoye, N. O.; Adewusi, S. R. A. *Adsorption* **2008**, *14*, 73.

(32) Mohan, D.; Pittman Jr, C. U. *Journal of Hazardous Materials* **2007**, *142*, 1.

(33) Say, R.; Yilmaz, N.; Denizli, A. *Separation Science and Technology* **2003**, *38*, 2039.

(34) Teixeira, M. C.; Ciminelli, V. S. T. *Environmental Science and Technology* **2005**, *39*, 895.

(35) Seki, H.; Suzuki, A.; Maruyama, H. *Journal of Colloid and Interface Science* **2005**, *281*, 261.

(36) Zouboulis, A. I.; Katsoyiannis, I. A. *Industrial and Engineering Chemistry Research* **2002**, *41*, 6149.

(37) Mallampati, R.; Valiyaveettil, S. *RSC Advances* **2012**, *2*, 9914.

(38) Ghimire, K. N.; Inoue, K.; Ohto, K.; Hayashida, T. *Bioresource Technology* **2008**, *99*, 32.

(39) Yoshida, I.; Konami, T.; Shimonishi, Y.; Morise, A.; Ueno, K. *Nippon Kagaku Kaishi* **1981**, 379.

(40) Suzuki, T. M.; Bomani, J. O.; Matsunaga, H.; Yokoyama, T. *Reactive and Functional Polymers* **2000**, *43*, 165.

(41) Sun J; Chu, Y.F.; Wu, X.; Liu, R. H. *Journal of Agricultural and Food Chemistry* **2002**, 50, 7449.

(42) Vinson Ja; Su, X.; Zubik, L.; Bose, P. *Journal of Agricultural and Food Chemistry* **2001**, 49, 5315.

(43) Biswas, B. K.; Inoue, J.-i.; Inoue, K.; Ghimire, K. N.; Harada, H.; Ohto, K.; Kawakita, H. *Journal of Hazardous Materials* **2008**, *154*, 1066.

CHAPTER 6

BIOMIMETIC METAL OXIDES FOR THE EXTRACTION OF NANOPARTICLES FROM WATER

Publication from this chapter

R. Mallampati and S. Valiyaveettil, Biomimetic synthesis of metal oxides for the extraction of nanoparticles from water, *Nanoscale*, 2013, 5, 3395-3399.

6.1. Introduction

One of the most important problems affecting people around the world is inadequate access to clean water and sanitation.[1] This problem is expected to grow worse in the future due to over usage, lack of conservation methods and dwindling natural supply of clean water even in countries with significant water resources. In order to make water accessible to majority of population, robust water purification methods at a lower cost and minimal energy consumption need to be developed, while at the same time decreasing the use of chemicals and reducing the impact on environment. Water is usually contaminated with pollutants such as dissolved organic pollutants and heavy metal ions. Even though, many technologies involving different chemical and physical methods have been developed,[2,3] water purification still requires multiple stages to remove pollutants. The most challenging task is to find cost and energy efficient technologies for eliminating all types of pollutants from water.

Research on nanomaterials is currently an area of intense scientific interest due to wide variety of potential applications in biomedical, catalytic and electronic fields.[4,5] However, such a wide range of applications tend to overlook at the dangers that nanoparticles pose to the environment and to human health. For instance, many *in vitro* and *in vivo* studies have demonstrated the toxicity of silver and gold nanoparticles to mammalian cells.[6-8] Silver nanoparticles are known to disrupt life processes by causing DNA damage and mitochondria impairment in mammalian cells.[9,10] Since environmental pollution from nanomaterials is imminent in the near future, it is important to design functional materials capable of removing nanomaterials from the environment. Ironically, various nanomaterials have been proposed for water purification due to their higher surface area with active sites, but no discussion on contamination of water with such materials is provided.[2, 3] In recent years, many metal oxides such as Fe_3O_4, CeO_2, TiO_2 and Al_2O_3 have been used to remove toxic metal ions and organic pollutants from water.[11-19] The material and method of choice should be based on

a few factors such as low cost, availability, mechanical strength, low toxicity, high extraction efficiency and fast adsorption rates for pollutants.

Eggshell membrane (ESM) serves as an attractive biotemplate for synthesizing bioinspired materials. ESM fibers consists of functional proteins and glycoproteins.[20] We hypothesize that the hydrophilic amino and carboxyl groups of the glycoproteins on the ESM fiber surface can be used to complex and deposit metal ions.[21] It is conceivable that such functional groups act as structure directing agents to assemble metal oxide nanocrystallites. In addition, ESM is readily available and offers unique porous interwoven fibrous structure which can act as an excellent template for inorganic material synthesis. In this work, ESM is used as a biotemplate for the synthesis of ZnO, NiO, CuO, Co_3O_4, and CeO_2 in large amounts and investigated the extraction efficiency towards nanoparticles in water.

6.2. Characterization

The TGA analysis was used to understand the calcination process of the metal oxides. The TGA traces in Figure 6.1 shows the decomposition patterns of ESM and composite with metal ions. Gradual weight loss for both pure ESM and the metal salt composites started at around 200 °C which corresponds to ESM decomposition,[23,24] and completed at a temperature of around 600 °C. Even though, ESM was completely decomposed at a temperature of 600 °C, the composite was heated in air up to 750 °C to remove traces of organic materials.
The constant weight (10 %) after 570 °C indicates the completion of organic matter decomposition and formation of stable metal oxides.

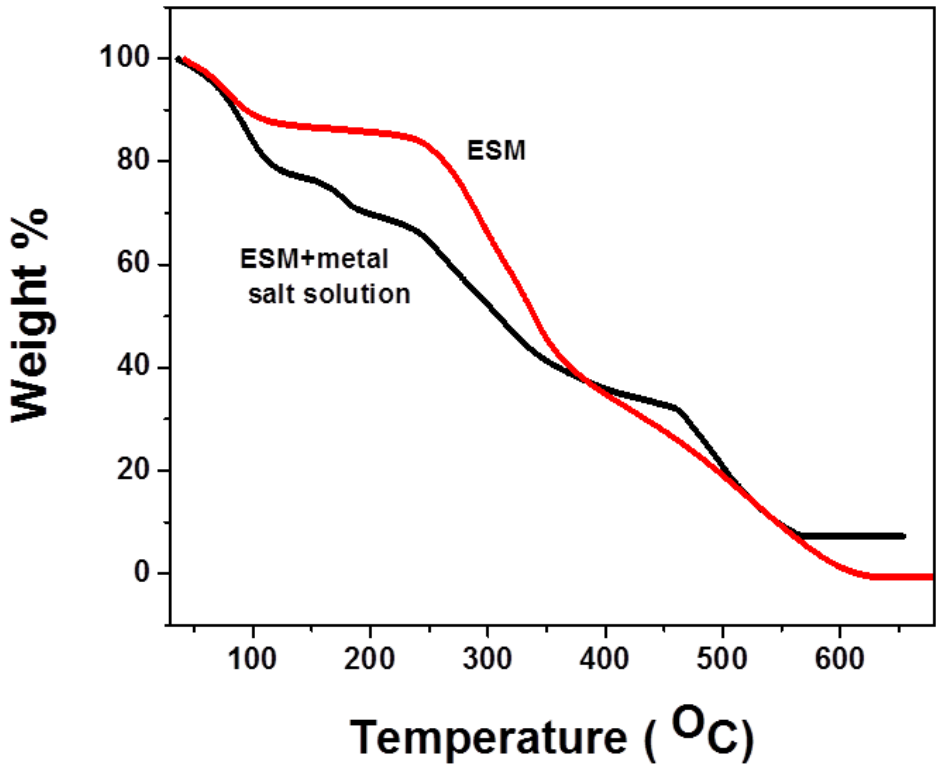

Figure 6.1. TGA curves of natural ESM and copper nitrate adsorbed on ESM

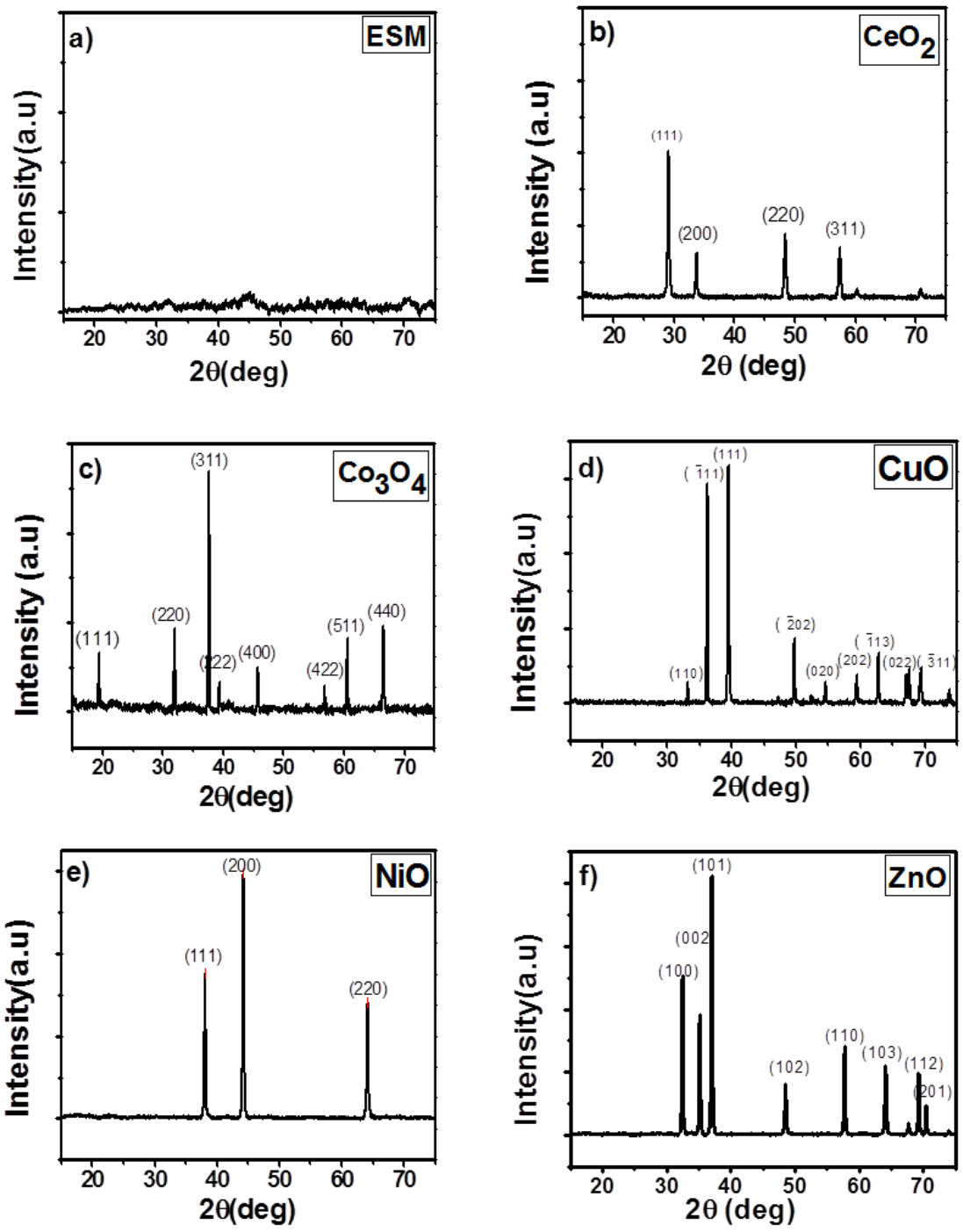

Figure 6.2. X-ray diffraction pattern of a) natural ESM, b) CeO_2, c) Co_3O_4, d) CuO, e) NiO and f) ZnO

XRD analyses were done to establish the chemical identities of the prepared metal oxides. Powder XRD patterns of ESM and the synthesized metal oxides are given

in the Figure 6.2, compared with reported literature and identified as ZnO (JCPDS 80-0075), CuO (JCPDS 80-1917), Co_3O_4 (JCPDS 80-1532) and CeO_2 (JCPDS 81-0792). The EDS analysis before and after the calcination of one of the ESM - CuO composites is shown in supporting information (Figure 6.3). The data shows the presence of carbon and sulphur associated with the organic components in ESM, but after calcination, those elements were removed from the sample.

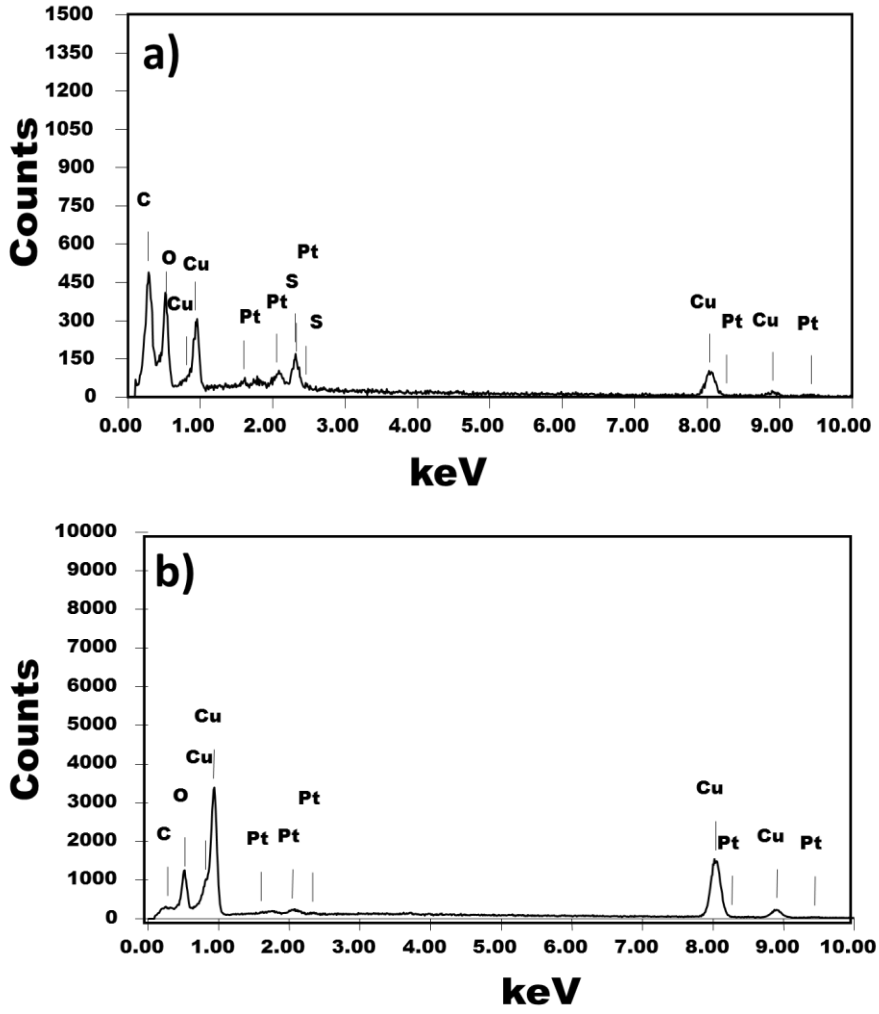

Figure 6.3. EDX analysis of ESM copper composite a) before calcination and b) after calcination

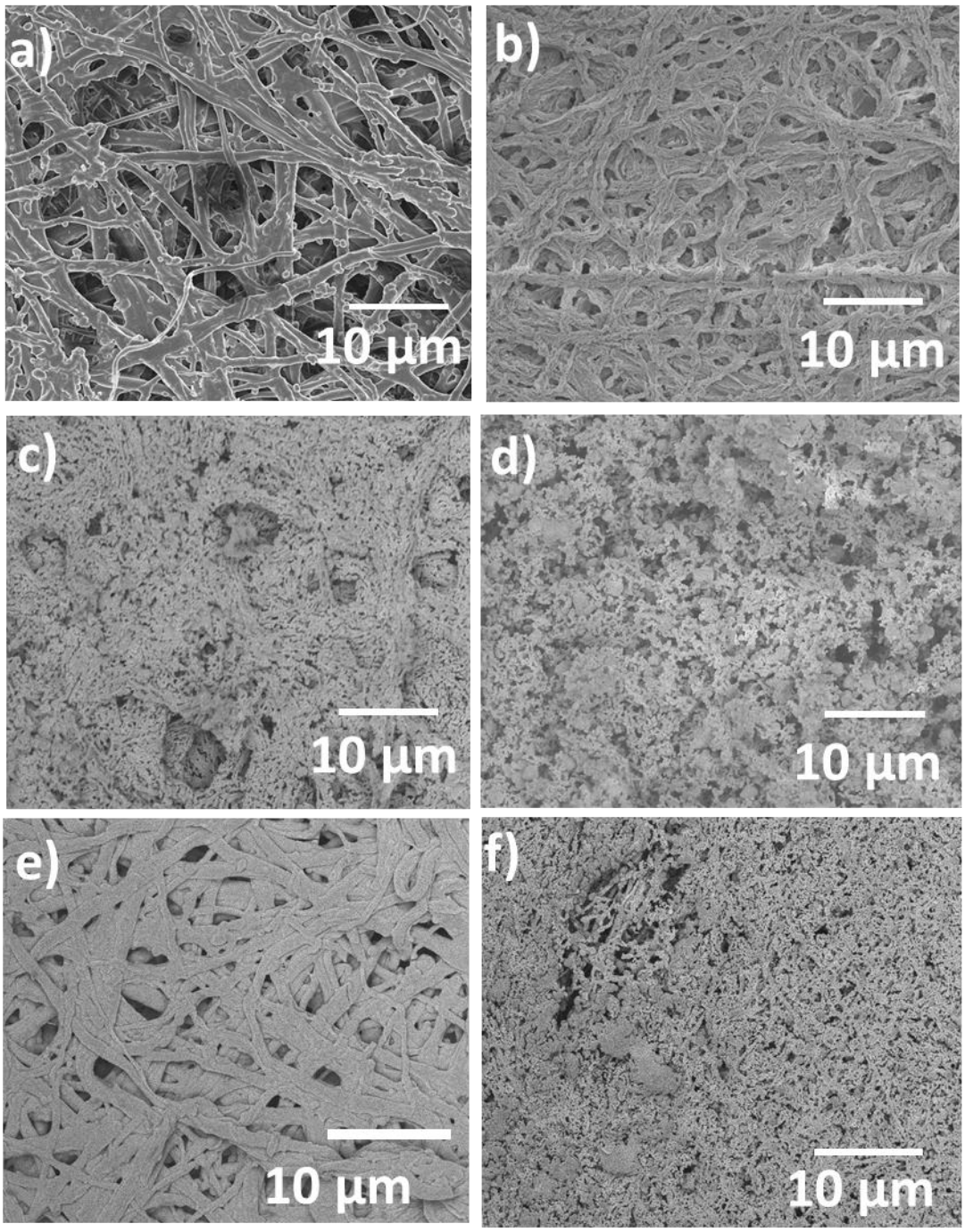

Figure 6.4. SEM images of (a) natural ESM and oxides (b) CeO_2, (c) Co_3O_4, (d) CuO, (e) NiO and (f) ZnO synthesized on ESM template.

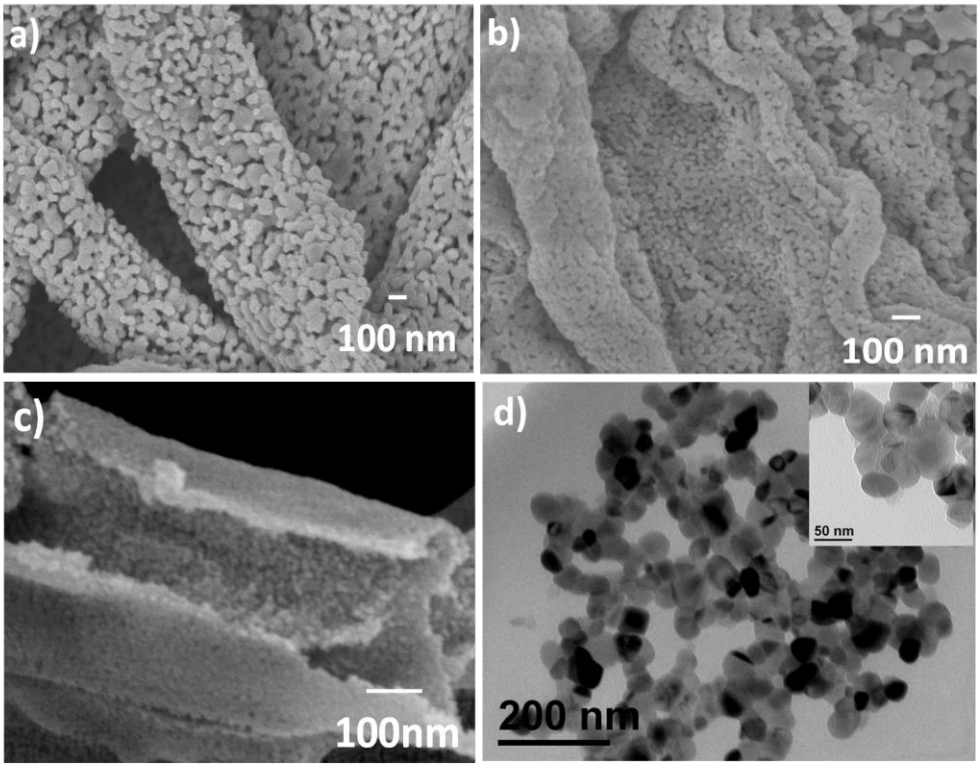

Figure 6.5. Magnified SEM images of (a) NiO, (b) CeO_2, (c) opened cavity of a CeO_2 tubes and (d) TEM of CeO_2 nanoparticles

The FESEM micrographs of pure ESM and metal oxides are shown in Figure 6.4. At a lower magnification, it can be seen that most of the metal oxides have the interwoven microporous structure of ESM. On closer inspection of the FESEM images (Figure 6.5), the tubes consist of many well-ordered nanocrystallites in the range of 20 – 50 nm. The large number of micro- and nanopores were formed due to the emission of gases such as CO_2, NO_x and H_2O during degradation of the template. From SEM images, the metal oxides showed a 3D micro / nanocomposite structure formed via a hierarchical organization of nanocrystals with a micrometer size range. The formation of such tubes (Figure 6.5c) is possible only through a biotemplate synthesis. The nanosized crystallites together with the multiple pores provide desirable physical properties such as high surface area, robustness, high efficiency of extraction and easy recovery for nanoparticle extraction from water. We tested the stability of metal oxides in water by examining the concentration of metal ions by ICP-OES after adsorption process and result showed that no detectable metal contents leached from the adsorbent.

The N_2 adsorption desorption method was carried out to measure the specific surface area of the materials. The BET technique utilizes physical adsorption behaviour of gas molecules on a solid surface at constant temperature. BET data (Table 6.1) indicates that the surface areas of all metal oxides vary significantly. It is hypothesized that metal oxides with larger surface area show high adsorption efficiencies for nanoparticles. It was determined that CeO_2 and NiO have the largest surface area of 17.22 m^2/g and 7.32 m^2/g, respectively, as compared to other metal oxides which are expected to show enhanced adsorption efficiency.

Table 6.1. Summary of the BET surface area (m2/g) and IEPS values for the metal oxides.

Metal oxides	Surface area (m^2/g)	Isoelectric point (IEPS)[27]	adsorption capacity (Q t)/ mg / g	
			Au - PVP	Ag - PVP
NiO	7.32	10.30	76.80	54.84
ZnO	17.22	7.10	48.94	47.56
CeO_2	3.68	9.30	45.84	41.89
Co_3O_4	1.43	7.30	32.27	51.04
CuO	1.21	9.50	3.38	5.02

6.3. Adsorption of nanoparticles

Ag-PVP and Au-PVP nanoparticles were chosen for the adsorption studies owing to the fact that such nanoparticles already exist in commercial products. PVP was chosen as the capping agent for the nanoparticles as it is nontoxic, water soluble and readily available. UV-Vis spectra were recorded (Figure 6.6) to study the optical properties of the nanoparticles.

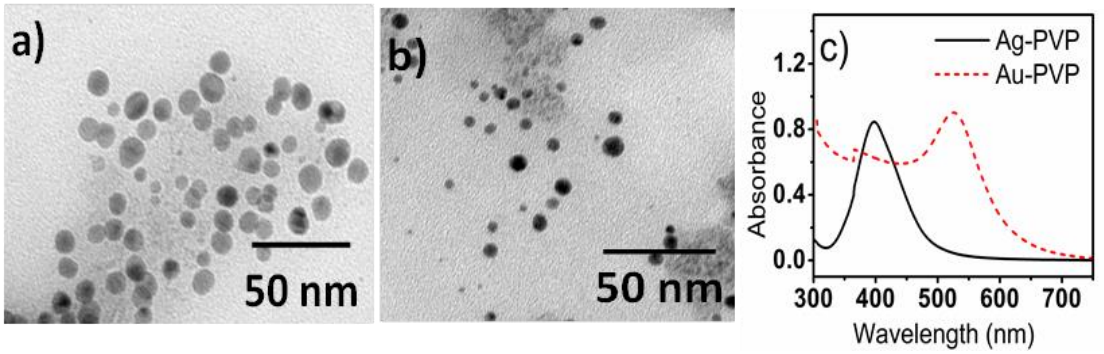

Figure 6.6. TEM images of (a) Ag-PVP, (b) Au-PVP nanoparticles and the corresponding (c) UV-VIS spectra

Adsorption maxima were observed at 514 nm and 400 nm for Au and Ag nanoparticles, respectively. TEM images shown in Figures 6.6 (a-b) indicated that the Au nanoparticles have a particle size distribution in the range of of 5 to 7 nm while the Ag nanoparticles have a wider particle distribution of 7 to 13 nm. Adsorption studies were carried out by adding 20 mg of metal oxides to 10 mL of 2.5 x 10^{-4} M nanoparticle solutions and recording the UV-Vis spectra of the aqueous solutions at different time intervals. Extraction data for nickel oxide for both nanoparticles are given in Figure 6.7. The intensities of absorption peaks at 514 nm (Au NP) and 400 nm (Ag NP) solutions were decreased with time. The optical images (Figure 6.7) of the nanoparticle solutions showed a decrease in color intensity with increase in time of extraction indicating the removal of nanoparticles. The maximum adsorption capacity at a given time (Q_t) explains the performance of the material towards extraction. Q_t was calculated for both Au and Ag NP solutions by using the equation, $Q_t = (C_0 - C_t)$ V/m where Q_t is the maximum adsorption capacity (mg g^{-1}) at a given time, C_0 is the initial concentration (mg L^{-1}), C_t is the final concentration (mg L^{-1}) at a given time, V is the volume (L) of the sample taken for analysis and m is the weight of the sorbent (g).

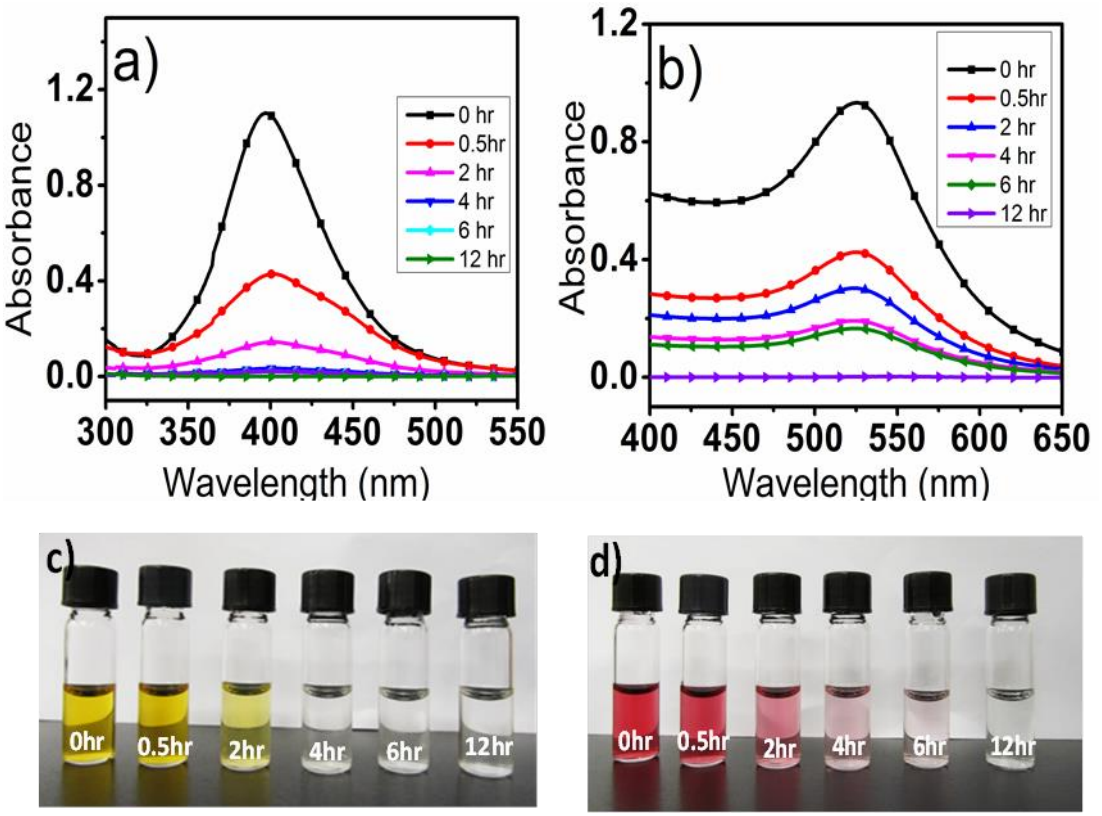

Figure 6.7. UV-VIS spectra (a) Ag-PVP and (b) Au-PVP and corresponding optical images of (c) Ag-PVP and (d) Au-PVP nanoparticle solutions at different time intervals.

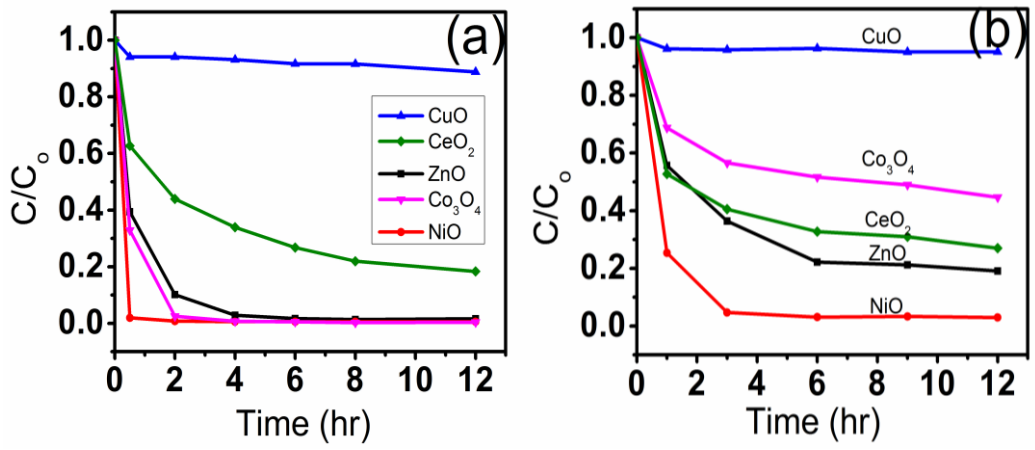

Figure 6.8. Adsorption capacities of different metal oxides towards (a) Ag-PVP and (b) Au-PVP nanoparticles. C_0 is the initial concentration of the nanoparticle solution and C is the remaining concentration at different time intervals during the extraction.

The calculated adsorption capacities of nanoparticles for various metal oxides are listed in Table 6.1. The results indicate that NiO showed quantitative adsorption for Au nanoparticles within 3 hours and Ag nanoparticles around 0.5 hours (Figure 6.8). However, CuO showed relatively low adsorption capacity for both nanoparticles. From these observations, the adsorption efficiencies of the metal oxides for Au nanoparticles can be ranked with decreasing order, NiO > ZnO> CeO_2 > Co_3O_4 > CuO and for Ag nanoparticles, NiO > Co_3O_4 > ZnO > CeO_2 > CuO. These results are in good agreement with the BET surface area analysis data of the metal oxides, indicating that higher surface area leads to higher extraction efficiency.

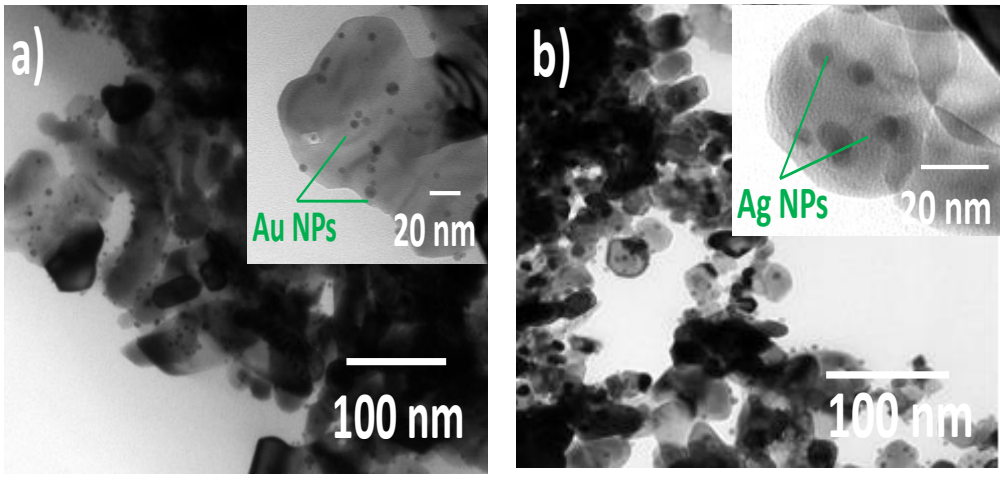

Figure 6.9. TEM images of (a) Au and (b) Ag nanoparticles on NiO particles after extraction. Inset shows the magnified images of metal oxide surface showing the presence of nanoparticles.

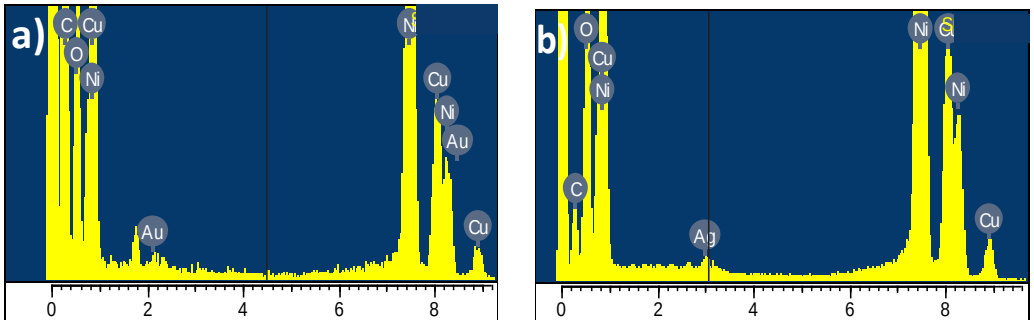

Figure 6.10. EDX analysis of a) Au NPs on NiO surface and b) Ag NPs on NiO surface

TEM analysis was performed using NiO samples after extraction to confirm the adsorption of nanoparticles on the surface of metal oxide crystals. From the TEM images (Figure 6.9), crystal grains of the metal oxides with a size of 50 nm were observed. A closer inspection of the magnified images (see inset) showed the presence of metal nanoparticles on the surface of the metal oxides. Further confirmation of nanoparticles on the surface of metal oxide before and after extraction was obtained from TEM-EDS analysis (Figure 6.10). Peaks corresponding to Au and Ag metal can be seen on the surface after extraction.

6.4. Plausible mechanism

Synthesis and mechanism of metal oxides were reported earlier.[23, 24] All metal oxides were fully characterized and used for the extraction of nanoparticles from water. In the case of metal oxide surfaces, the absence of sufficient number of neighboring atoms as compared to the bulk atoms result in a positive free energy of formation. Hence a metal oxide surface may exhibit surface relaxation or surface reconstruction in order to increase the symmetry and ligand coordination at the surface. For example, in the case of ZnO [25], Zn atoms tend to relax into a close-packed plane of oxygen atoms to increase coordination and to gain stability. Some of the adsorbates can help to reduce surface free energy by increasing the ligand coordination of surface ions and reducing the need for relaxation.[26] It is conceivable that electron rich Ag and Au nanoparticles could be adsorbed on the metal oxide surfaces and stabilize them by reducing the surface free energy. Since the metal oxide surface contain both negatively charged anions and positively charged cations, different types of adsorptions are possible such as physisorption, donor-acceptor interactions, oxidation / reduction with electron transfer and oxidation / reduction with oxygen transfer. Other factors such as (i) availability of polar and non-polar surfaces, (ii) presence of acidic metal and basic oxygen sites, (iii) complex and imperfectly understood defect chemistry and (iv) possibility of electron transfer may also influence the extraction and make it difficult to draw a conclusion. More theoretical and experimental investigations are needed to understand the nanoparticle adsorption mechanism. Further, acid - base properties

of an oxide surface are measured by its point of zero charge (Pzc) / isoelectric point of solid surface (abbreviated as IEPS for solids) and pH at which the surface is electrically neutral.[27] Table 6.1 shows that NiO has highest IEPS value followed by ZnO which matches the observed order for adsorption efficiency. Most of the metal oxides followed same trend as of IEPS values, except CeO_2 and CuO which could be due to the difference in surface area. Referring to Figures 6.4 and Table 6.1, it can be inferred that metal oxides with high surface area and high IEPS values showed high adsorption efficiency for both silver and gold nanoparticles. In addition, there are reports indicating surface area as one of the main factors responsible for the greater adsorption efficiencies of hierarchical metal oxides towards dyes and metal ions[13,18,19] and our results are consistent with such reports. It is conceivable that electrostatic attraction between metal oxide surfaces and nanoparticles and other factors mentioned above influence adsorption of nanoparticles on the surface. Other factors such as the size differences between Au and Ag nanoparticles and capping agents used for the synthesis of nanoparticles may also influence adsorption process. We are currently exploring some of these factors to understand the fate of nanoparticles in aqueous environment with time.

6.5. Conclusions

Readily available eggshell membrane was used to prepare metal oxide nanomaterials. SEM micrographs showed interwoven porous structures for the oxides. NiO was found to be an effective sorbent with adsorption capacities of 77 mg/g and 55 mg/g for gold and silver nanoparticles, respectively, from water within a period of 2 hours. TEM analysis of the metal oxide after extraction showed the presence of nanoparticles on the surface. The adsorption efficiencies of metal oxides for nanoparticles can be ranked with decreasing order, NiO > ZnO> CeO_2 > Co_3O_4 > CuO. Since the overall size of the prepared metal oxides tubes are in 10 - 20 micrometers, solid/liquid extraction would be fairly manageable and the relatively high density of metal oxides is also useful for real

time water treatment applications. We will be investigating such potential of these materials in the near future.

6.6. References

(1) Shannon, M. A.; Bohn, P. W.; Elimelech, M.; Georgiadis, J. G.; Marinas, B. J.; Mayes, A. M. *Nature* **2008**, *452*, 301.

(2) Zhang, L.; Fang, M. *Nano Today* **2010**, *5*, 128.

(3) Pradeep, T.; Anshup *Thin Solid Films* **2009**, *517*, 6441.

(4) Reiss, G.; Hutten, A. *Nat Mater* **2005**, *4*, 725.

(5) Nie, Z.; Petukhova, A.; Kumacheva, E. *Nat Nano* **2010**, *5*, 15.

(6) Khlebtsov, N.; Dykman, L. *Chemical Society Reviews* **2011**, *40*, 1647.

(7) Hackenberg, S.; Scherzed, A.; Kessler, M.; Hummel, S.; Technau, A.; Froelich, K.; Ginzkey, C.; Koehler, C.; Hagen, R.; Kleinsasser, N. *Toxicol Lett* **2011**, *201*, 27.

(8) Ahamed, M.; AlSalhi, M. S.; Siddiqui, M. K. J. *Clinica Chimica Acta* **2010**, *411*, 1841.

(9) Teow, Y.; Asharani, P. V.; Hande, M. P.; Valiyaveettil, S. *Chem Commun* **2011**, *47*, 7025.

(10) Teodoro, J. S.; Simões, A. M.; Duarte, F. V.; Rolo, A. P.; Murdoch, R. C.; Hussain, S. M.; Palmeira, C. M. *Toxicology in Vitro* **2011**, *25*, 664.

(11) Wu, H.; Lin, Y.; Wu, J.; Zeng, L.; Zeng, D.; Du, J. *Earth Science Frontiers* **2008**, *15*, 133.

(12) Valente, J. S.; Tzompantzi, F.; Prince, J. *Applied Catalysis B: Environmental* **2011**, *102*, 276.

(13) Srivastava, R. *Journal of Colloid and Interface Science* **2010**, *348*, 600.

(14) Pehlivan, E.; Özkan, A. M.; Dinç, S.; Parlayici, Ş. *Journal of Hazardous Materials* **2009**, *167*, 1044.

(15) Mallampati, R.; Valiyaveettil, S. *Journal of Nanoscience and Nanotechnology* **2012**, *12*, 618.

(16) Mahmoud, S. A.; Aal, A. A.; Aboul-Gheit, A. K. *ASME Conference Proceedings* **2008**, *2008*, 59.

(17) Li, J.; Lai, X.; Xing, C.; Wang, D. *Journal of Nanoscience and Nanotechnology* **2010**, *10*, 7707.

(18) Hu, J.-S.; Zhong, L.-S.; Song, W.-G.; Wan, L.-J. *Advanced Materials* **2008**, *20*, 2977.

(19) Al-Ghouti, M. A.; Al-Degs, Y. S.; Khraisheh, M. A.; Ahmad, M. N.; Allen, S. J. *J Environ Manage* **2009**, *90*, 3520.

(20) Nakano, T.; Ikawa, N.; Ozimek, L. *Poultry Science* **2003**, *82*, 510.

(21) Lakshminarayanan, R.; Kini, R. M.; Valiyaveettil, S. *Proc Natl Acad Sci U S A* **2002**, *99*, 5155.

(22) Dong, Q.; Su, H.; Song, F.; Zhang, D.; Wang, N. *Journal of the American Ceramic Society* **2007**, *90*, 376.

(23) Yang, D.; Qi, L.; Ma, J. *Journal of Materials Chemistry* **2003**, *13*, 1119.

(24) Dong, Q.; Su, H.; Xu, J.; Zhang, D.; Wang, R. *Materials Letters* **2007**, *61*, 2714.

(25) Heinrich, V. E.; Cox, P. A. *The Surface Science of Metal Oxides;* Cambridge University Press: Cambridge, U.K., 1994.

(26) Chen, M.; Wayne Goodman, D. In *The Chemical Physics of Solid Surfaces*; Woodruff, D. P., Ed.; Elsevier: 2007; Vol. Volume 12, p 201.

(27) Parks, G. A. *Chemical Reviews* **1965**, *65*, 177.

CHAPTER 7

BIOMIMETIC SYNTHESIS OF Mn_3O_4 HIERARCHICAL STRUCTURES AND THEIR APPLICATION IN WATER TREATMENT

Publications from the chapter:

R. Mallampati and S. Valiyaveettil, Simple and efficient biomimetic synthesis of Mn3O4 hierarchical structures and their application in water treatment, *Journal of Nanoscience and Nanotechnology*, 2011, 11, 1–5.

7.1. Introduction

Research on new materials focus on the production of materials with varying size, shape, multifunctionality and biocompatibility. These materials can be synthesized by different ways such as co-precipitation, sol-gel processing, microemulsions, hydrothermal / solvothermal, template synthesis and biomimetic synthesis.[1] During the last 5 years, there has been remarkable progress in the field of biosynthesis of functional materials. Researchers achieved excellent control over processes occurring at the biological-inorganic interface resulting in highly ordered nanostructures.[2-4] Owing to the structure and functions; it is interest to use natural biomaterials as template to fabricate bioinspired functional materials.[5] Various biomaterialsand their properties are used to synthesize wide range of materials.[6,7] The biomineralization strategy offers an efficient and novel synthetic route in preparing inorganic functional materials. The proteins associated with biominerals are responsible for synthesizing advanced materials with sophisticated hierarchical structures and excellent properties. This could be achieved by employing the characteristic architectures of biomaterials, functional groups of biomacromolecules and mimics the biological assembly.[8]

Eggshell membrane (ESM) is an interesting material as a biotemplate for directing the nucleation, assembly and patterning of new architectures. The resulting inorganic materials will be successfully tailored with characteristic hierarchical order. Glycoproteins of ESM are made up of large amounts of amido, carboxyl and hydroxyl groups,[9-11] which act as directing and capping functions of ESM for metal oxide nanocrystallites. In the biomineralization process, the hydrophilic anionic groups on ESM surface are responsible for extraction and transport of metal ions. The biotemplate ESM can be removed through calcination, leaving the metal oxide without disturbing the network like morphology. Different functional materials such as SnO_2[12], $BaSO_4$[13], $MnWO_4$[14], $Ce_xZr_{1-x}O_4$[15], PbSe[16], ZnO[17] and TiO_2[18] are synthesized by using ESM as template. Mn_3O_4 is synthesized by various techniques as it is used in batteries, high-density magnetic storage media, corrosion-inhibiting pigment, electrochromic materials and as catalyst.[19-29]

In this work, a simple, green, biotemplate synthesis was employed to synthesize Mn_3O_4 nanocrystallites with hierarchical network morphology. To

our knowledge, the reports on extraction of various contaminants from aqueous solution to Mn_3O_4 surface are rare. Emerging contaminants are chemicals or materials that are perceived to pose a threat to human health or the environment and have only in the past few decades gained closer attentions of environment regulators due to a lack of published health standards previously. It is also 'emerging' due to new source, new detection technology and new pathway to humans.[34] These include pesticides, pharmaceuticals, personal care products, veterinary products, industrial compounds/by-products, food additives, and engineered nano-materials.[35] As they are transported within the water cycle, they can also undergo various physical, chemical and biological transformations.[36] In many countries, chlorinated solvents is one of the 30 most commonly detected organic emerging pollutants and these organochlorine compounds are most widely applied pesticides. They resist degradation, hydrophobic and are notorious for their high toxicities.[37-39] One characteristic of emerging contaminants is that they are difficult to remove via traditional sewage or drinking water treatment using granulated activated carbon.[38] These include small and/or polar molecules. Many other adsorbents have also been tested to remove phenolic and organochlorine compounds such as activated clay,[40,41] activated carbon prepared on various precursors,[42] chitosan beads and functional chitosan,[43,44] biomass including eggshell membrane[45,46] and metal oxides.[47]

Phosphate is responsible for eutrophication, the excessive growth of algae in water. Eutrophication causes severe environmental damage, reducing dissolved oxygen in water, causing problems for water treatment and affecting perceived beauty. Secretions from algae can also poison humans and other animals.[37] Furthermore; anionic pollutants have proven difficult to remove with conventional methods. Among the various existing methods, adsorption is a popular method for removing them because high adsorption rates are achievable. Our study focused on the use of metal oxide for the removal of different pollutants including organic dyes, pesticides and phosphate anion. Here we show the excellent absorption capacity of Mn_3O_4 towards different pollutants. As an example of potential application, victoria blue (VB), alcian blue (AB), bromophenol blue (BB), neutral red (NR), phenol (P), p-nitrophenol (PNP), p-chlorophenol (PCP) and 2,4,6-trichlorophenol (TCP)

were chosen as typical water soluble organic waste for our extraction experiment due to their structural diversity. The amount of pollutant in the spiked solution before and after adsorption was quantified by using UV - Vis spectrophotometer (dyes), Ion exchange chrmotagraphy (PO_4^{3-}) and HPLC (pesticides) with C18 inverse phase (3.9 x 150 mm) column. Mobile phase was a mixture of water/methanol (60:40) injected in at a rate of 0.7 ml/min. UV spectrometer with maximum absorbance value set at 270 nm for P, 278 nm for PCP, 288 nm for TCP and 316 nm for PNP was used as detector.

7.2. Characterization

Collagen, glycoprotein and proteoglycans present on the ESM are responsible for the nucleation and deposition of Mn_3O_4. The mechanism of biomineralization process of calcium salts on ESM template was reported earlier.[14,15] The macromolecules in ESM contain ionic hydrophilic and hydrophobic domains. The hydrophilic groups interact with Mn^{2+} cations and induce nucleation and growth of nanocrystals. The intermolecular and intramolecular forces, such as hydrogen bonding, the electrostatic effect organize macromolecules and help to induce the assembly of nanoparticles and control the shape of the products.[24]

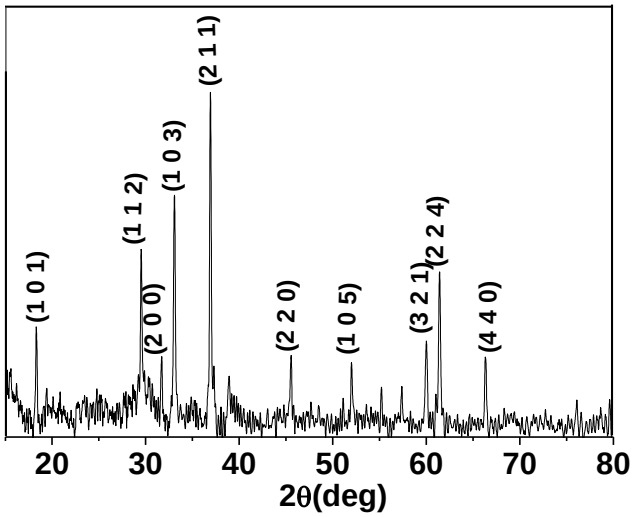

Figure 7.1. X-ray diffraction pattern of the Mn_3O_4 sample.

The powder XRD patterns of as synthesized samples calcinated at 700 ^{o}C are shown in Figure 7.1. The diffraction pattern corresponds to the body-centered structure of Mn_3O_4. The XRD pattern obtained was compared with reported pattern of Mn_3O_4 (JCPDS 80-0382). All major peaks are comparable with the reference data. The elemental composition of prepared sample can be confirmed by EDX analysis (Figure 7.2).

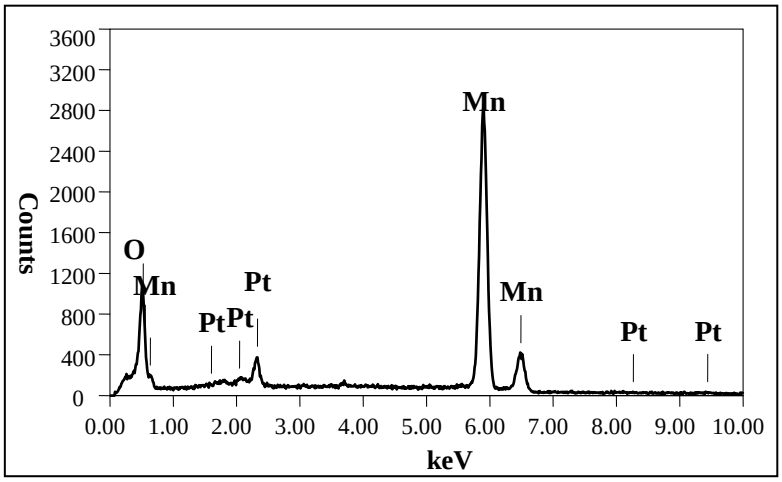

Figure 7.2. EDX spectra of Mn_3O_4, showing peaks corresponding to Manganese and Oxygen.

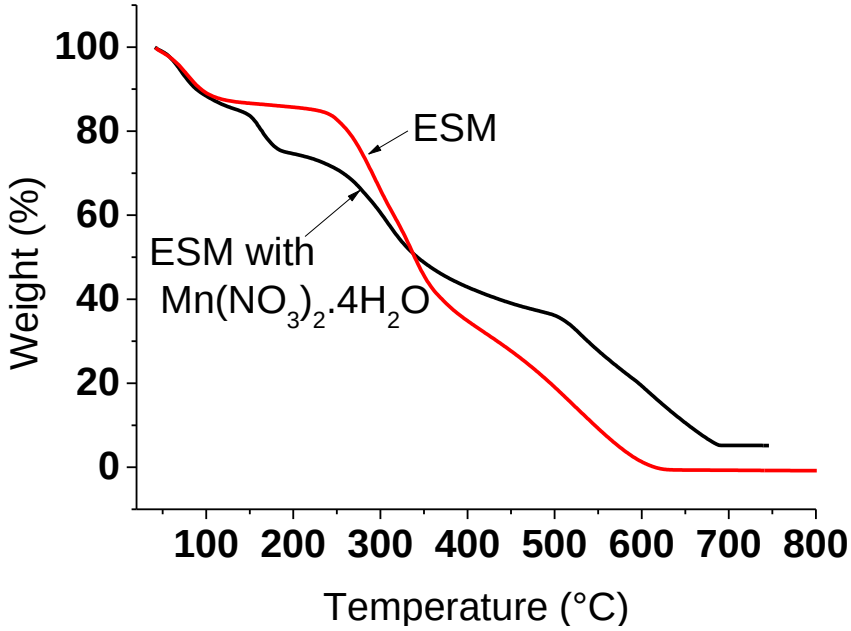

Figure 7.3. TGA curves of natural ESM and manganese nitrate impregnated egg membrane (ESM+ $Mn(NO_3)_2.4H_2O$)

The sample was coated with platinum before analysis to make sure that the surface of the sample is conductive. The TGA shown in Figure 7.3 gives the decomposition pattern of the ESM and ESM impregnated with $Mn(NO_3)_2.4H_2O$. The initial weight loss at 100 ^oC corresponds to loss of adsorbed water. A significant weight loss was observed up to ~ 700 ^oC in both samples, above which the total mass of the sample remained constant with further increase in temperature.

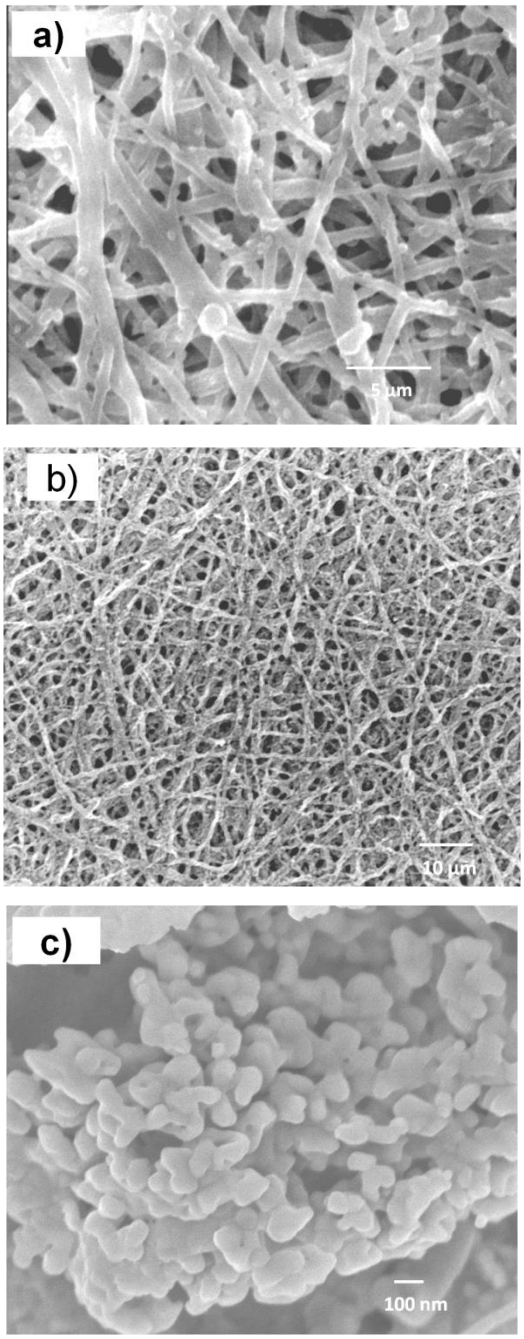

Figure 7.4. SEM image of a) natural ESM b) $Mn(NO_3)_2.4H_2O$ infiltred ESM composite calcinated at 700^oC and c) magnified image of b

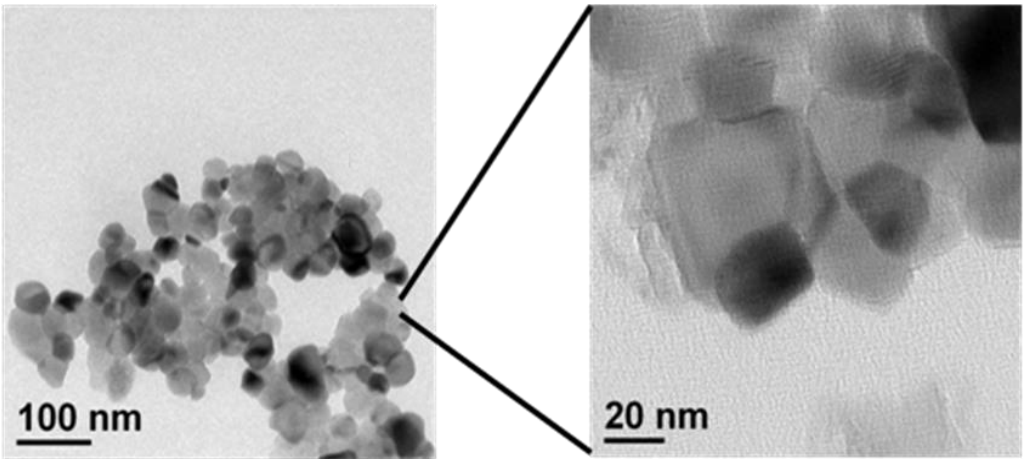

Figure 7.5. TEM image of Mn_3O_4 crystals dispersed in ethanol

Figure 7.4 shows SEM images of normal ESM and as prepared Mn_3O_4 crystals. During calcination, the organic materials of ESM were degraded and gases such as CO_2 or H_2O were released, which caused the formation of micro pores on the fibrous structure. The resulting Mn_3O_4 fibres are made up of nano crystallites with large number of micro and nano pores. Such pores are responsible for adsorption of higher amount of spiked organic pollutants. The morphology of ESM is translated to manganese oxide (Mn_3O_4) with varying pore sizes. TEM image (Figure 7.5) indicates that such microstructures of Mn_3O_4 composed of nanocrystallites of size around 20 nm.

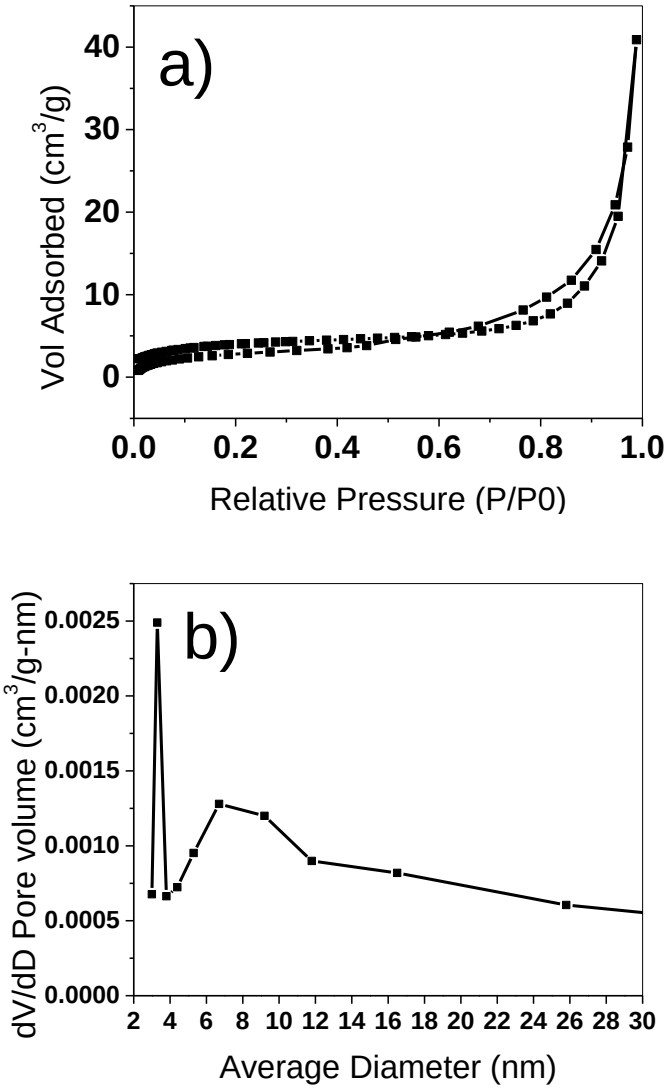

Figure 7.6. Nitrogen adsorption–desorption isotherms plot (a) and corresponding pore-size distribution plot (b) of Mn_3O_4.

The nitrogen adsorption-desorption isotherm and corresponding pore size distribution curves for as prepared manganese oxide are shown in Figure 7.6. According to Brunauer classification,[30] the isotherm indicates that the Mn_3O_4 has a mesoporous structure. The BET surface area of the substance was 13.13 m^2/g with an average pore size in the range of 10 nm.

7.3. Adsorption experiments

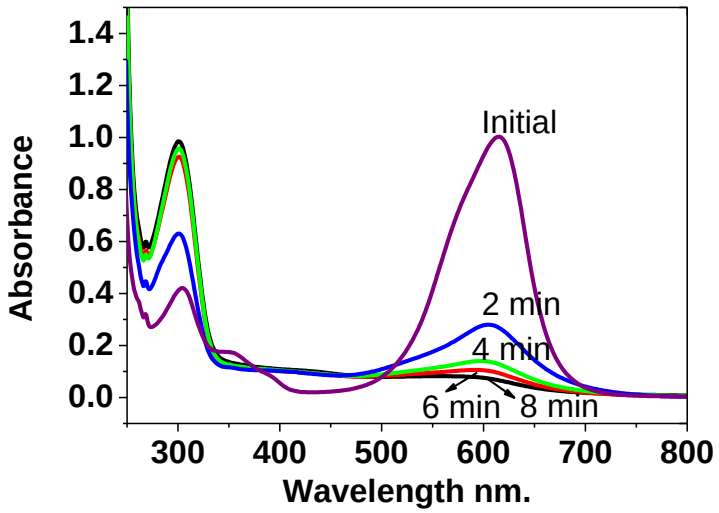

Figure 7.7. UV spectra of a solution of Victoria blue (100 mg L^{-1}, 50 mL) in the presence of Mn_3O_4 hollow microfibers (0.01 g) at different time intervals of 0, 2, 4, 6 and 8 min, respectively.

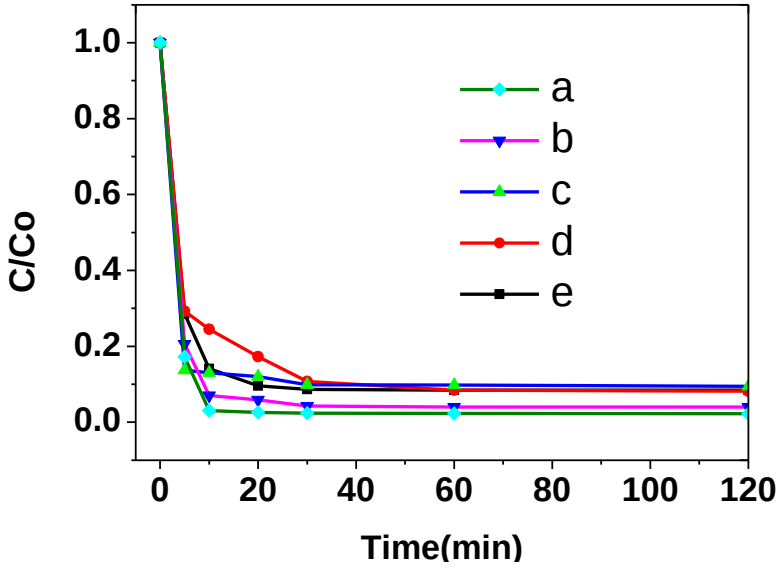

Figure 7.8. Adsorption rate of the Victoria Blue on a) as prepared Mn_3O_4; b) secondary; c) third; d) fourth regenerated particles, respectively. C_0 (mg L^{-1}) is the initial concentration of the Victoria Blue solution and C (mg L^{-1}) is the remaining concentration at different time intervals during the extraction.

In general, metal oxides act as adsorbents in textile industries to eliminate excess organic dyes at room temperature. As an example of potential applications of synthesized network structures of Mn_3O_4, extraction of water soluble dyes, pesticides and phosphate ions from spiked water samples were

carried out in the lab. Alcian blue, neutral red, bromophenol blue and victoria blue were chosen as typical organic dyes, because of their diversity in the molecular structures. It is clear that the adsorption capacity is not same for all four compounds. When the initial concentration of the dyes are 100 mg L^{-1}, Mn_3O_4 could remove about 98% of alcian Blue and victoria blue; 90% of neutral red and bromophenol blue, without any additives at room temperature. The UV-Vis spectra at different time intervals are shown in Figure 7.7. The colour of the dye solution disappears in 5 min. It indicates that the effective absorption takes place immediately when Mn_3O_4 comes in contact with dye molecules. The intensity of characteristic absorption peaks at 600 nm was chosen to monitor the extraction of victoria blue. It was established that 1 g of Mn_3O_4 prepared using template synthesis can remove about 400 mg of alcian blue or victoria blue. For comparison, the adsorption capacity of manganese oxide prepared without the template was also investigated, which showed a low adsorption of 125 mg/g of Mn_3O_4 of alcian blue in one hour. It is conceivable that the electrostatic attraction between the surface of Mn_3O_4 and organic compounds in solution at pH 2 was responsible for the dye removal.[31-33] The Mn_3O_4 could be regenerated via combustion at 300^{o} C in air for 5h, and purified Mn_3O_4 shows the same dye adsorption performance in the repeated extraction (Figure 7.8). This results proved that the prepared Mn_3O_4 can be reused and the method of preparation is cost effective. The size of as prepared material was several micrometers. The solid/liquid separation would be fairly easy because of their relatively high density, which is useful for potential applications.

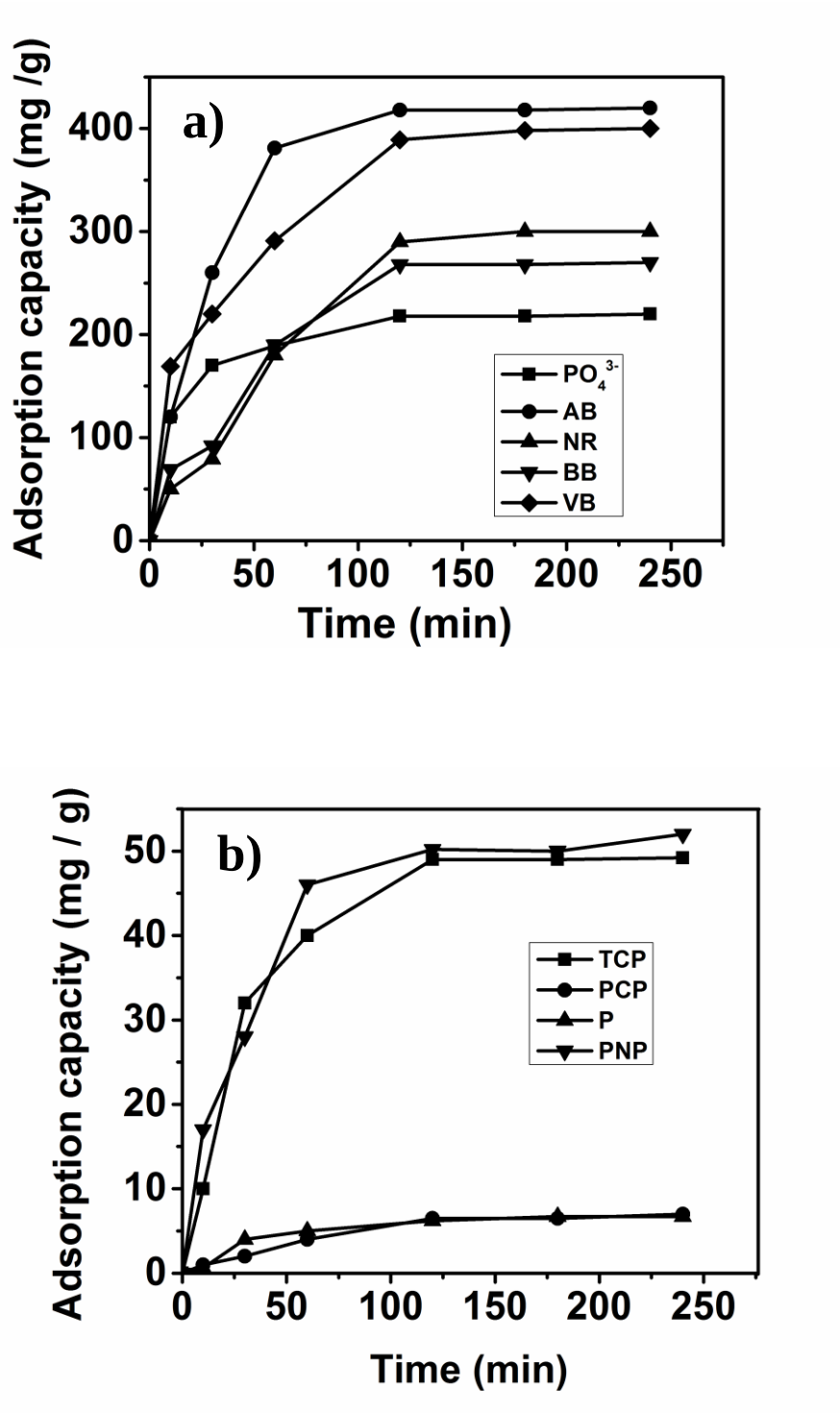

Figure 7.9. Adsorption capacities of dyes (a) and pesticides (b) using Mn_3O_4 as adsorbent.

The adsorption uptake versus the adsorption time for different pollutants at 30 ^oC is shown in Figure 7.9. The amount of pollutant adsorbed (mg/g) increased with increasing time and then reached equilibrium. Adsorption was fast for all pollutants at the initial stage of contact time after which it slowed down to

equilibrium. This is due to the many vacant sites at the initial stage. The maximum adsorption capacity is observed at 3 h for phosphate. HPLC result for TCP showed complete disappearance of reference peak at initial concentration of 200 mg/L within 1 minute. An equilibrium time of 15 – 30 min was reported for adsorbing TCP (initial concentration 25 -150 mg/L) on coconut husk-based activated carbon which was improved from coconut-shell based commercial grade activated carbon.[42] P and PCP showed lower adsorption compared to TCP and PNP and reached equilibrium by 4 h. Both TCP and PNP showed higher adsorption and reach equilibrium in less than 15 minutes. Based on the HPLC results for TCP, there is a high likelihood that TCP degraded as well during adsorption test. This work showed that Mn_3O_4 can be used to extract many pollutants efficiently from water.

7.4. Conclusions

Comparing with conventional methods of material syntheses, biomineralization is facile, eco-friendly and cost effective. Generally biomineralization process has minimum requirements for chemicals, equipments, and is carried out under ambient conditions. Biotemplate, such as eggshell membrane is available in large amounts at low costs, and biomorphic mineralization makes efficient uses of natural materials with a capability of turning biowastes into functional materials. We demonstrated the novel route to synthesize hierarchical structures of Mn_3O_4. The oxide crystals showed a good extraction efficiency toward the removal of victoria blue (400 mg/g), alcian blue (420 mg/g), bromophenol blue (270 mg/g), neutral red (300 mg/g), phenol (6.7 mg/g), p-nitrophenol (52 mg/g), p-chlorophenol (7 mg/g), 2,4,6-trichlorophenol (49.2 mg/g) and PO_4^{3-} (220 mg/g) from water sample and are expected to be useful for industrial water treatment applications.

7.5. References

(1) Cushing, B. L.; Kolesnichenko, V. L.; O'Connor, C. J. *Chem Rev* **2004**, *104*, 3893.

(2) Sotiropoulou, S.; Sierra-Sastre, Y.; Mark, S. S.; Batt, C. A. *Chemistry of Materials* **2008**, *20*, 821.

(3) Gazit, E. *FEBS Journal* **2007**, *274*, 317.

(4) Sanchez, C.; Arribart, H.; Guille, M. M. G. *Nature Materials* **2005**, *4*, 277.

(5) Torres, J. Q.; Giraudon, J. M.; Lamonier, J. F. *Catalysis Today* **2011**, *176*, 277.

(5) Fan, T. X.; Chow, S. K.; Zhang, D. *Progress in Materials Science* **2009**, *54*, 542.

(6) Cushing, B. L.; Kolesnichenko, V. L.; O'Connor, C. J. *Chemical Reviews* **2004**, *104*, 3893.

(6) Meldrum, F. C.; Wade, V. J.; Nimmo, D. L.; Heywood, B. R.; Mann, S. *Nature* **1991**, *349*, 684.

(7) Vukusic, P.; Sambles, J. R. *Nature* **2003**, *424*, 852.

(8) Sellinger, A.; Weiss, P. M.; Nguyen, A.; Lu, Y.; Assink, R. A.; Gong, W.; Brinker, C. J. *Nature* **1998**, *394*, 256.

(9) Zhao, Y. H.; Chi, Y. J. *Biotechnology* **2009**, *8*, 254.

(10) Mikšík, I.; Charvátová, J.; Eckhardt, A.; Deyl, Z. *Electrophoresis* **2003**, *24*, 843.

(11) Nakano, T.; Ikawa, N. I.; Ozimek, L. *Poultry Science* **2003**, *82*, 510.

(12) Dong, Q.; Su, H.; Zhang, D.; Cao, W.; Wang, N. *Langmuir* **2007**, *23*, 8108.

(13) Liu, J.; Wu, Q. *J. Mater. Res.* **2004**, *19*, 10.

(14) Zhang, R. H.; Chen, L. L.; Ren, Y. Z.; Wang, J. Y. *Russian Journal of Inorganic Chemistry* **2009**, *54*, 8.

(15) Li, J.; Chiu, K. L.; Kwong, F. L.; Ng, D. H. L.; Chan, S. L. I. *Current Applied Physics* **2009**, *9*, 1438.

(16) Su, H.; Wang, N.; Dong, Q.; Zhang, D. *Journal of Membrane Science* **2006**, *283*, 7.

(17) Dong, Q.; Su, H.; Xu, J.; Zhang, D.; Wang, R. *Materials Letters* **2007**, *61*, 2714.

(18) Yang, D.; Qi, L.; Ma, J. *Advanced Materials* **2002**, *14*, 1543.

(19) Lee, G. H.; Huh, S. H.; Jeong, J. W.; Choi, B. J.; Kim, S. H.; Ri, H. C. *Journal of the American Chemical Society* **2002**, *124*, 12094.

(20) Armstrong, A. R.; Bruce, P. G. *Nature* **1996**, *381*, 499.

(21) Nardi, J. C. *Journal of the Electrochemical Society* **1985**, *132*, 1787.

(23) Zarur, A. J.; Ying, J. V. *Nature* **2000**, *403*, 65.

(24) Hu, L.; Peng, Q.; Li, Y. *Journal of the American Chemical Society* **2008**, *130*, 16136.

(25) Sun, S.; Zeng, H. *Journal of the American Chemical Society* **2002**, *124*, 8204.

(26) Ge, J.; Hu, Y.; Biasini, M.; Beyermann, W. P.; Yin, Y. *Angew. Chem.* **2007**, *119*, 4420.

(27) Chen, L. L.; Wu, X. L.; Guo, Y. G.; Kong, Q. S.; Xia, Y. Z. *Journal of Nanoscience and Nanotechnology* **2010**, *10*, 8158.

(28) Zhang, X.; Yu, P.; Wang, D.; Ma, Y. *Journal of Nanoscience and Nanotechnology* **2010**, *10*, 898.

(29) Dong, H.; Koh, E. K.; Lee, S. Y. *Journal of Nanoscience and Nanotechnology* **2009**, *9*, 6511.

(30) Clavier, G. M.; Pozzo, J. L.; Bouas-Laurent, H.; Liere, C.; Roux, C.; Sanchez, C. *Journal of Materials Chemistry* **2000**, *10*, 1725.

(31) Zhong, L. S.; Hu, J. S.; Liang, H. P.; Cao, A. M.; Song, W. G.; Wan, L. J. *Advanced Materials* **2006**, *18*, 2426.

(32) Al-Ghouti, M. A.; Al-Degs, Y. S.; Khraisheh, M. A. M.; Ahmad, M. N.; Allen, S. J. *Journal of Environmental Management* **2009**, *90*, 3520.

(33) Li, J.; Lai, X.; Xing, C.; Wang, D. *Journal of Nanoscience and Nanotechnology* **2010**, *10*, 7707.

(34) Murnyak, G.; Vandenberg, J.; Yaroschak, P. J.; Williams, L.; Prabhakaran, K.; Hinz, J. *Toxicology and Applied Pharmacology* **2011**, *254*, 167.

(35) Lapworth, D. J.; Baran, N.; Stuart, M. E.; Ward, R. S. *Environmental Pollution* **2012**, *163*, 287.

(36) Xagoraraki I., Kuo D., (2008). Water Pollution: Emerging Contaminants Associated with Drinking Water. In: International Encyclopedia of Public Health (Heggenhougen K., Editor), Vol. 6, pp. 539-550. Academic Press, San Diego

(37) http://www.epa.gov/waterscience/methods/pollutants.htm

(38) M.E. Stuart, K. Manamsa, J.C. Talbot, E.J. Crane, British Geological Survey Open Report, 2011, **OR/11/013**.

(39) Nhan, D. D.; Carvalho, F. P.; Am, N. M.; Tuan, N. Q.; Yen, N. T. H.; Villeneuve, J. P.; Cattini, C. *Environmental Pollution* **2001**, *112*, 311.

(40) Vázquez, G.; González-Álvarez, J.; García, A. I.; Freire, M. S.; Antorrena, G. *Bioresource Technology* **2007**, *98*, 1535.

(41) Hameed, B. H. *Colloids and Surfaces A: Physicochemical and Engineering Aspects* **2007**, *307*, 45.

(42) Hameed, B. H.; Tan, I. A. W.; Ahmad, A. L. *Chemical Engineering Journal* **2008**, *144*, 235.

(43) Lu, L. C.; Wang, C. I.; Sye, W. F. *Carbohydrate Polymers* **2011**, *83*, 1984.

(44) Campos, J. L.; Otero, L.; Franco, A.; Mosquera-Corral, A.; Roca, E. *Bioresource Technology* **2009**, *100*, 1069.

(45) Achak, M.; Hafidi, A.; Ouazzani, N.; Sayadi, S.; Mandi, L. *Journal of Hazardous Materials* **2009**, *166*, 117.

(46) Koumanova, B.; Peeva, P.; Allen, S. J.; Gallagher, K. A.; Healy, M. G. *Journal of Chemical Technology & Biotechnology* **2002**, *77*, 539.

(47) Bandara, J.; Mielczarski, J. A.; Kiwi, J. *Applied Catalysis B: Environmental* **2001**, *34*, 307.

CHAPTER 8

EGGSHELL MEMBRANE SUPPORTED RECYCLABLE NOBLE METAL CATALYSTS FOR ORGANIC REACTIONS

Publication for this chapter.

R. Mallampati and S. Valiyaveettil, Efficient and recyclable noble metal catalysts for different organic reactions, *ChemCatChem*, 2013, (in press).

8.1. Introduction

Functional nanoparticles are used in different areas of material science such as catalysis,[1] electrochemistry,[2] bioimaging[3] and sensing.[4-6] Gold and silver nanoparticles (NPs) are particularly interesting due to their ease of preparation and control over size and shape using conventional synthesis.[7-25] Recently, nanostructured noble metals such as Au, Ag and Pt have been widely used as catalysts for variety of organic reactions owing to high surface to volume ratio and high surface energy which enhances the catalytic activity. Heterogeneous catalysis provides an opportunity for easy separation, recycling of the catalyst and product purification. For catalytic applications, the metal NPs are usually supported on a substrate such as metal oxide,[26] active carbon[27] or stabilized by polymer molecules.[28] Porous supports offer ordered pores with controllable size, high surface area, and large pore volume,[29] which can be used for the stabilization of metal NPs catalysts.[30] Catalysts supported on porous substrates face problems such as difficulty in characterization, possibility of clogging the pores and not accessible to reagents. Therefore, it is important to look for an alternative support with excellent textural characteristics and surface properties for the fabrication of highly stable catalytic NPs.

Herein, we report the synthesis of highly dispersed Au and Ag NPs with a size range of 10 - 25 nm on the surface of eggshell membrane (ESM) support. The functional groups on the fiber surfaces of ESM act as a stabilizing and reducing agent, which removes the need for additional reagents or surface modification. The fibrous nature of the ESM offers a large surface area for immobilization of catalyst particles. Use of natural waste material such as ESM with abundant functional groups such as $-NH_2$, -OH and –CHO[31] on the surface helps in a small way to reduce, reuse and recycle waste materials. It is also interesting to test the NPs on ESM surface towards their stability, catalytic activity and recyclability in various organic reactions. Catalytic performance of the NPs was evaluated using two different model reactions such as reduction of nitrophenols and one pot synthesis of functionalized propargylamines.

8.2. Characterization

Owing to the presence of large amounts of functional groups (-OH, -CO_2H, -NH_2, - CHO), it is conceivable that the surface adsorbed Au (III) or Ag (I) ions get reduced to nanoparticles on the ESM. This can be verified using SEM, XPS and visible changes in colour of the ESM. SEM images of the natural ESM and NPs adsorbed on to the surface are given in Figure 8.1.

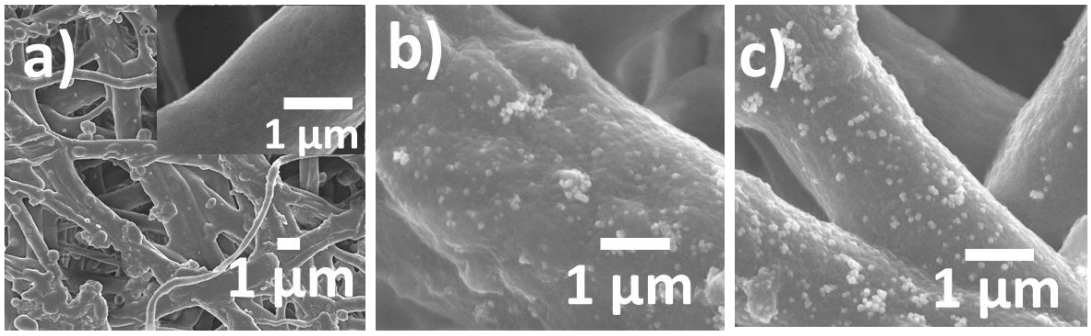

Figure 8.1. SEM images of natural ESM (a), Au NPs (b) and Ag NPs (c) on ESM fibers.

A network structure of fibers was observed for the natural ESM. It has been reported that collagen and saccharides are the main constituents of ESM fibers. Nakano *et al*.[31] reported that the main chemical constituents of chicken ESM are amino acids (Glycine and Alanine) and uronic acid. The aldehyde moiety of uronic acid and saccharides in ESM play a significant role in reducing the surface adsorbed metal ions to NPs.[32] In addition, other groups such as - NH_2 and -OH may also interact with Au (III) or Ag (I) ions. The presence of NPs on the surface of ESM was also established using energy dispersive spectroscopy (EDS) (Figure 8.2).

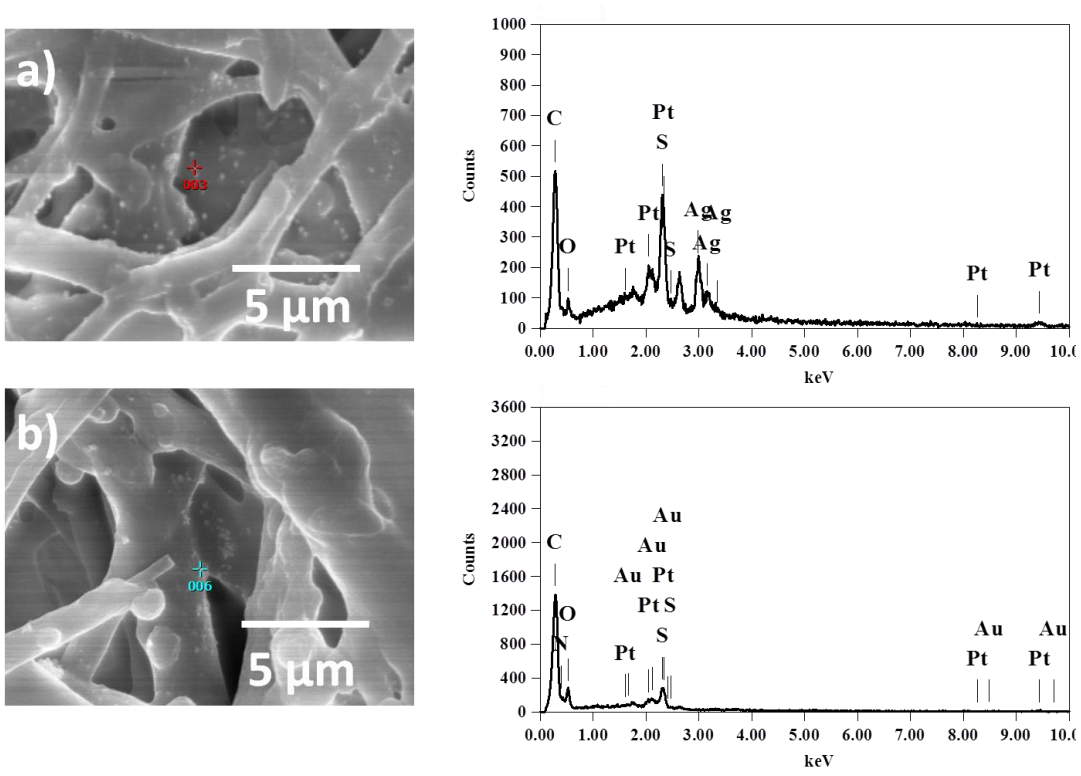

Figure 8.2. SEM - EDS spot analysis of Ag NP (a) and Au NP (b) on ESM

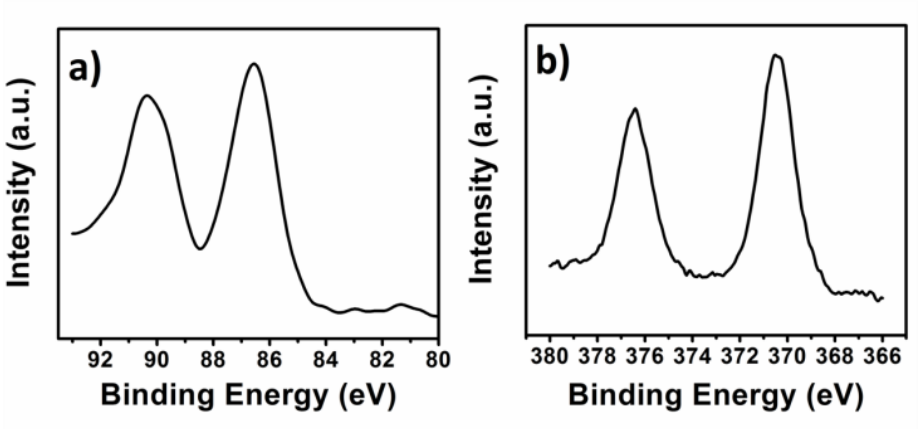

Figure 8.3. XPS spectra of Au NP (a) and Ag NP (b) on ESM. Spectra were recorded using ESM-NPs

A spot profile energy dispersive X-ray analysis of the NPs showed characteristic Au (0) peaks at 2.12 keV and 9.78 keV and Ag (0) peak at 3.1 keV. Oxidation states of gold and silver species in NPs were studied by XPS (Figure 8.3), which showed characteristic Au (4f) and Ag (3d) peaks in the spectrum. Binding energies (370 eV) for Ag $3d_{5/2}$ peak and (87.7 eV) for Au $4f_{7/2}$ peaks were also

observed. The XPS results are in good agreement with SEM and EDS data that zero valent gold and silver atoms were formed on the surface of ESM.

\

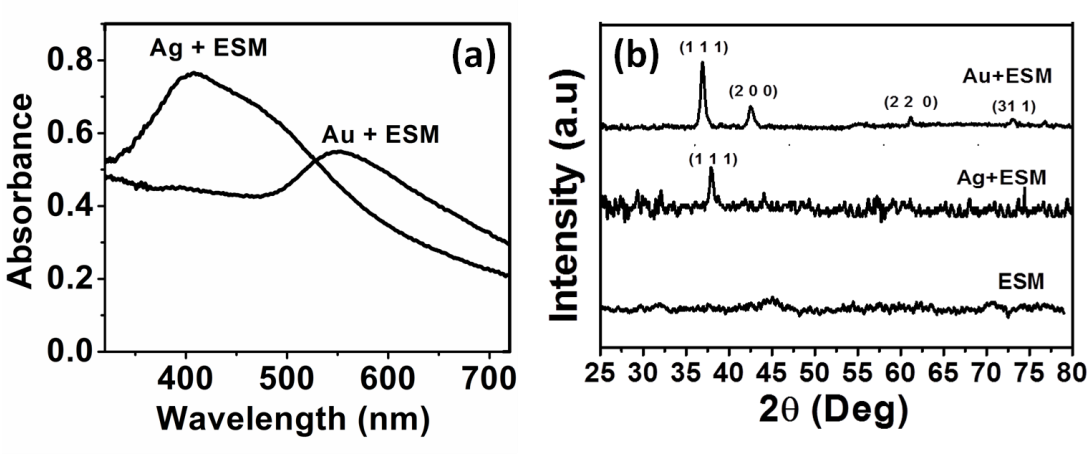

Figure 8.4. UV-Vis spectra (a) and XRD pattern (b) of Au-ESM and Ag-ESM at ambient conditions.

UV-Vis spectra were recorded for NP-ESMs (Figure 8.4a) to study the size and optical properties of nanoparticles. Small pieces of ESM composites were used to record UV-Vis spectra in reflectance mode with $BaSO_4$ as reference material. Broad surface plasmon resonance (SPR) absorption peaks with maximum at 514 nm for Au and 400 nm for Ag were observed. These results are consistent with previous reports on the synthesis of NPs. X-ray diffraction studies were performed to confirm the presence of NPs on ESM fibers and to study the crystalline nature of those NPs. The XRD patterns of ESM and NP-ESMs are shown in Figure 8.4b. All peaks were indexed and compared with reported literature values. Significant peaks corresponding to Au (111), (200), (220), (311) and (222) lattice planes confirm the presence of Au (JCPDS 7440-57-5) and peaks corresponding to Ag (111) lattice plane confirm the presence of Ag (JCPDS 7440-22-4) on ESM.

8.3. Reduction of *p*-nitrophenol

Aromatic amines are of significant industrial importance and widely used in the synthesis of pharmaceuticals, dyes and agrochemicals.[33,34] Two general methods were used for the reduction of aromatic nitrocompounds in industry, which

include stoichiometric reduction reaction[35] and catalytic hydrogenation.[36,37] The catalytic hydrogenation is a convenient method for producing amines in high yield. Reduction of aromatic nitrocompounds using various nanoparticles prepared by different techniques have been investigated earlier[38-40] and suffers from limitations in reusability and recovery of the catalyst after the reaction. Biotemplated nanoparticles as catalysts have also been explored owing to the fact that it can be recovered easily and reused for a number of times.[41] Here we investigated the efficiency of NP-ESMs as catalysts for the borohydride reduction of *p*-nitrophenol, owing to the solubility of nitrophenols in water. In the absence of Au-ESM, the mixture of *p*-nitrophenol and $NaBH_4$ showed an absorption maximum at 400 nm corresponding to the *p*-nitrophenolate ion. This peak was unchanged with time indicating that the reduction did not take place; however, the addition of a small amount of NP-ESMs to the above reaction mixture caused fading the yellow colour of the reaction mixture in quick succession. Time dependent absorption spectra of this reaction mixture showed the disappearance of the peak at 400 nm and a gradual development of a new peak at 300 nm corresponding to the formation of *p*-aminophenol (Figure 8.5).

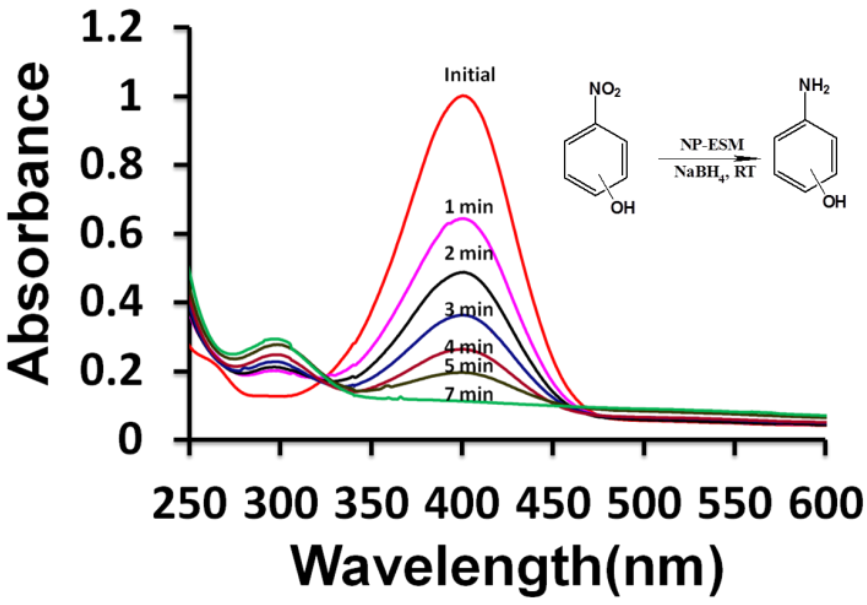

Figure 8.5. Time dependant UV- Vis spectra of the reduction of *p*-nitrophenol by Au-ESM with time.

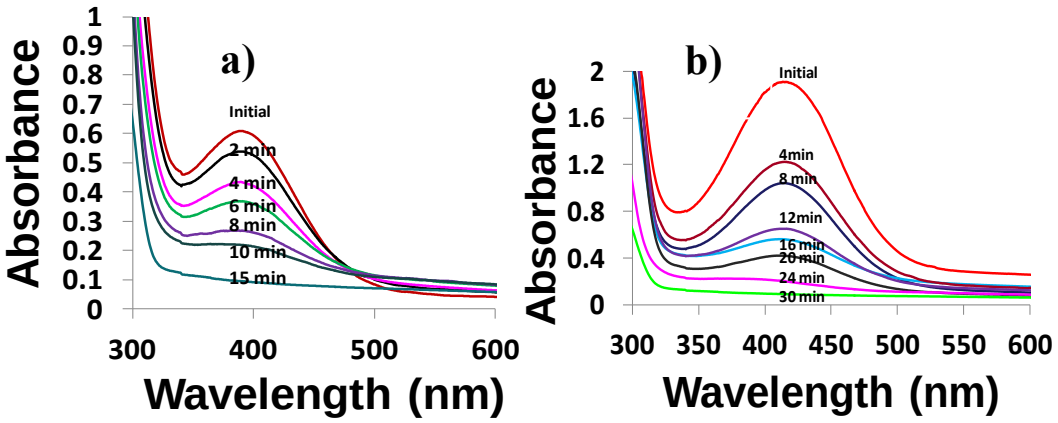

Figure 8.6. UV- Vis spectra of time dependant reduction of *ortho*-(a) and *meta* – nitrophenol (b) by Au-ESM

Similarly, borohydride reduction of *o*- and *m*-nitrophenol in presence of NP-ESMs were also investigated under similar conditions (Figure 8.6). The changes in the spectral patterns are similar to that observed in the case of *p*-nitrophenol reduction. These results indicated that NP-ESMs can successfully catalyze the reduction of *o*-nitrophenol and *m*-nitrophenol. Apparent rate constants (k_{app}) were calculated for all reactions from the graph of lnA Vs time (Figure 8.7), where A is absorbance. For comparison, the catalytic data of all three reactions are presented in Table 8.1.

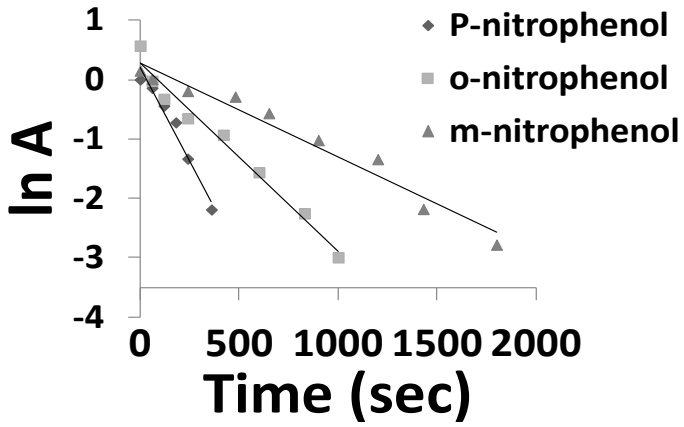

Figure 8.7. Graph of ln A versus Time (sec) where A is absorbance

Table 8.1. K_{app} of different borohydide reduction reactions in presence of Au + ESM and Ag + ESM.

Catalyst	Apparent rate constant ($k_{app / S}^{-1}$)		
	2-aminophenol	4-aminophenol	3-aminophenol
Au-ESM	3.2×10^{-3}	6.3×10^{-3}	1.6×10^{-3}
Ag-ESM	5.6×10^{-3}	11.2×10^{-3}	2.5×10^{-3}

The data shows that the rate of *p*-nitrophenol reduction catalyzed by NP-ESMs is higher than that of other two nitrophenols and follows the order of *p*-nitrophenol > *o*-nitrophenol > *m*-nitrophenol. Such differences in the reaction rate might be due to the influence of position of substituents. Generally, the rate of reduction of nitrophenols depends on the formation and stability of nitrophenolate ions that can be explained in more detail by comparing the resonance structure of three isomeric nitrophenolate ions.[42] In case of *o*- and *p*-nitrophenolate ion, the $-NO_2$ group is in resonance with the negative charge on oxygen that is delocalized throughout the benzene ring and hence stabilized. But due to steric hindrance, the influence of –I (inductive) effect of $-NO_2$ group in *o*-nitrophenolate ion is relatively less than the *p*-nitrophenolate ion. In the case of *m*-nitrophenol, $-NO_2$ group cannot enter into resonance stabilization of negative charge on oxygen and exert only a weak negative inductive effect. Therefore, the rate of reduction of different isomeric nitrophenols followed the order: *p*-nitrophenol > *o*-nitrophenol > *m*-nitrophenol. Ag-NPs shows higher activity as compared to Au-NPs. Reusability of the catalyst due to easy separation is another advantage of heterogeneous catalysts over homogeneous catalysts in industrial applications. Although, many catalytic studies have been reported in the literature using nanoparticles as catalyst, there are only a few reports where the catalyst were recovered for further use in consecutive cycles. In order to check the reusability, ESM-NPs were recovered and reused in repeated reduction reactions of *p*-nitrophenol. Generally, catalytic activity decreases as the number of reaction

cycles increases. The reaction times for complete conversion among the consecutive runs are recorded (Table 8.2).

Table 8.2. Table showing reaction time of five consecutive reactions using NP-ESM catalysts.

Run	Time taken for completion of paranitrophenol reduction (min)	
	Au-ESM	Ag-ESM
1	6	7
2	6	9
3	8	12
4	9	13
5	12	15

These results indicate that the NP-ESMs are active up to five cycles of nitrophenol reduction. During this recycling process, no significant loss of nanoparticles from ESM was observed indicating the high stability and recyclability of catalyst without significant decrease in activity.

8.4. Synthesis of propargylamine

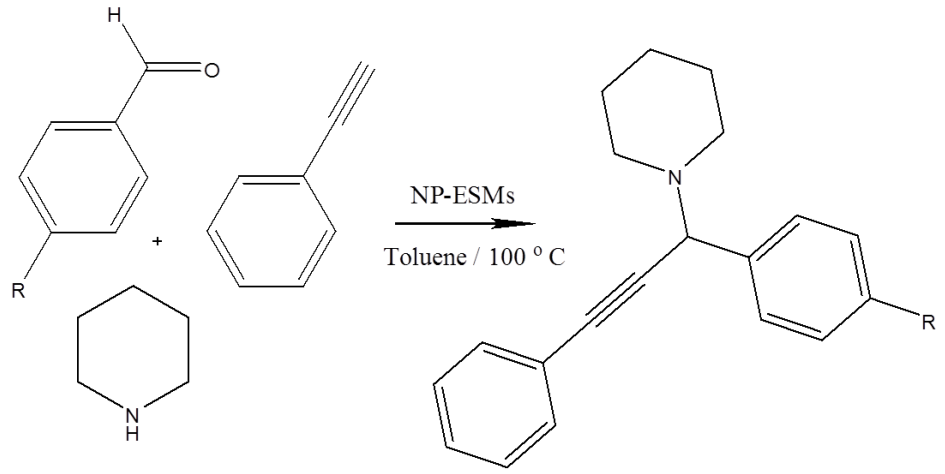

Figure 8.8. Nanoparticles catalysed coupling reactions to form propargylamine derivatives.

One pot multicomponent coupling reactions (MCR), where several organic moieties are coupled in one step is an attractive synthetic strategy.[43,44] The three-component coupling of aldehydes, amines and alkynes (A^3 coupling) is an example of MCR, and has received much attention in recent times.[45] The propargylamine derivatives obtained from A^3 coupling reactions are useful synthetic intermediates for biologically active compounds such as β-lactams, conformationally restricted peptides, natural products and therapeutic drug molecules.[46–48] Traditionally, propargylamines are prepared by the amination of propargylic halides, propargylic phosphates or propargylic triflates.[49,50] However, these reagents which are used in stoichiometric amounts are highly moisture sensitive and require controlled reaction conditions. Thus, the development of improved synthetic methods for the synthesis of propargylamines remained as an active area of research.[51] Recently, metal NPs, especially Au and Ag NPs with high surface to volume ratio have been exploited to activate the C-H bond of the terminal alkynes.[52] However, metal NPs in their pure form tend to agglomerate, which limits their efficiency in the catalytic processes. Herein, highly dispersed Au and Ag Nps grown over ESM were used as catalyst for the synthesis of propargylamines by an A^3 coupling reaction. This reaction shows the catalytic activity of NP-ESMs even in organic solvent. The catalytic efficiency of NP-ESMs was tested in three-component coupling of aldehyde, amine, and alkyne. Initially, benzaldehyde (1 mmol), piperidine (1.2 mmol), and phenylacetylene (1.2 mmol) were mixed with NP-ESMs (20 mg) in toluene (20 mL). The reaction was carried out at 100 °C and completed in 24 h with a quantitative yield of the final product (Figure 8.9).

Table 8.3. percentage yields of propargylamine reaction with different reactants.

Catalyst	Product when $R = CH_3$	$R = Cl$	$R = NO_2$
Au-ESM	99 %	68 %	0 %
Ag-ESM	99 %	77 %	0 %

Formation of the product was confirmed by spectroscopic methods. These results prompted us to study the substituent effects on the aromatic ring of benzaldehydes, for example, *p*-methyl enzaldehyde furnished the desired product in good yield (99%) whereas, no reaction was observed when *p*-nitrobenzaldehyde was used (Table 8.3). No product was formed in the absence of catalyst or in presence of pure ESM under identical conditions. It is understood that the A^3 coupling reaction proceeds by terminal alkyne C–H bond activation by NPs on ESM.[50] The NP acetylide intermediate then react with the iminium ion formed in situ from the aldehyde and the amine to generate the corresponding propargylamine. The reusability of the catalysts was demonstrated for five consecutive reactions. The membrane supported catalyst was recovered by filtration and washed with toluene.

Table 8.4. Percentage yields of propargylamine reactions for five consecutive runs.

Run	Au-ESM	Ag-ESM
1	99 %	99 %
2	99 %	98 %
3	82 %	90 %
4	80 %	85 %
5	78 %	82 %

The recovered catalyst was used for consecutive reactions. Results (Table 8.4) indicate that the NP-ESMs showed significant catalytic activity upto five cycles of reaction. The morphology and stability of the catalyst after the fifth cycle of the reaction was observed through SEM (Figure 8.9) which clearly shows the presence of NPs on ESM indicating that the NPs were stable on ESM and did not leach out during the reaction.

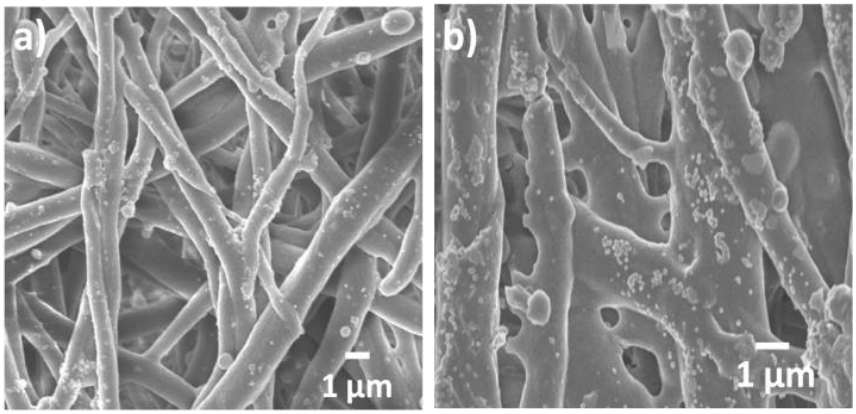

Figure 8.9. FESEM images of Au-ESM (a) and Ag-ESM (b) after five consecutive reactions.

8.5. Conclusions

Readily available biomaterial, ESM was employed for the synthesis of metal NPs using the surface functionalities for the auto reduction of metal ions. Immobilizing NPs on ESM enabled easy handling of the catalyst compared to free nanoparticles. Catalytic efficiencies of NP-ESMs were evaluated for two different types of organic reactions. NP-ESM catalysts can be used for the efficient reduction of nitro to amine functional groups within a short period of time (10 min) and A^3 coupling reactions with high yield (99%). It is believed that these simple catalytic systems can be further explored for other important organic reactions. Our catalysts offer an added advantage in terms of low cost, non-toxicity, easy synthesis and reusability. Such biotemplated synthesis which is a facile, green and cost effective method is able to offer many fascinating possibilities for designing new catalysts for different organic reactions and expected to be useful in industrial applications.

8.6. References

(1) Narayanan, R.; El-Sayed, M. A. *The Journal of Physical Chemistry B* **2005**, *109*, 12663.

(2) Rashid, M. H.; Bhattacharjee, R. R.; Kotal, A.; Mandal, T. K. *Langmuir* **2006**, *22*, 7141.

(3) Rashid, M. H.; Mandal, T. K. *The Journal of Physical Chemistry C* **2007**, *111*, 16750.

(4) Rashid, M. H.; Bhattacharjee, R. R.; Mandal, T. K. *The Journal of Physical Chemistry C* **2007**, *111*, 9684.

(5) Li, C.-Z.; Male, K. B.; Hrapovic, S.; Luong, J. H. T. *Chemical Communications* **2005**, *0*, 3924.

(6) Xia, Y.; Yang, P.; Sun, Y.; Wu, Y.; Mayers, B.; Gates, B.; Yin, Y.; Kim, F.; Yan, H. *Advanced Materials* **2003**, *15*, 353.

(7) Sun, Y.; Xia, Y. *Science* **2002**, *298*, 2176.

(8) Hao, E.; Bailey, R. C.; Schatz, G. C.; Hupp, J. T.; Li, S. *Nano Letters* **2004**, *4*, 327.

(9) Suzuki, M.; Niidome, Y.; Kuwahara, Y.; Terasaki, N.; Inoue, K.; Yamada, S. *The Journal of Physical Chemistry B* **2004**, *108*, 11660.

(10) Murphy, C. J.; Sau, T. K.; Gole, A. M.; Orendorff, C. J.; Gao, J.; Gou, L.; Hunyadi, S. E.; Li, T. *The Journal of Physical Chemistry B* **2005**, *109*, 13857.

(11) Miyamura, H.; Matsubara, R.; Miyazaki, Y.; Kobayashi, S. *Angewandte Chemie International Edition* **2007**, *46*, 4151.

(12) Kanaoka, S.; Yagi, N.; Fukuyama, Y.; Aoshima, S.; Tsunoyama, H.; Tsukuda, T.; Sakurai, H. *Journal of the American Chemical Society* **2007**, *129*, 12060.

(13) Kim, F.; Song, J. H.; Yang, P. *Journal of the American Chemical Society* **2002**, *124*, 14316.

(14) Gole, A.; Murphy, C. J. *Chemistry of Materials* **2004**, *16*, 3633.

(15) Jin, R.; Egusa, S.; Scherer, N. F. *Journal of the American Chemical Society* **2004**, *126*, 9900.

(16) Seo, D.; Park, J. C.; Song, H. *Journal of the American Chemical Society* **2006**, *128*, 14863.

(17) Li, C.; Shuford, K. L.; Park, Q. H.; Cai, W.; Li, Y.; Lee, E. J.; Cho, S. O. *Angewandte Chemie International Edition* **2007**, *46*, 3264.

(18) Kwon, K.; Lee, K. Y.; Lee, Y. W.; Kim, M.; Heo, J.; Ahn, S. J.; Han, S. W. *The Journal of Physical Chemistry C* **2006**, *111*, 1161.

(19) Chen, H. M.; Hsin, C. F.; Liu, R.-S.; Lee, J.-F.; Jang, L.-Y. *The Journal of Physical Chemistry C* **2007**, *111*, 5909.

(20) Chu, H.-C.; Kuo, C.-H.; Huang, M. H. *Inorganic Chemistry* **2005**, *45*, 808.

(21) Ha, T. H.; Koo, H.-J.; Chung, B. H. *The Journal of Physical Chemistry C* **2006**, *111*, 1123.

(22) Pileni M. P. *Nature Materials* **2003**, 2, 145.

(23) Brown, S.; Sarikaya, M.; Johnson, E. *Journal of Molecular Biology* **2000**, *299*, 725.

(24) Shankar, S. S.; Rai, A.; Ahmad, A.; Sastry, M. *Chemistry of Materials* **2005**, *17*, 566.

(25) Lisiecki, I.; Pileni, M. P. *Journal of the American Chemical Society* **1993**, *115*, 3887.

(26) Enache, D.; Knight, D.; Hutchings, G. *Catal Lett* **2005**, *103*, 43.

(27) Carrettin, S.; McMorn, P.; Johnston, P.; Griffin, K.; Hutchings, G. J. *Chemical Communications* **2002**, *0*, 696.

(28) Praharaj, S.; Nath, S.; Ghosh, S. K.; Kundu, S.; Pal, T. *Langmuir* **2004**, *20*, 9889.

(29) Fukuoka, A.; Higuchi, T.; Ohtake, T.; Oshio, T.; Kimura, J.-i.; Sakamoto, Y.; Shimomura, N.; Inagaki, S.; Ichikawa, M. *Chemistry of Materials* **2005**, *18*, 337.

(30) Besson, E.; Mehdi, A.; Reye, C.; Corriu, R. J. P. *Journal of Materials Chemistry* **2009**, *19*, 4746.

(31) Nakano, T.; Ikawa, N. I.; Ozimek, L. *Poult Sci* **2003**, *82*, 510.

(32) Zheng, B.; Qian, L.; Yuan, H.; Xiao, D.; Yang, X.; Paau, M. C.; Choi, M. M. F. *Talanta* **2010**, *82*, 177.

(33) Neilson A.H., The Handbook of Environmental Chemistry, vol. 3: Anthropogenic compounds, Part J: PAHs and Related Compounds: Biology, Lewis Publishers, Boca Raton, FL, 1997, p. 346.

(34) Schwab, C. E.; Huber, W. W.; Parzefall, W.; Hietsch, G.; Kassie, F.; Schulte-Hermann, R.; Knasmuller, S. *Crit Rev Toxicol* **2000**, *30*, 1.

(35) Xu, S.; Xi, X.; Shi, J.; Cao, S. *Journal of Molecular Catalysis A: Chemical* **2000**, *160*, 287.

(36) Downing, R. S.; Kunkeler, P. J.; van Bekkum, H. *Catalysis Today* **1997**, *37*, 121.

(37) Deshpande, R. M.; Mahajan, A. N.; Diwakar, M. M.; Ozarde, P. S.; Chaudhari, R. V. *The Journal of Organic Chemistry* **2004**, *69*, 4835.

(38) Praharaj, S.; Nath, S.; Ghosh, S. K.; Kundu, S.; Pal, T. *Langmuir* **2004**, *20*, 9889.

(39) Esumi, K.; Isono, R.; Yoshimura, T. *Langmuir* **2003**, *20*, 237.

(40) Liu, J.; Qin, G.; Raveendran, P.; Ikushima, Y. *Chemistry – A European Journal* **2006**, *12*, 2131.

(41) Hayakawa, K.; Yoshimura, T.; Esumi, K. *Langmuir* **2003**, *19*, 5517.

(42) Finar I. L., Organic Chemistry. The Fundamental Principles, Vol. 1, 6th ed., English Language Book Society, London, UK 1973.

(43) Armstrong, R. W.; Combs, A. P.; Tempest, P. A.; Brown, S. D.; Keating, T. A. *Accounts of Chemical Research* **1996**, *29*, 123.

(44) Kamijo, S.; Yamamoto, Y. *Journal of the American Chemical Society* **2002**, *124*, 11940.

(45) Ringdahl B., The Muscarinic Receptors (Ed. Brown JH), Humana Press, Clifton, N J, 1989, 377-418

(46) Miura, M.; Enna, M.; Okuro, K.; Nomura, M. *The Journal of Organic Chemistry* **1995**, *60*, 4999.

(47) Jenmalm, A.; Berts, W.; Li, Y.-L.; Luthman, K.; Csoeregh, I.; Hacksell, U. *The Journal of Organic Chemistry* **1994**, *59*, 1139.

(48) Dyker, G. *Angewandte Chemie International Edition* **1999**, *38*, 1698.

(49) Imada, Y.; Yuasa, M.; Nakamura, I.; Murahashi, S.-I. *The Journal of Organic Chemistry* **1994**, *59*, 2282.

(50) Czernecki, S.; Valéry, J.-M. *Journal of Carbohydrate Chemistry* **1990**, *9*, 767.

(51) Wei, C.; Li, C.-J. *Journal of the American Chemical Society* **2003**, *125*, 9584.

(52) Wei, C.; Li, Z.; Li, C.-J. *Organic Letters* **2003**, *5*, 4473.

CHAPTER 9

CONCLUSIONS AND FUTURE STUDIES

9.1. Conclusions

The focus of this study was to develop an efficient and stable biomaterial based adsorbent for water treatment. Biowastes such as apple and tomato peels were used as efficient adsorbents to remove different pollutants in water such as pesticides, dyes, heavy metal ions and nanoparticles. Adsorption capacities of different biopeels were measured towards different pollutants and noted that biopeels were able to adsorb cationic pollutants more efficiently than anionic pollutants. Tomato peels showed efficient removal of Pb^{2+}, Ni^{2+}, alcian blue, and brilliant blue. Unmodified apple peels showed limited selectivity towards different pollutants. The functional groups on biomembranes can be further modified for the extraction of desirable contaminants from water. We prepared chemically modified apple peel by loading Zr on its surface and by surface grafting. Such chemically modified apple peel showed enhanced extraction of anions. Zr immobilized apple peel was employed to extract anions and nanoparticles from water. Raw apple peel and immobilised apple peel together make a complete system to adsorb most of the pollutants from water simultaneously. Langmuir and Freundlich isotherm models were used to validate the adsorption process. Kinetic studies were done to further understand the adsorption process. Experimental factors such as pH and temperature of the medium also influenced the extraction efficiency. Many biowaste materials have been reported as different adsorbents by other research groups however these targeted adsorbents were used to remove only a single class of pollutants. There was no report which shows the removal of different classes of pollutants by using single adsorbent. From the results, it is conceivable that the use of such biowaste is a simple, cost effective and efficient method for water treatment and can be used in large scale applications.

We also explored the use of eggshell membrane as template to prepare hierarchical metal oxide nanotubes. This work demonstrates the novel route to synthesize hierarchical superstructures with unique morphology and the as-prepared Mn_3O_4 crystals showed efficient removal of organic pollutants in waste water. It was further tested for other anionic pollutants such as phosphate,

arsenate and chromate ions. This prompted us to synthesize other metal oxides for water treatment and many metal oxides were screened for efficient adsorption of different pollutants in water. SEM micrographs showed interwoven porous structures for NiO and CeO_2. NiO was found to be an effective sorbent with adsorption capacities of 77 mg/g and 55 mg/g for gold and silver nanoparticles respectively, from water within a period of 2 hours. TEM analysis of the metal oxide after extraction showed the presence of nanoparticles on the surface. Mn_3O_4 showed efficient adsorption towards pesticides, dyes and phosphates. Combination of these two metal oxides can remove all pollutants from water and use of such metal oxides as adsorbents is expected to reduce many steps in water purification process. Since the overall size of the prepared metal oxides tubes are in 10 - 20 micrometres, solid/liquid extraction would be fairly manageable and the relatively high density of metal oxides is also useful for real time water treatment applications. In comparison with conventional methods of materials production such as precipitation, hydrothermal and calcination, biomineralization is facile, eco-friendly and cost effective. Generally biomineralization process has minimum requirements for chemicals, equipment and is carried out under ambient conditions. Biotemplate such as eggshell membrane is available in large amounts at low costs and biomorphic mineralization makes efficient uses of natural materials with a capability of turning biowastes into functional materials. Biomorphic products are usually inherited with specific pore morphologies and unique intricate microstructures. The proposed synthesis could offer interesting possibilities for developing new materials for water purification.

9.2. Future studies

Biodegradation and stability of the adsorbent at high concentrations of acid or alkali are not discussed or tested in reported literatures. Laboratory experiments were done in small quantities and materials were under observation for limited time period only. It was difficult to predict material properties on prolonged usage. Some of the thermodynamic and kinetic parameters need to be studied

systematically before using these materials in industrial applications. Design of new materials, optimization of such parameters, and exploring the efficiency in the removal of different pollutants from water are investigated in this thesis. Collaborative research with engineers and environmental chemists may help to further develop these adsorbents for industrial or large scale applications. Such adsorbents can be used to recycle waste water from different sources. Certain engineering parameters such as water flux, contact time, regeneration speed and waste generation are crucial factors in large scale water purification processes. These parameters help us to understand the efficiency in removal of pollutants and durability of the adsorbent. Since biowaste is available abundantly throughout the world, this study may provide viable solution for clean water access in many developing countries. Simple design and user friendly materials make the water treatment process more efficient. The adsorption process decreases number of steps in water purification process and may contribute to minimum energy consumption.